

2019-01-24

Paleoenvironmental Reconstruction of Kalodirr and Moruorot, Kenya using Stable Carbon Isotopes

Butts, Catherine Frances Rita

Butts, C. F. R. (2019). Paleoenvironmental Reconstruction of Kalodirr and Moruorot, Kenya using Stable Carbon Isotopes (Master's thesis, University of Calgary, Calgary, Canada).

Retrieved from <https://prism.ucalgary.ca>.

<http://hdl.handle.net/1880/109862>

Downloaded from PRISM Repository, University of Calgary

UNIVERSITY OF CALGARY

Paleoenvironmental Reconstruction of Kalodirr and Moruorot, Kenya using Stable
Carbon Isotopes

by

Catherine Frances Rita Butts

A THESIS

SUBMITTED TO THE FACULTY OF GRADUATE STUDIES

IN PARTIAL FULFILLMENT OF THE REQUIREMENTS FOR THE

DEGREE OF MASTER OF ARTS

GRADUATE PROGRAM IN ANTHROPOLOGY

CALGARY, ALBERTA

JANUARY, 2019

© Catherine Frances Rita Butts 2019

Abstract

Early Miocene environments in East Africa are proposed to have consisted of entirely dense forest systems composed strictly of C_3 vegetation, which has affected our understanding of Miocene ape habitats. However, new environmental data from the early Miocene sites of Moroto (21 Ma), Napak (20 Ma), Tinderet (20 Ma), Rusinga Island (20-18 Ma), and Bukwa (19 Ma) indicate a more open environment consisting of open canopied forests, woodlands and wooded grasslands with evidence of some C_4 vegetation. This study builds on this new data by analyzing stable carbon isotopes in mammalian tooth enamel collected from Kalodirr and Moruorot, Kenya (17.5-16.8 Ma). These $\delta^{13}C_{\text{enamel}}$ signatures suggest a mosaic of C_3 vegetation too enriched to indicate a closed canopy forest. Rather, they are more similar to values found in woodlands, with some indications of C_4 vegetation. This supports the hypothesis that the forest canopies of East Africa were opening before the middle Miocene, demonstrating that the environmental history of East Africa was more dynamic than previously described.

Preface

This thesis is original, unpublished work by the author, C. Butts.

Dedication

In dedication to my loving parents and grandparents. Thank you for all your support and advice throughout the years, as well as allowing me to pursue every wim no matter how strange.

I love you.

Acknowledgements

I am eternally grateful to my amazing supervisor (aka. Academic Mom) Susanne Cote. You have provided me with opportunities I never believed possible. I have learned and grown so much in the past two years due to your positivity, guidance, patience, feedback and support.

I would also like to thank my committee members, Annie Katzenberg and Jessica Theodor for your thoughtful feedback and encouragement. A special thank you to Annie Katzenberg for allowing me to use her lab for my acid treatments.

Abigail Hall and Madison Bradley, you are the best Science siblings I could ask for! Thank you for the camping tips, the constant support, and forcing me to get out of the thesis bubble once and a while. An additionally shout out to Laura Tucker, thank you for the isotope talks.

Thank you to the National Museums of Kenya and the Turkana Basin Institute for permitting this work to be done. Also, to their field workers and the people of Turkana for helping in the collection of my specimens and their hospitality.

This work is partially supported by the University of Calgary, as well as the Natural Sciences and Engineering Council (NSERC) and the National Science Foundation (NSF), which funded Dr. Susanne Cote.

Table of Contents

ABSTRACT	I
PREFACE.....	II
DEDICATION	III
ACKNOWLEDGEMENTS	IV
TABLE OF CONTENTS.....	V
LIST OF FIGURES	VII
LIST OF TABLES.....	VIII
EPIGRAPH	IX
CHAPTER 1: INTRODUCTION	1
CHAPTER 2: ENVIRONNEMENTAL INTERPRETATIONS, $\delta^{13}\text{C}$ ISOTOPE CONCEPTS, AND SITE RELEVANCE	3
2.1 ENVIRONMENTS OF EAST AFRICA: HISTORICAL INTERPRETATIONS VS. NEW DATA	3
2.2 GRASSES AND ENVIRONMENTS: DEVELOPMENT AND PREHISTORIC CONTEXT	8
2.3 SITE RELEVANCE	11
CHAPTER 3: HYPOTHESES AND PREDICTIONS, SITE DESCRIPTION, AND STUDY DESIGN.....	13
3.1 SITE DESCRIPTION	14
3.1.1 <i>Geographic Setting and Alternative Names</i>	14
3.1.2 <i>Geology</i>	15
3.2 MATERIALS	17
3.2.1 <i>Artiodactyla</i>	19
3.2.2 <i>Perissodactyla</i>	21
3.2.3 <i>Proboscidea</i>	22
3.2.4 <i>Hyracoidea</i>	23
3.3 $\delta^{13}\text{C}$ ISOTOPE CONCEPTS	23
3.3.1 <i>Plants</i>	23
3.3.2 <i>Mammalian Tooth Enamel</i>	25
3.3.3 <i>Mammalian Diet</i>	26
3.4 METHODS	28
3.4.1 <i>Sampling Protocol</i>	28
3.4.2 <i>Sample Analysis</i>	28
3.4.3 <i>Dietary Calculations</i>	30
3.4.4 <i>Habitat Reconstructions using Dietary Isotopes</i>	33
3.5 HYPOTHESES AND PREDICTIONS	35

CHAPTER 4: RESULTS AND DISCUSSION	38
4.1 RESULTS	38
<i>4.1.1 Kalodirr and Moruorot Isotope Ranges</i>	<i>38</i>
<i>4.1.2 C₃ vs C₄ Diets.....</i>	<i>42</i>
<i>4.1.3 Species Differences.....</i>	<i>45</i>
<i>4.1.4 Habitat Reconstruction.....</i>	<i>47</i>
4.2 DISCUSSION	49
<i>4.2.1 Isotopic Signals.....</i>	<i>49</i>
<i>4.2.2 C₃ vs C₄.....</i>	<i>50</i>
<i>4.2.3 Habitat Interpretation.....</i>	<i>52</i>
CHAPTER 5: PRETREATMENT ANALYSIS	54
5.1 ENAMEL FORMATION AND DIAGENESIS	54
<i>5.1.1 Formation and Chemistry</i>	<i>54</i>
<i>5.1.2 Diagenesis and Pretreatments</i>	<i>55</i>
5.2 STUDY DESIGN.....	58
<i>5.2.1 Methods.....</i>	<i>58</i>
5.3 RESULTS	62
5.4 DISCUSSION	67
CHAPTER 6: CONCLUSIONS	69
6.1 SUMMARY	69
6.2 SIGNIFICANCE	71
6.3 FUTURE DIRECTIONS	72
CITATIONS	74
SUPPLEMENTARY INFORMATION.....	87
LIST OF FIGURES.....	87
LIST OF TABLES.....	87

List of Figures

Figure 1: Diagram of the eastern branch of the East African Rift System. The red circle represents Kalodirr and Moruorot. Rift lines accessed through: https://services7.arcgis.com/Gw2vEo9WjwgQp6Er/arcgis/rest/services/East_African_Rift_System/FeatureServer (no author listed).	6
Figure 2: Map of the Lothidok Range, edited from Boschetto (1988). Kalodirr and Moruorot are labelled by the red 'X' shapes.	15
Figure 3: Simplified Stratigraphy of Kalodirr and Moruorot, Kenya.....	16
Figure 4: Dietary ranges of all samples collected from Kalodirr and Moruorot using the conservative dietary model.	42
Figure 5: Dietary ranges of all samples collected from Kalodirr and Moruorot using the standard dietary model.	43
Figure 6: Summary of species distribution along with box and whisker plots of $\delta^{13}\text{C}$ enamel values of families at both Kalodirr and Moruorot.	45
Figure 7: Box and whisker plots comparing $\delta^{13}\text{C}$ enamel range of individual species; , c) suid/sanithere species <i>Diamantohyus africanus</i> , <i>Kenyasus rusingensis</i> , <i>Libycochoerus jeanelli</i> and <i>Namachoerus moruoroti</i> , b) giraffid/pecoran species <i>Canthumeryx sirtensis</i> and <i>Walangania africanus</i> , c) tragulids species <i>Dorcatherium chappuisi</i> and <i>Dorcatherium pigotti</i> , d) anthracothere species <i>Brachyodus aequatorialis</i> and <i>Sivameryx africanus</i>	46
Figure 8: Box and whisker plot of $\delta^{13}\text{C}$ enamel values of families at both Kalodirr and Moruorot.....	48
Figure 9: Box and whisker plot displaying the $\delta^{13}\text{C}_{\text{enamel}}$ values of the various treatment types.	65
Figure 10: Box and whisker plot displaying the percentage of weight lost in treatments B, C and D.	66

List of Tables

Table 1: List of families analyzed from Kalodirr and Moruorot where “K” represents Kalodirr and “M” represents Moruorot.	19
Table 2: Conversions accounting for change in $\delta^{13}\text{C}_{\text{atm}}$ from modern values to 17.5 - 16.8 Ma and its effect on plant and enamel $\delta^{13}\text{C}$ values for standard and conservative models.	28
Table 3: Calculated environmental analogues using plant values collected from Cerling et al. (2003, 2011). $\delta^{13}\text{C}$ values are adjusted to account for atmospheric change.	34
Table 4: $\delta^{13}\text{C}_{\text{enamel}}$ ranges and median values retrieved from the mammalian families retrieved from both Kalodirr and Moruorot.	38
Table 5: Results of comparative Mann-Whitney U tests of $\delta^{13}\text{C}$ enamel values between families from both Kalodirr and Moruorot. Cells with significant values are highlighted in light grey.	40
Table 6: Results of Mann-Whitney U tests comparing families found from both Kalodirr and Moruorot.	41
Table 7: Calculated percentage of individuals, using the standard dietary model, classified by dietary types, grouped by family.	44
Table 8: Results of comparative Mann-Whitney U tests of $\delta^{13}\text{C}$ enamel values between Suidae/Sanitheriidae species from Kalodirr and Moruorot.	46
Table 9: Results of Shapiro-Wilk normality tests for the $\delta^{13}\text{C}$ enamel values of the treatment types.	62
Table 10: Results of Shapiro-Wilk normality tests for the percentage of weight loss of treatment types B, C, and D.	63
Table 11: List of the alteration of enamel weight and $\delta^{13}\text{C}$ by pretreatment type for all specimens in this experiment. KAL = Kalodirr, KAR = Karungu, MOR = Moruorot. Error! Bookmark not defined.	
Table 12: Results of a Welch Two Sample t-test comparing the acid treatments B, C and D $\delta^{13}\text{C}_{\text{enamel}}$ values. Significant values are highlighted in light grey.	65
Table 13: Weight percent loss comparisons between treatment types. The type of statistical tests used are listed where Mann-Whitney U tests are used when at least one of the treatments are non-normal and Welch Two Sample t-test are used when both treatments have a normal distribution. Significant results are highlighted in grey.	67

Epigraph

*Why, sometimes I've believed as many as
six impossible things before breakfast.*

-Lewis Carroll

Chapter 1: Introduction

The early Miocene (23 to 16 Ma) of East Africa is critical to the study of the diversification and distribution of apes. Traditionally, it is believed that these early fossil apes utilized lowland, closed canopy forests like all modern apes, which are found exclusively in dense forests. This environmental interpretation was supported by early work on paleogeography, gastropod index species identification, and climatic modelling (Verdcourt 1963; Frakes & Kemp 1972; Andrews & Van Couvering 1975; Evans et al. 1980). These lowland forests would have been composed of strictly C_3 vegetation (Verdcourt 1963) because C_4 vegetation is not believed to be in East Africa during the early Miocene. This interpretation was consistent with models that suggested that the C_4 photosynthetic pathway arose as a derivative of the C_3 photosynthetic pathway due to the global decrease in CO_2 levels during the middle Miocene (Ehleringer et al. 1991; Freeman & Hayes 1992). These models were not only supported by global atmospheric pCO_2 estimates but also by the earliest indications of C_4 photosynthesis in East Africa, dated to 15.5 Ma from paleosols at the Tugen Hills of Kenya, and the increased incorporation of C_4 into herbivorous mammalian diets by 9.9 Ma (Kingston et al. 1994; Morgan et al. 1994; Pagani et al. 2005; Uno et al. 2011). This makes the timing of the appearance of C_4 vegetation of Africa later than observed in other continents. For example, in North America the first indication of C_4 vegetation is ≥ 23 Ma in the central Great Plains, and its first incorporation into mammalian diets was in hypsodont Great Plains horses around 16 to 14.8 Ma (Fox & Koch 2003; Edwards et al. 2010; Muhlbachler et al. 2011; Stromberg 2011; Stromberg & McInerney 2011). The late transition from C_3 dominant to C_4 dominant environments in East Africa, paired with early paleoenvironmental reconstruction work led to the hypothesis that East African environments were dominated by stable and closed canopy forests until the middle Miocene (Verdcourt 1963; Andrews & Van Couvering 1975; Evans et al. 1980; Quade et al. 1989; Ehleringer et al. 1991; Freeman & Hayes 1992). These forests gave way to transitional environments such as open

forests, woodlands and wooded grasslands, and finally grassland dominated environments in the late Miocene around 9.9 Ma (Verdcourt 1963; Andrews & Van Couvering 1975; Evans et al. 1980; Quade et al. 1989; Ehleringer et al. 1991; Freeman & Hayes 1992; Uno et al. 2011).

However, emerging mammalian tooth enamel isotopic evidence from the fossil sites of Napak (~20 Ma), Moroto (~20-21 Ma; Kingston et al. 2009; 2011) and Bukwa (~19 Ma; Kingston et al. 2018) Uganda, and Rusinga Island (20-17 Ma; Garrett et al. 2015) and Tinderet (~20 Ma; Arney et al. 2009), Kenya indicate the presence of open environments such as open canopy forests, forest mosaics and woodlands in the early Miocene. This suggests that forest canopies were opening before the middle Miocene. I speculate that this would be due to local and continental disturbance factors, such as an increase in localized volcanic events and early rifting in the East African Rift System (EARS).

This study contributes to this environmental story by adding new data for the fossil localities of Kalodirr and Moruorot, dated to 17.5 to 16.8 Ma (Boschetto 1988). In order to reconstruct these environments, this study will analyze the stable carbon isotopic signatures of herbivorous mammalian tooth enamel. An additional goal of this project is to place these teeth into stratigraphic context, by mapping the regional geology, in order to determine if there was any dietary change over time. I hypothesize that Kalodirr and Moruorot will indicate a more open environment than the other East African early Miocene sites, providing additional support that forest canopies were opening prior to the middle Miocene.

Chapter 2: **Environmental Interpretations, $\delta^{13}\text{C}$ Isotope Concepts, and Site Relevance**

2.1 Environments of East Africa: Historical Interpretations vs. New Data

Verdcourt (1963) led early environmental reconstruction work in East Africa using gastropod assemblages from Miocene sites across the region. He concluded that their shell forms were similar to modern forms that are recovered in evergreen forest or riverine forest systems (Verdcourt 1963). Andrews & Van Couvering (1975) built on Verdcourt's work by drawing on multiple sources of data. They stated that the equatorial belt, an area of increased rainfall and high temperatures, was extended causing the formation of a continuous lowland forest across western, central and eastern Africa (Andrews & Van Couvering 1975). Two major factors that influenced their interpretations of vegetation zones were: (1) the placement of the continents during the Cenozoic and (2) the changes in worldwide humidity and heat (Andrews & Van Couvering 1975). First they drew on Frakes & Kemp's (1972) reconstructions, which indicated that by the Eocene Africa was 5° south of its present position and migrated into its current position by the Oligocene and Miocene. During the Oligo-Miocene, the Indian continent obstructed the warm waters of the Pacific Ocean from reaching East Africa due to its position in the middle of the Indian Ocean (Frakes & Kemp 1972). Andrews & Van Couvering (1975) hypothesized that these warm Pacific waters could have moved northward through the 'Straits of Zinj' and increased rainfall across East Africa. This rainfall would be amplified in the monsoonal season when the northeast winds off the Tethys Ocean spread across East Africa (Frakes & Kemp 1972; Andrews & Van Couvering 1975). Additionally, the continental divide of East Africa was reconstructed to be west of the present-day EARS, which would have caused the equatorial trough to extend across Uganda and Kenya (Andrews & Van Couvering 1975). These factors would cause the Oligo-Miocene of eastern Africa to have a high precipitation rate until uplift occurred in the Kenyan Rift in the late Miocene (Andrews & Van Couvering 1975). This has been further

augmented by multiple studies that suggest that precipitation rates would not have changed until this uplift at 10 Ma, causing a major aridification event during the end Miocene-early Pliocene and the subsequent opening of tropical forests (Pickford et al. 1993; Slingo et al. 2005; Sepulchre et al. 2006; Maslin & Christensen 2007; Kaspar et al. 2010; Prommel et al. 2013). Additionally, climatic trends indicated that the Miocene was globally a warm period hitting its maximum during the Mid-Miocene Climatic Optimum followed by a period of global cooling by 10 Ma (Edwards 1968; Jenkins 1973; Haq 1980; Miller et al. 1987; Flower & Kennett 1993; Kennett 1995; Zachos et al. 2001). These initial interpretations and continued support led to the conclusion that a stable and dense lowland forest dominated the early Miocene of East Africa until the middle Miocene. After the middle Miocene there was a marked increase in open environments, including dry and arid woodlands and wooded grasslands along with the increased presence of fossil grasses and phytoliths (Cerling et al. 1991, 1997a, 1997b; Wynn & Retallack 2001; Retallack et al. 2002). Furthermore, it is commonly accepted that C₄ vegetation was not present in East Africa until 15.5 Ma, where it is first recorded in the paleosols of the Muruyur Beds at Kipsaramon in the Tugen Hills (Kingston et al. 1994; Morgan et al. 1994). C₄ does not become common in East Africa until 10 Ma, with a gradual increase in C₄ dominated grasslands starting in the late Miocene at 8 Ma (Cerling 1992; Cerling et al. 1998; Uno et al. 2016). However, new data suggests a different, more complex environmental story. Data from multiple disciplines can be used in order to establish a well-rounded understanding of both the large scale and localized pressures, such as volcanic activity and localized rifting, acting on East Africa and will be described in the following paragraphs.

Since the late Cretaceous, Africa has migrated ~14° north (Smith & Hurley 1982). This movement had a number of influences, including the break off of Arabia and its collision with Eurasia and the subsequent slowed movement of the underlying mantle, which caused localized rifting events and increased volcanism across the EARS (McConnell 1972; Schilling 1973;

Karson & Curtis 1989; Nyblade & Robinson 1994; Burke 1996; Chorowicz 2005; Partridge 2010). The breakup of Afro-Arabia began in the late Oligocene along the Gulf of Aden, indicated by offshore deposits dated to 29.9 Ma to 28.7 Ma (Azzaroli 1968; Bosworth et al. 2005; Guiraud et al. 2005). By the Oligo-Miocene, this rifting and stretching had spread through the Afar and Red Sea system (Azzaroli 1968; Berggren & Van Couvering 1974; Steininger & Rogl 1984; Bernor et al. 1987; Bosworth et al. 2005; Guiraud et al. 2005). While geologists have encountered difficulty constraining the time of this collision, paleontologists accept an early Miocene collision due to the presence of deinotheres and gomphotheres in the Eastern Mediterranean at 18.4 Ma as well as in India at 18.3 Ma (Barry et al. 1985; Bernor et al. 1987; Tassy 1990; Allen et al. 2004; Bosworth et al. 2005; Koufos et al. 2005).

The collision of Eurasia and Arabia resulted in the slowed movement of the African Plate relative to the underlying mantle (Partridge 2010). This caused the EARS to be dominated by the intrusion of the ductile asthenosphere into the solid lithospheric mantle, creating a system of heat flow into cool continental environments (McConnell 1972; Karson & Curtis 1989; Burke 1996; Chorowicz 2005; Partridge 2010). In other words, the shallow crust was fractured to such an extent that rifting is controlled by localized influences rather than large-scale tectonic strain. This would not have been considered in the large-scale reconstructions used in the past, as it would not affect the dynamics of the African Plate. Today, the EARS is a belt of rift valleys composed of two main branches, eastern and western, spanning from the Red Sea and Gulf of Aden to the Zambezi River in Mozambique (McConnell 1972). It is important to note that the term EARS is typically applied to Cenozoic rifts, although rifting was initiated as early as the Permo-Triassic (Kreuser 1995, Morley et al. 1992, MacGregor 2015). As Kalodirr and Moruorot are constrained to the eastern branch, this section will focus on this branch.

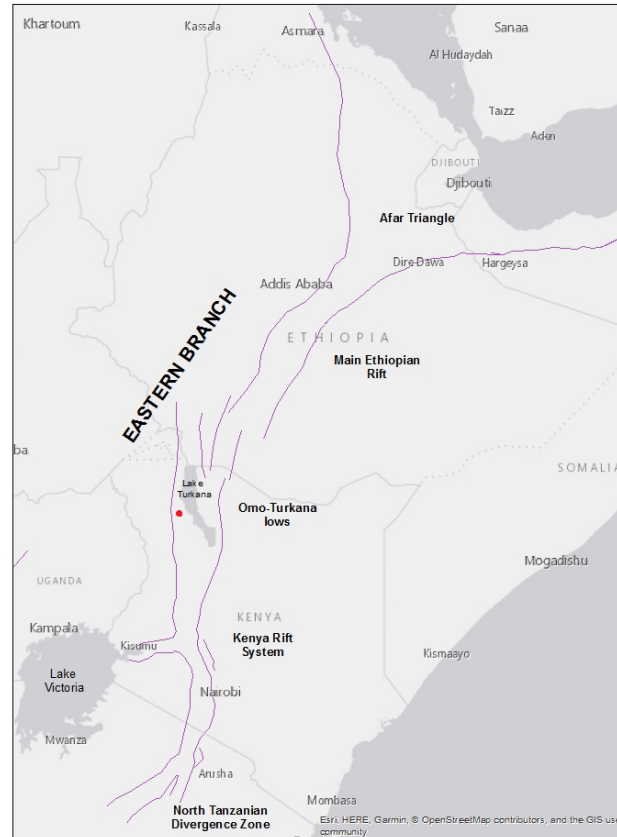


Figure 1: Diagram of the eastern branch of the East African Rift System. The red circle represents Kalodirr and Moruorot. Rift lines accessed through: https://services7.arcgis.com/Gw2vEo9WjwgQp6Er/arcgis/rest/services/East_African_Rift_System/FeatureServer (no author listed).

The eastern branch extends from the Afar Triangle in the north, through the Main Ethiopian rift (MER), the Omo-Turkana lows, and the Kenyan (Gregory) rifts, ending in the basin of the North-Tanzanian divergence zone in the south, a total distance of 2200 km (Figure 1; Chorowicz 2005). In the eastern branch, the initiation of basin subsidence in the Turkana Basin at ~25 Ma (Omo-Turkana lows) resulted due to half graben (i.e. a block between two faults that is displaced downward relative to the blocks on either side) basins, which formed and extended from Turkana to the Tugen Hills of the Kenyan Rift system (Morley et al. 1992; Ebinger et al. 2000). Rifting migrated both southward from Turkana to Kerio and northward into the Main Ethiopian Rift (MER) during the mid to late Miocene (Morley et al. 1992). To the south,

subsidence activity continued until ~14 Ma, which caused the alignment of volcanic centers along the fault borders (Morley et al. 1992). This subsidence resulted in the uplift of the East African plateau that created a heterogeneous landscape by 10 Ma (Sepulchre et al. 2006; Maslin & Christensen 2007; Kasper et al. 2010; Prommel et al. 2012).

Coinciding with this rifting, the eastern branch had a heavy concentration of volcanic activity during the early Miocene (McConnel 1972; Burke 1996; Partridge 1998; Chorowicz 2005). Increased volcanism is not typically correlated with the expansion of rift systems, exemplified by the west European rift (Prodehl 1981), and can be attributed to factors including the weakened lithosphere and the occurrence of multiple mantle plumes within the continental crust (Bullard 1936; McConnell 1972; Schilling 1973; Schilling et al. 1992; Karson & Curtis 1989; Nyblade & Robinson 1994; Burke 1996; Partridge 1997; Chorowicz 2005). The bulk of volcanic eruptions were concentrated at the northern end of the Kenyan rift, emitting ~140,000 km³ of material since the early Miocene (Partridge 1997). The Lothidok Range in the Turkana Depression exemplifies this increase of volcanic activity in Kenya during the Miocene, represented by the presence of both pyroclastic material (volcanic ejecta; e.g. tuffs and lahars) and basalts (Boschetto 1988). The pyroclastic rocks consist of two petrologically distinct types: mafic alkaline tephra, emitted at 17.7 Ma, and trachytic tuffs, emitted at 16.8 and 13 Ma (Boschetto 1988). This suggests at least two different volcanic sources (Boschetto 1988). Three major basaltic flows, which consist of multiple smaller flows, have been recorded in the Lothidok Range and consist of: the Kalakol Basalts consisting of three intermediate basaltic flows (27.5 to 26.9 Ma; 24.5 Ma; 18 to 17.7 Ma), basalts overlying sediments at Loperot and capping the Lothidok Peak (15.3 to 13.7 Ma), and the Loperi Basalts (12.4 to 10.9 Ma; Boschetto 1988; Boschetto et al. 1992).

While large-scale factors such as climate and uplift are important to the environmental story of East Africa, it is also important to consider localized influences. Andrews & Van

Couving (1975) considered volcanic activity and rifting on a continental scale rather than regional, primarily their influences on elevation and topography. The concentration of rifting and increase of volcanism during the early Miocene of East Africa may have altered localized climate and vegetation patterns. This would ultimately create unstable and dynamic environments across East Africa, rather than the hypothesized stable and dense forests. These changes are recorded in the flora, fauna and soils from the Miocene recovered across East Africa.

2.2 Grasses and Environments: Development and Paleontological Context

By the early Cretaceous, the grass family Poaceae, previously known as Gramineae, are recorded in East Africa (Stromberg 2011). The family Poaceae contains the major clades of grasses including the C₃-dominated BEP grass clade (Bambusoideae, Ehrhartoideae and Pooideae) and the C₄-dominated PACCMAD grass clade (Panicoideae, Chloridoideae, Centothecoideae, Micrairoideae, Aristidoideae and Danthonioideae; Grass Phylogeny Working Group (GPWG) 2001). These early grasses were adapted to warm, mesic, and closed environments and likely utilized the C₃ pathway (Osborne & Freckleton 2009; Edwards & Smith 2010; Stromberg 2011). The C₄ pathway evolved from the C₃ pathway multiple times, mainly within the subfamilies of the PACCMAD clade and typically in response to open and arid environments (GPWG 2001; Kellogg 2001; Osborne & Freckleton 2009; Bouchenak-Khelladi et al. 2010; Edwards & Smith 2010). Until recently, the first record of C₄ grasses in East Africa was during the middle Miocene, ~15.5 Ma (Kingston et al. 1994; Morgan et al. 1994). Grasses found in East Africa before this time, including Poaceae from the Lokichar Basin (Oligo-Miocene boundary) and monocot grasses from Bukwa (~19 Ma), are considered to use C₃ photosynthesis (GPWG 2001; Pickford 2002; Vincens et al. 2006).

Continued research across the early Miocene has increased insights into the environmental changes of East Africa. Fossil sites, such as Bukwa, Rusinga Island and Karungu, all indicate heterogeneous environments with evidence indicating closed to open forests, seasonal woodlands and wooded grasslands (Brock & MacDonald 1969; Evans et al. 1981; Bonnefille 1985; Pickford 2002; Collinson et al. 2009; Ungar et al. 2012; Driese et al. 2015; Lukens et al. 2017; Novello et al. 2017; Kingston et al. 2018). Leaves, flowers and fruits recovered from Bukwa, Uganda (~19 Ma) indicate a forested environment, monocot grasses and rhizomes indicate woodlands, and gastropods and phytoliths indicate grasslands (Brock & MacDonald 1969; Walker 1969; Bonnefille 1985; Pickford 2002; Kingston et al. 2018). Similarly, fruit and seed assemblages from Rusinga Island, Kenya (20-18 Ma) suggest a wet lowland forest, while the distribution of seeds suggests deciduous woodland indicating spatially heterogeneous environments (Chesters 1957; Andrews & Van Couvering 1975; Andrews et al. 1979; Evans et al. 1981; Collinson et al. 2009). In contrast, paleoclimate reconstructions of Rusinga Island indicate semi-arid to arid environments and new phytolith data indicates the presence of PACCMAD grasses (Novello et al. 2017; Hillis et al. 2018). The paleosols of Karungu, Kenya (17.8 Ma) suggest the presence of a seasonal riparian forest, woodland and wooded grasslands (Driese et al. 2015; Lukens et al. 2017). Additionally, isotope analysis from Napak (20 Ma) and Moroto (~20-21 Ma; Kingston et al. 2009; 2011), and Bukwa (~19 Ma; Kingston et al. 2018) Uganda and Rusinga Island (20-17 Ma; Garrett et al. 2015) and Tinderet (20 Ma; Arney et al. 2017), Kenya retrieved $\delta^{13}\text{C}_{\text{enamel}}$ values that indicate either open forest or woodland conditions, with indications of mixed C_3 and C_4 plant materials. This new evidence indicates that the environmental history of the East African early Miocene was complex and dynamic rather than the previous stable models, with more open environments including open forests, woodlands and wooded grasslands with C_4 vegetation.

These data suggest different environmental interpretations for East Africa, which would be similar to those observed in North America. Data collected from North America indicate that the early and middle Eocene was dominated by subtropical forests with widespread but rare grasses (Crepet & Feldman 1991; Graham 1999; Stromberg 2011). PACCMAD and Pooideae (a subfamily of C_3 grasses) may have originated by 42 to 38 Ma in South America and migrated into the closed forest and woodland environments of North America by the earliest Oligocene (Manchester 2001; Hembree & Hasiotis 2007; Stromberg 2003; 2004; 2005; 2011). This record indicates that the earliest grasses were adapted to closed environments and began to expand their environmental zones (Osborne & Freckleton 2009; Edwards & Smith 2010; Stromberg 2011). These forests gave way to a mix of woodlands, shrublands and bunch grasslands (Retallack 1997; Retallack 2007; Stromberg 2003; 2004; 2011). By the Miocene, open-habitat grasses were widespread (Stromberg 2011). In the early Miocene of North America, these environments became C_3 dominated grasslands characterized by a mix of grasses and dicotyledons (Retallack 1997; Retallack 2007; Stromberg 2003; 2004; 2011). C_4 grasses were present in the Great Plains (≥ 23 Ma) and moved into California by the middle Miocene and continued to increase in abundance (Nambudiri et al. 1978; Fox & Koch 2003; Stromberg 2003; 2004; 2005; 2011). Fauna also began to adapt toward more open habitat locomotor morphologies and abrasive diets during the late Oligocene to early Miocene with hypsodont horses appearing by 16 to 14.8 Ma (Jacobs et al. 1999; Janis et al. 2000; Janis et al. 2002; Muhlbachler & Solounias 2006; Muhlbachler et al. 2011). Horses began incorporating small quantities of C_4 in their diets at ~ 15 Ma (Wang et al. 1996; MacFadden & Cerling 1996; Cerling et al. 1997b; Passey et al. 2002). This indicates a time lag between the appearance of C_4 vegetation in the North American record and its incorporation into mammalian diets (Wang et al. 1996; MacFadden & Cerling 1996; Cerling et al. 1997B; Passey et al. 2002). The diets of these horses shift from C_3 dominated to C_4 dominated by 6.6 Ma before the environment was C_4 dominated, although C_4 grasses were moderately abundant (Wang et al. 1994; Passey et al. 2002; McInerney et al. 2011; Stromberg 2011). C_4 grasslands become

the dominant grasslands by 6 Ma (Stromberg 2011). However, modern North American grasslands consist of both C₃ and C₄ grass types (Fredlund & Tieszen 1994) unlike modern African grasslands, which are dominantly C₄ vegetated.

2.3 Site Relevance

This study aims to augment the previous environmental data collected from East Africa during the early Miocene by adding new data for the fossil localities of Kalodirr and Moruorot, Kenya. This study analyzes stable carbon isotopes signatures of herbivorous mammals collected from Kalodirr and Moruorot. The isotopes from these herbivorous will be compared to modern vegetation and mammalian analogues to determine the likely C₃ and/or C₄ composition of their diets. These data will then be used to infer the likely habitats that these herbivorous mammals were living in, as a proxy for reconstructing the environments of Kalodirr and Moruorot. I hypothesize that $\delta^{13}\text{C}_{\text{enamel}}$ values recovered will indicate a more open environment than the other East African early Miocene sites, providing additional support that the forest canopies were opening before the middle Miocene.

Kalodirr and Moruorot are located further north than the other early Miocene sites of East Africa and are also slightly younger, dated to 17.5 to 16.8 Ma (Boschetto 1988). Due to their northern position and younger age, I have hypothesized more open environments. If forest canopies were opening progressively prior to the middle Miocene it would be logical that these younger sites that are further from the equator would be more open than the older sites that are closer to the equator. Additionally, the fauna from these sites suggest a different environmental niche. First, Kalodirr and Moruorot have an increased diversity of suids, which are represented by four species, with some taxa favouring more open environments (Bishop et al. 2010; Leakey et al. 2011). Three hominoids were also recovered from Kalodirr and Moruorot: *Simiolus enjiessi*, *Afropithecus turkanensis*, and *Turkanapithecus kalakolensis* (Leakey & Leakey 1986a, 1986b,

1987). The postcrania of these three hominoids suggest that they were arboreal quadrupeds (Rose et al. 1992; Rose 1994, 1997). This arboreal locomotion along with the frugivorous dentition of *Simiolus* and *Turkanapithecus* suggest forested habitats (Rose et al. 1992; Rose 1994, 1997; Kay & Ungar 1997; Leakey & Walker 1997; McCrossin & Benefit 1997; Ward 1997, 1998; Harrison 2002, 2010). However, the dentition of *Afropithecus*, namely the canines, incisors and premolars, suggests sclerocarp harvesting (Rossie & MacLachy 2013). Along with the thick enamel this dentition suggests feeding on hard fruits surrounded by a tough Pericarp and seeds or more abrasive materials, which are typically found in drier habitats (Rossie & MacLachy 2013). This more derived dentition may indicate a more open habitat for *Afropithecus* than the predicted closed canopy forests.

Chapter 3: Hypotheses and Predictions, Site Description, and Study Design.

This study used $\delta^{13}\text{C}$ of available mammalian tooth enamel collected from Kalodirr and Moruorot, Kenya in order to analyze the likely diets of these mammals, by comparing the recovered $\delta^{13}\text{C}_{\text{enamel}}$ values to modern plant and mammal analogues. This determined the likely C_3 and/or C_4 diets of these mammals, which can be extrapolated to predict the habitats of these mammals. This proxy is then used to determine the environments of Kalodirr and Moruorot, which was the primary objective of this study.

This study also maps the geology of these fossil localities in order to compare $\delta^{13}\text{C}_{\text{enamel}}$ signatures by stratigraphic level. The stratigraphy of both Moruorot and Kalodirr were recorded and compared to original sections provided by Boschetto (1988) who mapped the regional geology of the Lothidok Range. The fossils sampled for this summary were then mapped into their likely stratigraphic association using GPS waypoints. The two complete sections of Kalodirr and Moruorot that were mapped during the 2018 field season are provided in the Supplementary Information. These sections were compared to one another in the hopes of correlating the geology of the two sites and comparing $\delta^{13}\text{C}_{\text{enamel}}$ signatures over stratigraphic time. The stratigraphy was placed into two time bins, an upper and a lower, where the increased appearance of yellow tephra was the cutoff between both bins.

Ultimately, this work will add to the environmental history of East Africa and further address the hypothesis that the forest canopies were opening before the middle Miocene.

3.1 Site Description

3.1.1 *Geographic Setting and Alternative Names*

The Kalodirr and Moruorot fossil sites are located in the Lothidok Range of northern Kenya (Boschetto 1988; Boschetto et al. 1992). The Lothidok Range, halfway between Lake Turkana (formerly Lake Rudolf) and the town of Lodwar, is located in the Turkana Depression (Boschetto et al. 1992; Figure 2). The term ‘Lothidok’ refers to the entire range as well as the highest peak of the range (ie. Lothidok Hill). Previous work has used the spelling ‘Losodok’ or ‘Losidok’ to refer to the same area or hill (Boschetto 1988). The Lothidok Range is also labelled ‘Muruarot’ on the 1:250,000 Lodwar sheet, which is referenced in Boschetto (1988). Additionally, it is a late Oligocene fossil site known as Losodok or Lothidok (Madden 1972). ‘Lothidok’ will hereafter refer to the entire range and the geological formation named after it.

Kalodirr is located on the western slopes of the Lothidok Range near the headwaters of the Kalodirr River (3°20’ N, 35°45’ E) (Boschetto et al. 1992). The total area of Kalodirr extends from south of the Kalakol-Lodwar road to the northern portion of the Lokipenata Ridge (Boschetto et al. 1992).

Moruorot Hill is the second largest hill on the eastern edge of the Lothidok range, 11 km south of Lothidok Hill (Boschetto et al. 1992). The Moruorot fossil localities lie both on the northern and southern flanks of Moruorot Hill (3°17’ N, 35°50’ E) (Boschetto et al. 1992; Leakey et al. 2011). Previous spellings include ‘Murualet’ (Fuchs, 1939), ‘Muruarot’ (Walsh & Dodson 1969), and ‘Morualet’ and ‘Moruarot’ (Leakey & Leakey, 1986a). According to Boschetto (1988), this hill was also referred to as ‘Losodok’ by Arambourg (1943). It will hereafter be referred to as ‘Moruorot.’

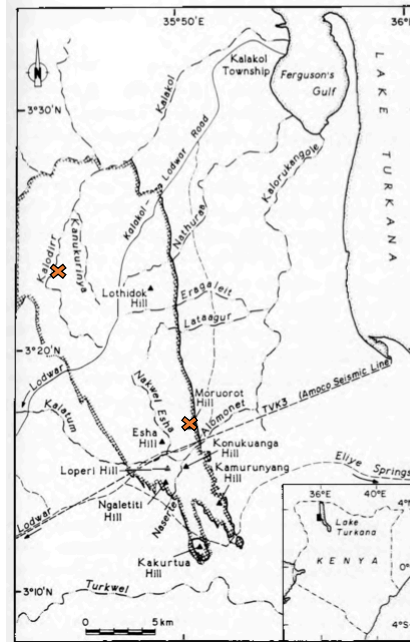


Figure 2: Map of the Lothidok Range, edited from Boschetto (1988). Kalodirr and Moruorot are labelled by the red 'X' shapes.

3.1.2 Geology

The Lothidok Formation is exposed across the Lothidok Range and is best represented along the southwestern portion of the region. Harold Boschetto (1988) mapped the detailed geology of this area, therefore the stratigraphic sections I collected for Kalodirr and Moruorot during the 2018 field season are compared to his stratigraphy. This Formation consists of all strata between the upper contact of the Kalakol basalts and the lower contact of the Loperi basalts (Boschetto 1988; Boschetto et al. 1992). It is informally divided into lower (Tll) and upper (Tlu) units (Boschetto 1988). The Kalodirr and Moruorot fossil sites are composed on Tll strata (Boschetto 1988).

The Tll consists of three formally defined members listed in depositional succession: the Moruorot Member (formerly the Basal Conglomerate Member), the Kalodirr Member (formerly the Kalodirr Tuff Member), and the Naserte Member (formerly the Naserte Tuffs), with an

informal fourth member, the Nakwel Esha beds (Boschetto 1988; Boschetto et al. 1992).

According to my stratigraphic sections Kalodirr and Moruorot are primarily composed of the Kalodirr Member, while other members make up a few smaller outcrops.

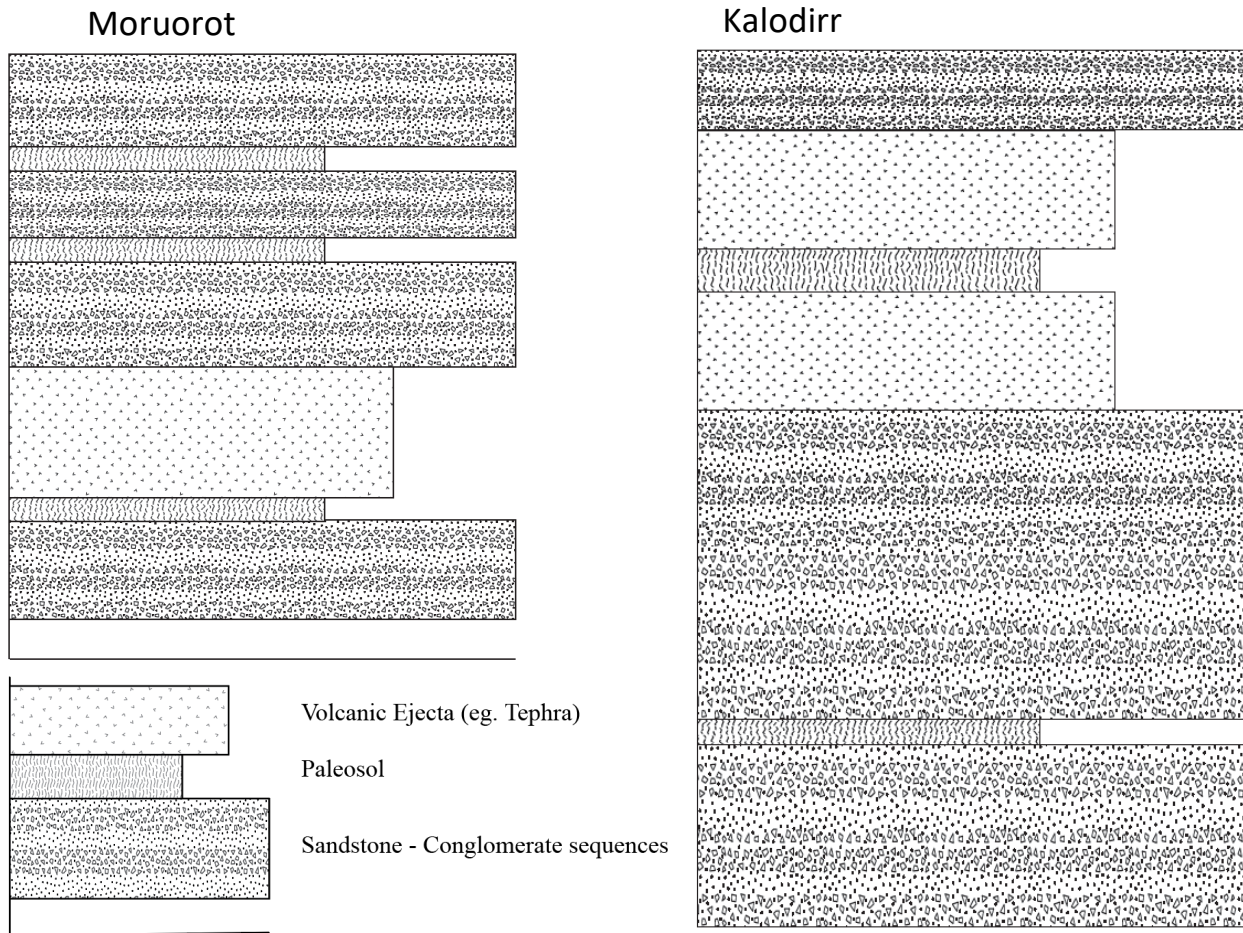


Figure 3: Simplified Stratigraphy of Kalodirr and Moruorot, Kenya.

Stratigraphic sections were collected across Moruorot and Kalodirr during the 2018 summer field season in hopes of placing the sampled fossils into stratigraphic association. My sections largely agree with Boschetto's (1988) summary of the TII members, mainly the Kalodirr Member, summarized in Figure 3. Strata are primarily composed of conglomerate-sandstone-

mudstone (CSM) associations, which fine upwards in section. In general, the conglomerates are clast-supported, with clasts that are volcanoclastic and subrounded. These conglomerates grade both vertically and laterally into poorly sorted, coarse-grained conglomeritic sandstones, leading into fine grained and rippled sandstones. These fine-grained sandstones progress vertically, but not horizontally, into siltstones and mudstones that are massive with raindrop impressions. These CSM associations resemble braided stream deposits, mapped according to the dominance of large clasts and coarse-grained matrix. The larger the clast and grain size, the higher the energy level of the stream. When analyzing the clasts in the conglomerates, you can map the flow direction of the stream by analyzing the direction of the longest axis of the clast. My observations led me to discern a primary paleoflow direction of NE-SW, similar to Boschetto (1988), with some minor flows in the N-S direction.

The fossils used in this study are from the Kalodirr Member at both Kalodirr and Moruorot. As described previously, fossils were placed into stratigraphic association based on GPS data and surrounding strata (Figure S1 and S2). Correlations between Kalodirr and Moruorot have proven difficult, as Kalodirr preserves more of the stratigraphy than Moruorot, therefore stratigraphic analysis could not confidently take place. The stratigraphy was placed into two-time bins, an upper and lower, where the increased presence of yellow tephra was the cutoff between the bins (Figure S1 and S2). A basic analysis of the stratigraphic differences in gomphothere diets took place to determine if there was a stratigraphic difference between the Kalodirr and Moruorot samples.

3.2 Materials

One of the primary methods used is the comparison of fossil morphologies to living representatives, which includes the analysis of crown structure, enamel thickness and hypsodonty.

The following section describes compiled data on the likely diets of the identified mammals recovered from Kalodirr and Moruorot based on morphology. Morphological terms used in the following section include (Janis 2008):

Bunodont: rounded, bumpy cusps. Designed to process non-brittle foods.

Lophodont: ridged type of molar where individual cusps are thrown into higher occlusal relief and run together as longitudinal or horizontal ridges. The individual ridges run in the labio-lingual direction and broaden the grinding surface. Designed to shred fibrous and or tough vegetation.

Selenodont: crescent shaped lophs that run in the antero-posterior direction, creating an elongated cutting surface. Designed to break up tough vegetation.

Brachyodont: short, low-crowned teeth. Designed for a browsing diet of leaves.

Hypsodont: tall, high-crowned teeth. Designed for a grazing diet of grasses.

Although morphology is an important indicator into behaviour and diet, it may be subject to Liem's Paradox, the occurrence when species with highly specialized morphology act as ecological generalists (Liem 1980). Along with morphology, diets are also determined using modern taxa from the same families. While this does help us to understand the behavior of extinct species, it is not always accurate. For example, it is unlikely that the modern species with low diversity, such as tragulids, giraffids, rhinocerotids and proboscideans, accurately represent the ecological diversity of the fossil forms. Therefore, other dietary analyses, including microwear and mesowear, are implemented. However, it is best to retrieve confirmation that dietary inferences made using morphologies are correct by using morphologically independent methods, such as isotopes.

Table 1: List of families analyzed from Kalodirr and Moruorot where “K” represents Kalodirr and “M” represents Moruorot.

Order	Family	Species	K	M
Artiodactyla	Sanitheriidae (n = 8)	<i>Diamantohyus africanus</i>	6	2
	Suidae (n = 9)	<i>Kenyasus rusingensis</i>	2	0
		<i>Libcochoerus jeanelli</i>	1	1
		<i>Namachoerus moruoroti</i>	4	1
	Anthracotheriidae (n = 7)	<i>Brachyodus aequatorialis</i>	3	0
		<i>Sivameryx africanus</i>	4	0
	Tragulidae (n = 11)	<i>Dorcatherium chappuisi</i>	7	0
		<i>Dorcatherium pigotti</i>	4	0
Giraffidae (n = 10)	<i>Canthumeryx sirtensis</i>	5	5	
Pecora (n = 2)	<i>Walangania africanus</i>	1	1	
Perrissodactyla	Rhinocerotidae (n = 11)	<i>Brachypotherium sp.</i>	1	0
		<i>Turkanatherium sp.</i>	0	1
		<i>Indet sp.</i>	6	3
Proboscidea	Deinotheriidae (n = 5)	<i>Prodeinotherium hobleyi</i>	2	3
	Gomphotheriidae (n = 21)	<i>Protanancus macinnesi</i>	2	0
		<i>Indet sp.</i>	11	10
Hyracoidea	Titanohyracidae (n = 9)	<i>Afrohyrax championi</i>	7	2
Total			66	29

3.2.1 Artiodactyla

Suidae/Sanitheriidae. The superfamily Suoidea encapsulates the families Suidae, Tayassuidae and Sanitheriidae (Bishop 2010). The taxonomy of Suoidea is complex, partially due to the rapid divergence of suoid lineages through time and space as well as a lack of consensus on

the relationship between sanitheres and suids (Bishop 2010). Due to this complexity sanithere and suid specimens will be analyzed together. The species *Namachoerus moruoroti*, *Diamantohyus africanus*, *Kenyasus rusingensis* and *Libycochoerus jeanelli* from Kalodirr and Moruorot are included in this study (Table 1). These four pigs can be divided into two types, small and lophodont (*Namachoerus moruoroti* and *Diamantohyus africanus*) and large and bunodont (*Kenyasus rusingensis* and *Libycochoerus jeanelli*; Bishop 2010). These diverse tooth morphologies suggest the incorporation of a broad range of dietary sources, such as leaves and grasses.

Anthracotheriidae. Anthracotheres are a group of suiform ungulates that differ primarily in size (ranging from a small dog to a hippopotamus), specializations of the anterior dentition, and the degree of brachydonty and selenodonty (i.e. crescent-shaped cusps; Lihoreau & Ducrocq 2007; Holroyd et al. 2010). Anthracotheres are also suggested to be generalist species with the ability to colonize many habitats (Lihoreau & Ducrocq 2007). The anthracotheres of Kalodirr and Moruorot are thought to be semi-aquatic, which may alter interpretations of diet if they were feeding on aquatic vegetation. As we do not know the values of the aquatic $\delta^{13}\text{C}$ that would be present in these environments, we consider them to be feeding on terrestrial vegetation. The species *Brachyodus aequatorialis* and *Sivameryx africanus* are found at Kalodirr and Moruorot (Table 1; Holroyd et al. 2010). Both *Brachyodus aequatorialis* and *Sivameryx africanus* have selenodont dentition with pentacuspitate upper molars where the mesostyle is invaded by the transverse valley (Lihoreau & Ducrocq 2007). This is a higher complexity in cheek tooth morphology than typically observed in modern browsers (Archer & Sanson 2002). Additionally, Rowan et al. (2015) described the morphology of a skull of *Sivameryx africanus* from Kalodirr, concluding that the cheek teeth showed advanced selenodonty and relatively short cusps. The combination of brachydont and selenodont molar patterns suggests a cutting diet, which would be effective on foods like the stems of leaves (Archer & Sanson 2002; Janis 2008; Holroyd et al.

2010; Rowan et al. 2015). Alternatively, the increased complexity of the molar patterns may indicate the incorporation of tough foods (Archer & Sanson 2002).

Tragulidae. All Miocene forms of tragulids are included in *Dorcatherium*, a genus that is described primarily from the Asian and European fossil records (Geraads 2010b). African specimens are known from isolated teeth and postcrania as well as a single skull, which makes taxonomic characterization difficult; therefore classifications occur largely based on size (Geraads 2010b). Two tragulid species were sampled, *Dorcatherium chappuisi* and *Dorcatherium pigotti* (Table 1). *Dorcatherium* has bunoselenodont (i.e the inner cusps are rounded and the outer ones are modified into crescents) upper molars (Barmann & Rossner 2011; Khan & Akhtar 2011). Modern tragulids forage from forest floors, feeding on fallen fruits and seeds, flowers, leaves, shoots and mushrooms (Barmann & Rossner 2011). The complex upper molar pattern of *Dorcatherium* could have allowed the utilization of a broad diet, though they are found primarily in rainforests and woodlands indicating a browsing diet (Geraads 2010b).

Giraffidae/Pecora. Pecora is one of two infraorders within Ruminantia and encompasses five modern families: Giraffidae, Bovidae, Moschidae, Antilocapridae, and Cervidae (Cote 2010). These sites preserve both stem pecorans and giraffids, which will be analyzed together. Within this group two species have been identified, *Walangania africanus* (stem pecoran) and *Canthumeryx sirtensis* (early giraffid; Table 1). Pecorans are characterized by selenodont cheek teeth (Archer & Sanson 2002; Janis 2008). The high relief of *Walangania* and *Canthumeryx* molar ridges suggests a diet of tough foods, either in the form of stems or grasses (Hamilton 1978; Archer & Sanson 2002; Cote 2010).

3.2.2 *Perissodactyla*

Rhinocerotidae. This study uses fragmentary teeth of rhinocerotids making it difficult to identify our samples beyond the family level, though there were likely multiple species present

(Table 1). However, two samples, KNM-WK-18391A and KNM-MO-43, have been identified as *Brachypotherium* and *Turkanatherium*, respectively (Table 1; Hooijer 1968; Geraads 2010a; Geraads 2013). The morphology of rhinocerotid cheek teeth differs between the upper and lower teeth. The upper teeth are shaped similarly to the symbol “ π ” with the exception of the M3, which is triangular (Geraads 2010a). The lower cheek teeth are low crowned with a V-shaped cross-section (Fortelius et al. 2003). The low crowns suggest a diet dominated by browse, however the complexity of occlusal pattern in the upper molars may provide an opportunity for mixed feeding (Janis 2008).

3.2.3 Proboscidea

Deinotheriidae. African Miocene fossil assemblages contain the genus *Prodeinotherium*, which are small deinotheres (Table 1) (Sanders et al. 2010). During the mid- to late Miocene the larger *Deinotherium* replaced these prodeinotheres (Sanders et al. 2010). In general, *Prodeinotherium* and *Deinotherium* are characterized by the retention of only the lower tusks and low-crowned, lophodont cheek teeth, which is characteristic of a specialized browsing diet (Sanders et al. 2010).

Gomphotheriidae. Gomphotheres originated in the late Oligocene of East Africa and underwent a series of adaptive radiations during the Miocene, persisting into the Pliocene (Sanders et al. 2010). Gomphotheres are characterized by the enlargement and differentiation of tusk forms and the increase in size and elaboration of molars through the addition of lophids, cementum and accessory central conules (Sanders et al. 2010). Two of our specimens were identified as *Protanancus macinnesi* while the remaining 19 specimens could not be identified beyond the family level (Table 1; Sanders et al. 2010). The molars of earlier gomphotheres have low crowned teeth with rounded cusps that may or may not be oriented into transverse ridges. This morphology is interpreted as a browsing adaptation (Janis 2008; Sanders et al. 2010).

3.2.4 Hyracoidea

Titanohyracidae. The African Paleogene fossil record has a high diversity of hyracoids (with large to small statures; Rasmussen & Guitierrez 2010). Morphology is also diverse in this order, ranging from bunodont molars to lophoselenodont (Rasmussen & Guitierrez 2010).

Titanohyracids are medium to large hyracoids characterized by highly lophoselenodont cheek teeth, specialized lower incisors, and a cursorial postcranium (Rasmussen & Guitierrez 2010).

Afrohyrax championi is the only hyracoid species found at Kalodirr and Moruorot (Table 1). This species is described as a potentially open country animal with dietary specializations that indicate a degree of folivory (Rasmussen & Guitierrez 2010). The cursorial postcranium indicates that *Afrohyrax championi* could have been utilizing vegetation from more open habitats.

3.3 $\delta^{13}\text{C}$ Isotope Concepts

3.3.1 Plants

There are three photosynthetic pathways: The Calvin cycle (C_3), the Hatch-Slack cycle (C_4) and the Crassulacean acid metabolism cycle (CAM) (Michene & Lajtha 2008). These photosynthetic pathways are successful in environments with differing degrees of openness and amounts of humidity (Cerling & Harris 1999; Cerling et al. 2003; Uno et al. 2011). As terrestrial plants intake atmospheric CO_2 to perform photosynthesis they discriminate against the heavier ^{13}C in favour of ^{12}C , causing the plant to be depleted in ^{13}C relative to the surrounding atmosphere (Park & Epstein 1960, 1961). These photosynthetic cycles utilize different physiologies, which determines the $\delta^{13}\text{C}$ values of the plant. $\delta^{13}\text{C}$ values are expressed in “permil (‰)” notation, meaning per thousand, and are measured against the universal standard for carbon, the Vienna Pee Dee Belemnite (VPDB). Most plants have less ^{13}C than this standard making their values negative.

Plants utilizing the C_3 cycle have the highest discrimination rates of the photosynthetic pathways (Michene & Lajtha 2008). Deines (1980) display the ranges of C_3 and C_4 vegetation, showing the offset between the photosynthetic pathways. This graph describes the C_3 range of known plants, ranging between -23 ‰ to -33 ‰ (Deines 1980), with an average value of -26.5 ‰ (Farquhar et al. 1989). However, further work in the Amazon rain forests (van der Merwe & Medina 1989) and the Ituri Forest (Cerling et al. 2004) has extended this range, demonstrating that C_3 vegetation can be as depleted as -36 ‰. C_3 plant carbon signatures are highly influenced by environmental factors, with the most negative values found in closed canopy forests (Deines 1980; van der Merwe & Medina 1989; Cerling & Harris 1999; Cerling et al. 2004; Kohn 2010). C_3 vegetation with a value of -23‰, the absolute maximum for C_3 values, is restricted to areas with a mean annual precipitation (MAP) of less than 10mm per year (Kohn 2010). Kohn (2010) also suggest that C_3 vegetation with values below -31.5‰ are only found in the understories of dense closed-canopy forests, including the Amazon and the Ituri Forest (Congo).

The C_4 photosynthetic pathway utilizes the same enzymes as the C_3 pathway as well as a secondary enzyme that decreases the discrimination rate (Deines 1980). Therefore, C_4 plants are more enriched in ^{13}C than C_3 plants with a $\delta^{13}C$ range of -14‰ to -9‰ (Deines 1980), with an average of -13 ‰ (Farquhar et al. 1989).

The CAM pathway is represented by plants that are in arid ecosystems and are less common than the other two pathways with $\delta^{13}C$ values that fall between the C_3 and C_4 signals (Deines 1980; van der Merwe 1989; Michene & Lajtha 2008). It is possible that the mammals that are classified as mixed feeders could be CAM specialists, though CAM plants are not widely consumed by extant herbivores in East Africa (Uno et al. 2011) and are therefore not considered further in this study.

3.3.2 Mammalian Tooth Enamel

During tooth formation, carbon derived from diet is incorporated into enamel as carbonate anions (DeNiro & Epstein 1976; Lee-Thorp & van der Merwe 1987; Cerling & Harris 1999). The difference between the stable isotope ratios of diet ($\delta^{13}\text{C}_{\text{diet}}$) and enamel ($\delta^{13}\text{C}_{\text{enamel}}$) is expressed as an apparent fractionation factor (α^*) where (Cerling & Harris 1999):

$$\alpha^*_{\text{enamel-diet}} = (1000 + \delta^{13}\text{C}_{\text{enamel}}) / (\delta^{13}\text{C}_{\text{diet}} + 1000)$$

This can then be calculated as an enrichment or discrimination factor (ϵ^*) where (Cerling & Harris 1999):

$$\epsilon^* = (\alpha^* - 1)$$

This enrichment value allows $\delta^{13}\text{C}_{\text{enamel}}$ to be compared to $\delta^{13}\text{C}_{\text{diet}}$ values, which is synonymous with $\delta^{13}\text{C}_{\text{plant}}$ values and used to obtain information on diet (Deines 1980; Cerling & Harris 1999; Cerling et al 2003; Cerling et al. 2013). Within mammals, $\delta^{13}\text{C}_{\text{enamel}}$ has an isotope enrichment factor ranging from -9‰ to -14‰ when compared to $\delta^{13}\text{C}_{\text{diet}}$, with mice having a value of -9‰ and primates and ungulates having a value of -14.1‰ (Cerling & Harris 1999; Cerling et al 2003).

While this study considers the fractionation rate of our mammals to be 14.1 ‰ (Cerling & Harris 1999), this value may not represent the dietary values of all mammals. As carbon must transfer through the digestion system of the mammals in order to be incorporated into their tooth enamel, there is likely a difference between ruminating foregut fermenters (eg. giraffids, tragulids) and non-ruminating hindgut fermenters (eg. proboscideans, suids). The diet-enamel fractionation value originally proposed by Cerling & Harris (1999) was determined using ruminating foregut fermenters. Cerling & Harris (1999) hypothesized a similar fractionation rate in non-ruminants with a change of + 1 ‰. Modern studies have begun to further investigate the fractionation differences between ruminants and non-ruminants. Hedges & Van Klinken (2002)

introduce a conceptual model, which includes isotopic discrimination between methanogenesis (process utilized during rumination), rates of digestion, and metabolic fluxes. They predict body isotopic composition through mathematical modeling, showing that due to the digestive physiologies of ruminants they tend to have larger bioapatite spacing than non-ruminating mammals (Hedges & Van Klinken 2002). This was verified by Passey et al. (2004), who tested the carbon isotope fractionation of voles, rabbits, pigs and cattle. They determined that the largest measured fractionation (expressed as isotope enrichment) between enamel and diet was for cattle ($14.6 \pm 0.3 \text{‰}$), while the pigs had a rate of $13.3 \pm 0.3 \text{‰}$ (Passey et al. 2004). These data indicate that there are differences in fractionation based on digestion. However, these offsets are not large and still preliminary. This study recognizes that $\pm 14.1 \text{‰}$ is the measured value of modern ruminants (Cerling & Harris 1999) and there may be variation among the mammals that are sampled by this study. However, this fractionation value is still widely used in African isotopic studies and will be used in this study.

3.3.3 Mammalian Diet

The system that ^{13}C travels through must be considered when measuring the $\delta^{13}\text{C}$ values of C_3 and C_4 diets of herbivorous mammals. The first facet is vegetation and the influence that atmospheric carbon has on the $\delta^{13}\text{C}$ values of this vegetation. Atmospheric CO_2 is taken into the cells of plants in order to perform photosynthesis. The $\delta^{13}\text{C}$ value of atmospheric CO_2 ($\delta^{13}\text{C}_{\text{atm}}$) has changed since prehistoric times. The current $\delta^{13}\text{C}_{\text{atm}}$ value is approximately -8.2‰ but has fluctuated between -6.8 to -4.9‰ over the last 20 Ma (Tippie & Pagani 2010). The $\delta^{13}\text{C}_{\text{atm}}$ values calculated between 17.5 to 16.8 Ma are: $-6.207 \text{‰} \pm 0.055$ (upper 90% CI) and $-4.997 \text{‰} \pm 0.055$ (lower 90% CI). They are then used to adjust modern plant values to indicate the change in atmospheric CO_2 . These calculations follow the Supplementary Information descriptions found in

Uno et al. (2011) and are found in the Supplementary Information section (Table S1). Due to the alteration of $\delta^{13}\text{C}_{\text{atm}}$ the $\delta^{13}\text{C}$ values of plants must be adjusted to account for atmospheric change.

$\delta^{13}\text{C}$ values of modern C_3 and C_4 plants were adjusted for atmospheric change in order to represent vegetation at 17.5 to 16.8 Ma, following calculations by Uno et al. (2011; Table 2).

These values are used to represent a standard and conservative model for C_3 and C_4 vegetation and diets during this time period. The standard model uses the average value for C_3 and C_4 plants and is used in many East African studies, especially after the late Miocene and Pliocene (eg. Lee-Thorp et al. 1989; Quade et al. 1992; Bocherens et al. 1996; Macfadden & Cerling 1996; Harris & Cerling 2002; Sponheimer et al. 2003; Kingston & Harrison 2007; Cerling et al. 2011). However, due to the Miocene age of these fossil localities they are considered to be C_3 dominated and may have included more enriched C_3 vegetation than is observed today. Therefore, this conservative model was introduced to expand the range of potential C_3 vegetation by using the maximum $\delta^{13}\text{C}$ of C_3 plants observed in East Africa today, which were collected from a savannah in Mpala Kenya (Cerling et al. 2003). These plant values were then altered into enamel values in order to compare them to the recovered $\delta^{13}\text{C}_{\text{enamel}}$ values from the specimens analyzed in this study, by applying a fractionation factor of 14.1 ‰.

Table 2: Conversions accounting for change in $\delta^{13}\text{C}_{\text{atm}}$ from modern values to 17.5 - 16.8 Ma and its effect on plant and enamel $\delta^{13}\text{C}$ values for standard and conservative models.

	ATMOSPHERIC VALUES		PLANT VALUES				ENAMEL VALUES			
Dietary Models	$\delta^{13}\text{C}_{\text{atm}}$ C ₃ plants (‰)	$\delta^{13}\text{C}_{\text{atm}}$ C ₄ plants (‰)	$\delta^{13}\text{C}$ Average C ₃ plants (‰)	$\delta^{13}\text{C}$ Max C ₃ plants (‰)	$\delta^{13}\text{C}$ Average C ₄ plants (‰)	$\delta^{13}\text{C}$ Min C ₄ plants (‰)	$\delta^{13}\text{C}$ Average C ₃ enamel (‰)	$\delta^{13}\text{C}$ Max C ₃ enamel (‰)	$\delta^{13}\text{C}$ Average C ₄ enamel (‰)	$\delta^{13}\text{C}$ Min C ₄ enamel (‰)
Modern Values	-8.2	-8.2	-27.3	-24.6	-12.8	-14.4	-13.2	-10.5	0.3	-0.3
Standard Model	-5.603	-6.207	-24.097		-10.807		-9.997		3.293	
Conservative Model	-5.603	-6.207		-21.397		-12.407		-7.297		1.693

3.4 Methods

3.4.1 Sampling Protocol

Teeth were hand inspected for any signs of weathering (i.e. discolouration) and were not sampled if determined to be unsuitable. Sampling was also conducted along fractured surfaces in order to distinguish enamel from dentin, cementum, and matrix. Surfaces of suitable teeth were cleaned with water to remove any matrix and dried. Once dried, the outer layer of the enamel was removed using a high-speed rotary drill paired with a diamond tipped bur and discarded. A new diamond bur was then fitted to the drill, and sampling was done along fractured surfaces. After each use the drill bur was cleaned using acetone followed by water and dried. Enamel was collected as powder onto weighing papers and placed into micro-centrifuge tubes.

3.4.2 Sample Analysis

All samples were sent to the University of Florida for isotopic analysis, conducted by Dr. Jason Curtis. A Finnigan-MAT 252 isotope mass spectrometer coupled with a Kiel III carbonate

preparation device was used for analysis, which had a precision of 0.02074981 for carbon. The Kiel III carbonate preparation device uses an individual acid bath set to 70°C to allow the appropriate reaction between the acid and carbonate to occur (Mucciarone 2003). Approximately 600 micrograms of enamel sample were loaded into glass jars (Curtis, personal communication). These samples are acidified with two drops of purified phosphoric acid and left to react for 470 seconds (Mucciarone 2003). At the end of this reaction time, non-condensable gases are pumped away for 30 seconds (Mucciarone 2003). A two-trap system is then initiated in order to create and isolate the CO₂ gas from the reaction and transfer it to the changeover valve (Mucciarone 2003). Attached to the other side of this changeover valve is the mass spectrometer inlet system. This inlet system is composed of a symmetrical system of valves composed of a reference and sample side, where the valve volume and configuration are identical on both sides (Mucciarone 2003). A reference CO₂ gas is placed into the reference side of the inlet system for comparison with the sample gas from the carbonate device (Mucciarone 2003). The 30 to 50 micrograms of standard (NBS-19: TS limestone) were loaded (Mucciarone 2003; Curtis, personal communication). In order to obtain useful isotopic data, it is necessary to balance the pressure and volume between the reference and sample gasses (Mucciarone 2003). Gas from the inlet system (reference side) and the carbonate device flow through changeover valves into the ion source (Mucciarone 2003). In this ion source, the gas molecules are ionized by colliding with an electron beam (Mucciarone 2003). This allows them to be focused into a beam and directed through a flight tube into the analyzer zone. These beams are separated into different ion beams (based on mass) and directed into Faraday cup collectors (Mucciarone 2003). The signals received by the collectors are amplified and transferred to voltage to frequency converters (VFC) on a system control board in a microprocessor, which analyzes these signals and displays them on an interfaced computer (Mucciarone 2003). This data is expressed in the conventional delta (δ) notation, where the $\delta^{13}\text{C}/\delta^{12}\text{C}$ are compared to the international PDB standard defined by:

$$\delta (\text{‰}) = [(\text{Ratio}_{\text{sample}} - \text{Ratio}_{\text{standard}})/(\text{Ratio}_{\text{standard}})] \times 1000$$

PDB refers to a Cretaceous belemnite called *Belemnitella americana* from the Pee Dee Formation in South Carolina, though its supply has been exhausted. The carbonate standard NBS-19 is the current substitute for PDB.

3.4.3 Dietary Calculations

Recently, East African isotopic work on mammalian diets has set isotopic values to definitions used to describe modern observable diets. This serves as an extension of early analysis of consumer tissues, which describe browsers (C_3 - based), grazers (C_4 - based) and mixed feeders (Vogel 1978; DeNiro & Epstein 1978; Lee-Thorp 1989; Cerling & Harris 1999). These definitions include: hyperbrowsers (100% C_3), browsers ($\geq 75\%$ C_3), mixed feeders with intermediate diets, grazers ($\geq 75\%$ C_4), and hypergrazers (100% C_4) (Cerling et al. 2003; Cerling et al. 2015). Using an isotopic mixing model, Cerling et al. (2003) analyzed the enamel of modern mammals across East Africa to set dietary definitions to isotopic values. Cerling et al. (2003) indicate that dietary definitions of mammals can be paired with isotopic values in modern East Africa due to the separation of C_3 and C_4 vegetation between habitats. The partitioning of East African environments indicates that closed forest environments are strictly C_3 vegetation and open environments are strictly C_4 vegetation (Cerling et al. 2003; Cerling et al. 2011). For example, while in modern North America grazers have mixed isotopic signals as grasslands are composed of a mixture of C_3 and C_4 grasses (Fredlund & Tieszen 1994), modern African grasslands are strictly composed of C_4 grasses (Tieszen et al. 1979) giving a pure C_4 isotopic signal. Intermediate environments such as open forests, woodlands and wooded grasslands follow a continuum of C_3 and C_4 proportions (Cerling et al. 2011). This isotopic model of dietary types is

applied in both modern and Pliocene mammal studies in East Africa as this partitioning of C₃ and C₄ vegetation between environments has likely remained stable for the last 5 Ma.

However, environments of the early Miocene were likely less clear-cut, incorporating a higher proportion of C₃ open environment vegetation. For example, while today C₃ grasses of modern Africa are restricted to elevations of 2,500 m and above (Tieszen et al. 1979), they may have existed in low elevation environments during the early Miocene. This likely parallels the North American fossil record, where C₃ grasses were first developed in closed environments and became a primary component on the landscape once the forest canopies opened (Retallack 1997; Retallack 2007; Osborne & Freckleton 2009; Edwards & Smith 2010; Stromberg 2003; 2004; 2011). The presence of C₃ grasses could cause a C₃ grazer to be misidentified as a browser; therefore, the dietary definitions set by Cerling et al. (2003; 2015) are unsuitable for this epoch. Rather, I suggest replacing these terms with ones that are more indicative of the isotopic signals rather than dietary types. The thresholds of these terms will use the same ranges outlined by Cerling et al. (2015) without specifying grazing or browsing diets:

Pure C₄ Feeder = 100% C₄

C₄ Dominated Feeder = 100% to 75% C₄; 0 to 25% C₃

C₃-C₄ Mixed Feeder = 75% to 25% C₄; 75% to 25% C₃

C₃ Dominated Feeder = 100% to 75% C₃; 0 to 25% C₄

Pure C₃ Feeder = 100% C₃

The constraints for these diets are calculated using an isotopic mixing model (Cerling et al. 2015):

$$\delta^{13}\text{C}_{\text{enamel}} = f_{\text{C}_3} \delta^{13}\text{C}_{\text{C}_3} + f_{\text{C}_4} \delta^{13}\text{C}_{\text{C}_4}$$

Where:

$\delta^{13}\text{C}_{\text{enamel}}$ is the value of the measured tooth enamel

f_{C_3} is the fraction of C_3 biomass incorporated into the tooth enamel

$\delta^{13}\text{C}_{\text{C}_3}$ is the value of the C_3 biomass end-member

f_{C_4} is the fraction of C_4 biomass incorporated into the tooth enamel

$\delta^{13}\text{C}_{\text{C}_4}$ is the value of the C_4 biomass end-member

This study uses both a conservative dietary model and a standard dietary model for C_3 and C_4 inputs. These two models are calculated in order to demonstrate the standard predictions for diet types, which are used in modern and Pliocene studies, as well as the largest possible range of pure C_3 that may have been present during the early Miocene. The standard model uses the average values of modern C_3 and C_4 plants. This model is more accurate when comparing it to modern environments and used in many studies, especially after late Miocene and the Pliocene (eg. Lee-Thorp et al. 1989; Quade et al. 1992; Bocherens et al. 1996; Macfadden & Cerling 1996; Harris & Cerling 2002; Sponheimer et al. 2003; Kingston & Harrison 2007; Cerling et al. 2011). The conservative model indicates the maximum range of C_3 vegetation in these environments. Therefore, any indications of C_4 under this model will further support the hypothesis that C_4 was present in the landscape. The comparison of these models will demonstrate the potential diets of these specimens and how the parameters set for these calculations may change dietary interpretations.

The conservative values will indicate the largest dietary range of C_3 . Using the mixing model outlined above, $\delta^{13}\text{C}_{\text{C}_3} = -7.30 \text{‰}$ and $\delta^{13}\text{C}_{\text{C}_4} = 1.69 \text{‰}$. The conservative dietary definitions were calculated to be:

Pure C_4 Feeder = $\geq 1.69 \text{‰}$

C_4 Dominated Feeder = -0.55‰ to 1.69‰

C_3 - C_4 Mixed Feeder = -5.05 ‰ to -0.55 ‰

C_3 Dominated Feeder = -7.30 ‰ to -5.05 ‰

Pure C_3 Feeder = \leq -7.30 ‰

The standard values will indicate the standard dietary range of C_3 and C_4 vegetation. Using the mixing model outlined above, $\delta^{13}C_{C_3} = -10.00$ ‰ and $\delta^{13}C_{C_4} = 3.29$ ‰. The standard dietary definitions were calculated to be:

Pure C_4 Feeder = ≥ 3.29 ‰

C_4 Dominated Feeder = -0.03 ‰ to 3.29 ‰

C_3 - C_4 Mixed Feeder = -6.67 ‰ to -0.03 ‰

C_3 Dominated Feeder = -10.00 ‰ to -6.67 ‰

Pure C_3 Feeder = \leq -10.00 ‰

3.4.4 Habitat Reconstructions using Dietary Isotopes

$\delta^{13}C$ values derived from mammalian tooth enamel are used not only to reconstruct diet, but can also be used to infer the habitats of these mammals and the environments of these fossil sites in general (eg. Cerling et al. 1997a). This is a second order inference, as $\delta^{13}C$ signals are used to determine the vegetation that these mammals incorporated into their diets, which is further extrapolated to interpreting habitats and environments. The environments used by this study were based on definitions set by the United Nations Educational and Cultural Organization (White 1982) and a woody cover continuum developed by Cerling et al. (2011). This continuum was developed using ‘paleo-shade’ proxies, including woody cover measurements and $\delta^{13}C$ from soil organic matter (SOM) collected from modern environments (Cerling et al. 2011). They

indicate a relationship between the $\delta^{13}\text{C}$ of the soils reflects the amount of woody cover and use this relationship to classify environments (Cerling et al. 2011). This allowed them to create a woody cover continuum for the principal environments, which include (White 1982; Cerling et al. 2011):

Forest: continuous stand of trees at least 10m tall with interlocking crowns, with woody cover of >80%.

Woodland: open stand of trees at least 8m tall with woody cover of 40% or more, and grasses dominating the lower field layer.

Wooded grassland: land covered with grasses and other herbs, with woody plants covering between 10 and 40%.

Grasslands: land covered with grasses and other herbs with < 10% woody cover.

Environmental analogues were then set using $\delta^{13}\text{C}$ values of modern vegetation. This study uses $\delta^{13}\text{C}$ values of plants collected from environments in East Africa by Cerling et al. (2003; 2011). These $\delta^{13}\text{C}$ values were adjusted to account for the change in atmospheric CO_2 and plant-enamel fractionation and were used as environmental analogues (Table 3).

Table 3: Calculated environmental analogues using plant values collected from Cerling et al. (2003, 2011). $\delta^{13}\text{C}$ values are adjusted to account for atmospheric change.

Environment	Percent wood cover (%)	$\delta^{13}\text{C}_{\text{enamel}}$ Range (‰)
Forest	100 - 80	< -11.1
Woodland	80 - 40	-11.1 to -6.9
Wooded Grassland	40 - 10	-6.9 to -4.9
Grassland	10 - 0	> -4.9

$\delta^{13}\text{C}$ of mammalian enamel can then be compared to these values to aid in the identification of habitat. While mammalian tooth enamel is still used it does have limitations. These mammals may have been selectively feeding, sampling only a portion of the vegetation

available across the landscape. Alternatively, they may have been sampling a wide range of vegetation. For example, they may have been grazing on C₄ vegetation while foraging on fruits from a closed canopy. This would confuse the signals indicating a mixed feeder from an intermediate environment, such as a woodland.

3.5 Hypotheses and Predictions

1. $\delta^{13}\text{C}_{\text{enamel}}$ values will fall between -14 ‰ to -6 ‰, similar to the values from other East African early Miocene fossil sites. A higher proportion of values will fall on the more enriched end of this range, reflecting a slightly more open environment than these other sites.
 - a. This is because Kalodirr and Moruorot are younger and more northern than these other sites. If the forest canopies were opening progressively during the early Miocene, Kalodirr and Moruorot should reflect this change.
2. $\delta^{13}\text{C}_{\text{enamel}}$ values will reflect either highly enriched C₃ diets or diets with low proportions of C₄. This will reflect the opening of the forest canopies and the decreased availability of dense canopy browse.
3. Isotopic signatures will vary between the mammalian families.
 - a. The deinotheres, giraffids and pecorans will have the lowest $\delta^{13}\text{C}_{\text{enamel}}$ values, reflecting diets of C₃ sources from more enclosed environments.
 - i. Deinotheres have heavily specialized “shearing browser” diet (Harris 1975). Additionally, they disappear from the fossil record in the open environments of the Pliocene (Harris 1975).
 - ii. Giraffids and pecoran molars and tooth row angles are typically described as similar to browsing bovids (Archer & Sanson 2002; Solounias 2007).

- b. The suids, sanitheres and anthracotheres will have a wide range of $\delta^{13}\text{C}_{\text{enamel}}$ values, due to their capability to incorporate different types of vegetation. This is due to the generalized dentition and diversity of suids and the increased molar complexity of the anthracotheres (Archer & Sanson 2002; Lihoreau & Ducrocq 2007; Bishop 2010). These families are also known to have broad and diversified diets (Lihoreau & Ducrocq 2007; Uno et al. 2011).
 - c. The tragulids, rhinocertids, gomphotheres, and hyraxes will have browsing diets composed of more enriched C_3 components.
 - i. The molars of the rhinocerotids and gomphotheres suggest a browsing diet while later fossil sites indicate enriched C_3 (Cerling et al. 1997; Geraads 2010a; Janis 2008; Uno et al. 2011).
 - ii. While modern tragulids are known to be highly selective browsers, focusing on fruits (Rossner 2007), the combination of complex upper molars and the bunodont lower molars of *Dorcatherium* suggests the ability to feed on multiple vegetation sources (Barmann & Rossner 2011; Khan & Akhtar 2011).
 - iii. While hyraxes have lophoselenodont tooth morphology indicating a folivorous diet, their postcrania has been described as cursorial (Rasmussen & Guitierrez 2010). This would indicate a folivorous diet of more enriched sources.
 - d. Families represented by multiple species will show dietary partitioning between species. These families include the suids/sanitheres, the giraffids/pecorans, the tragulids, and the anthracotheres.
4. There will be a stratigraphic difference in $\delta^{13}\text{C}_{\text{enamel}}$ values, indicating dietary change. This will reflect environmental change through time.

- a. Specimens will be sorted into and compared using two-time bins, an upper and a lower, based on stratigraphic position and compared by family. Specimens in the lower time bin will be more depleted in ^{13}C than the upper time bin.

Chapter 4: Results and Discussion

4.1 Results

4.1.1 Kalodirr and Moruorot Isotope Ranges

The total range of $\delta^{13}\text{C}_{\text{enamel}}$ values for all sampled teeth is -11.91 ‰ to -6.01 ‰. Table 4 summarizes the total range of the isotopes for each family.

Table 4: $\delta^{13}\text{C}_{\text{enamel}}$ ranges and median values retrieved from the mammalian families retrieved from both Kalodirr and Moruorot.

Family	Median (‰)	Min (‰)	Max (‰)
Suidae/Sanitheriidae (n = 17)	-9.84	-10.99	-8.58
Giraffidae/ Pecora (n = 12)	-8.93	-11.00	-7.67
Tragulidae (n = 11)	-8.90	-10.22	-7.51
Rhinocerotidae (n = 11)	-9.86	-11.91	-7.78
Gomphotheriidae (n = 23)	-9.65	-11.05	-6.01
Deinotheriidae (n = 5)	-10.23	-11.18	-9.11
Anthracotheriidae (n = 7)	-9.77	-10.80	-6.77
Titanohyracidae (n = 9)	-10.10	-10.88	-9.57

A Shapiro-Wilk normality test (Shapiro & Wilk 1965) demonstrates that the distribution of $\delta^{13}\text{C}$ enamel values is not normal ($W = 0.96805$, $p\text{-value} = 0.02011$). Due to the non-normal nature of the data, Mann-Whitney U tests were used to test for differences in the median values between families (Table 5). The majority of family-level comparisons indicated a non-significant difference. The giraffids/small pecorans, hyraxes and suids are significantly different from two out of seven families. The giraffids/small pecorans and hyraxes generally had a more enriched median value relative to the other families. The suids were found to be significantly different

from the giraffids/small pecorans and the tragulids and had a median that was comparatively depleted in ^{13}C relative to these families. The tragulids are significantly different from 5 out of 7 families with a median value that is more enriched than the other families. In general, the tragulids are more enriched than the other families indicating a difference in potential dietary sources.

Table 5: Results of comparative Mann-Whitney U tests of $\delta^{13}\text{C}$ enamel values between families from both Kalodirr and Moruorot. Cells with significant values are highlighted in light grey.

Families	Suidae/ Sanitheriidae	Giraffidae/ Pecora	Tragulidae	Rhinocerotidae	Gomphotheriidae	Deinotheriidae	Anthracotheriidae	Titanohyracidae
Suidae/ Sanitheriidae								
Giraffidae/ Pecora	W=156.5 p-value = 0.01677							
Tragulidae	W=35 p-value = 0.004909	W=55.5 p-value = 0.5381						
Rhinocerotidae	W=97 p-value = 0.8878	W=97 p-value = 0.06037	W=27 p-value = 0.03019					
Gomphotheriidae	W=237 p-value = 0.2653	W=176.5 p-value = 0.1866	W=73 p-value = 0.04998	W=144 p-value = 0.5314				
Deinotheriidae	W=56 p-value = 0.3193	W=52 p-value = 0.02335	W=50 p-value = 0.0087	W=37 p-value = 0.3065	W=84 p-value = 0.1214			
Anthracotheriidae	W=70 p-value = 0.5342	W=32 p-value = 0.4218	W=24 p-value = 0.3434	W=43 p-value = 0.717	W=75.5 p-value = 0.8253	W=24 p-value = 0.3434		
Titanohyracidae	W=99 p-value = 0.2356	W=93 p-value = 0.006134	W=11.5 p-value = 0.004356	W=63 p-value = 0.323	W=150.5 p-value = 0.05126	W=28.5 p-value = 0.4624	W=39 p-value = 0.4584	

$\delta^{13}\text{C}$ enamel values were compared using a Mann-Whitney U test in order to compare the data between families that were found at both Kalodirr and Moruorot. The anthracotheres and the tragulids were excluded as they were only recovered from Kalodirr. The first Mann-Whitney U test indicated that there is not a significant difference between the total $\delta^{13}\text{C}$ enamel values of Kalodirr and Moruorot ($W=1196.5$, $p\text{-value}=0.0534$; Table 6), although it approaches significance. This suggests that the families at Kalodirr and Moruorot may have been digesting slightly different vegetation from one another.

Table 6: Results of Mann-Whitney U tests comparing families found from both Kalodirr and Moruorot.

Family	Sample Size	W	P
Suidae/Sanitheriidae	16	38	0.2017
Giraffidae/Pecora	10	15.5	0.7483
Rhinocerotidae	11	15	0.9245
Gomphotheriidae	21	100	0.03033
Deinotheriidae	5	1	0.4
Titanohyracidae	9	14	0.05601
All Values	72	1196.5	0.0534

The results of the tests between the specific families of each site are shown on Table 5. While only the gomphotheres show significantly different values between Kalodirr and Moruorot ($W=15.5$, $p\text{-value}=0.03033$), the hyrax values are also close to significance ($W=14$, $P=0.05601$). Unfortunately, the hyraxes could not be analyzed stratigraphically as they were collected from areas in Kalodirr that was unmapped during the 2018 field season. However, the gomphotheres were placed into stratigraphic context. They were divided into two time bins, upper ($n=7$) and lower ($n=13$). When analyzed they were determined to have an insignificant stratigraphic difference ($W=59$, $p\text{-value}=0.3114$). This indicates a dietary difference between the gomphotheres of Kalodirr and Moruorot rather than a dietary difference through time.

4.1.2 C₃ vs C₄ Diets

4.1.2.1 Conservative dietary model

Under the conservative dietary model, the majority of our specimens are defined as pure C₃ feeders, incorporating only C₃ sources into their diets. (Figure 4). The percentages of C₃ and C₄ consumption and dietary classification for each specimen are found on Table S3 in the Supplementary Information.

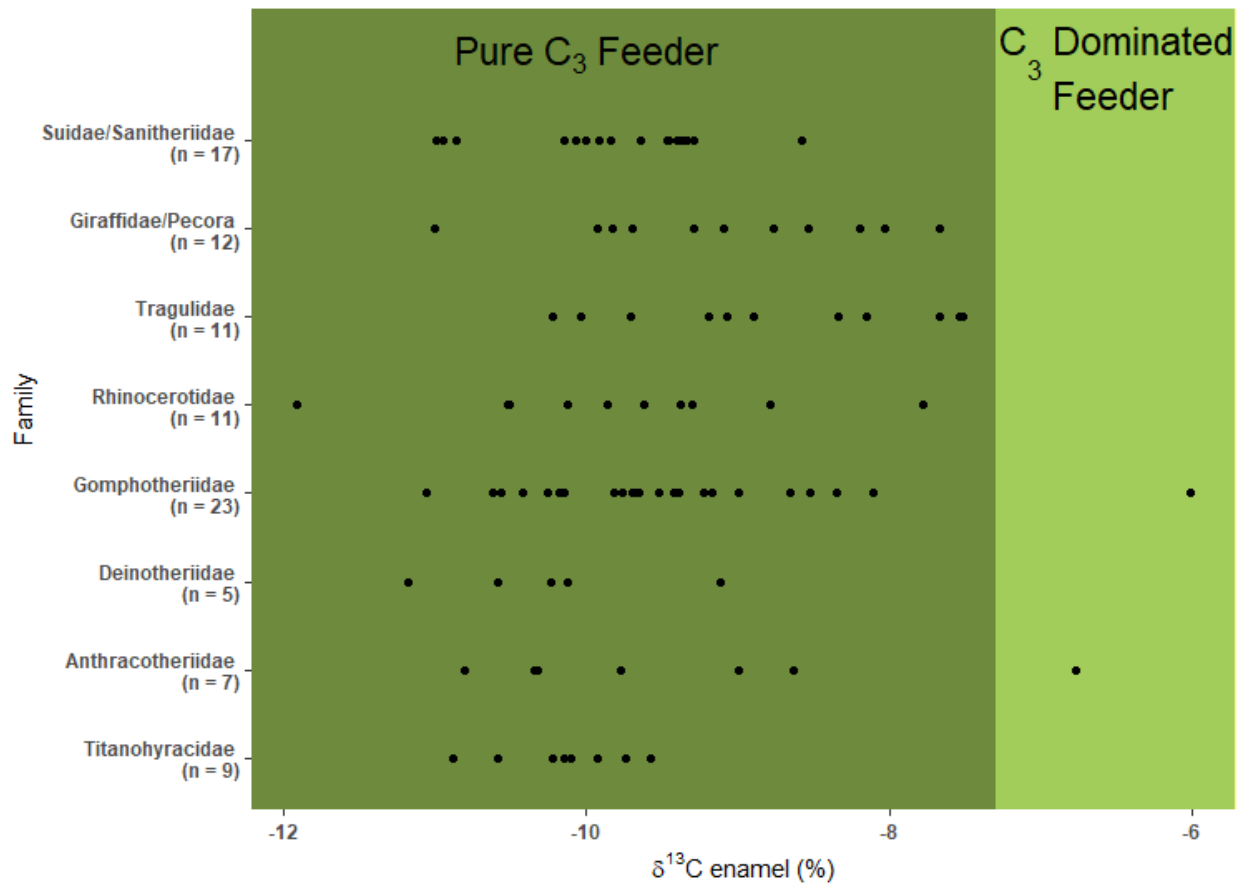


Figure 4: Dietary ranges of all samples collected from Kalodirr and Moruorot using the conservative dietary model.

Out of the 95 samples, 2 fell into the C₃ dominated feeder range, a gomphothere (KNM-MO 71279) and anthracothere (KNM-WK16924), indicating some C₄ vegetation was incorporated (< 25%

C₄). These calculations indicate that under this model, the gomphothere had a diet of 86% C₃ and 14% C₄ and the anthracothere had a diet of 94% C₃ and 6% C₄.

4.1.2.2 Standard dietary model

Under the standard dietary model we observe a wider range of diet types (Figure 5). For the percentages of C₃ and C₄ consumption and dietary classification for each specimen refer to the Supplementary Information (Table S4).

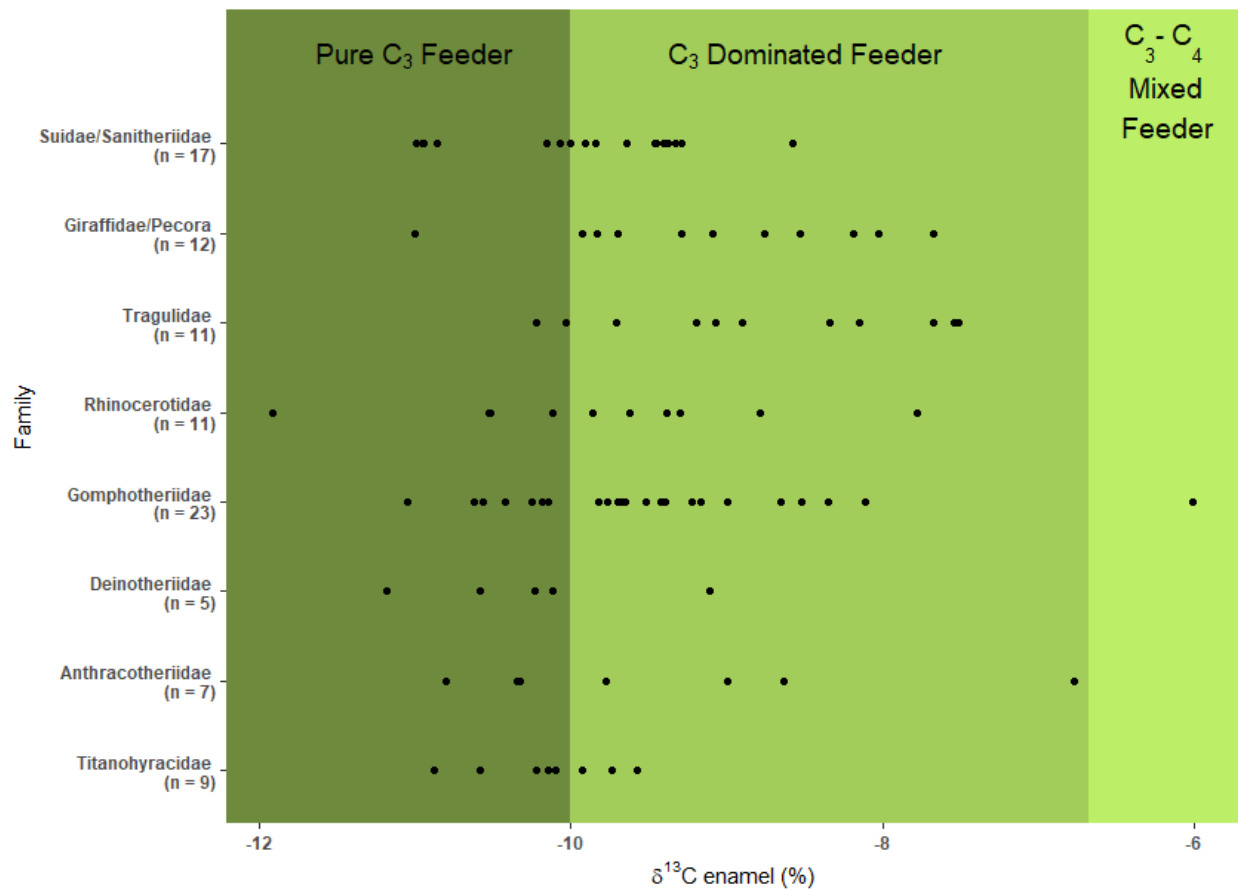


Figure 5: Dietary ranges of all samples collected from Kalodirr and Moruorot using the standard dietary model.

Majority of specimens are classified as C₃ dominated feeders under the standard dietary model. Table 7 summarizes the percentages of individual that have been assigned to each dietary type, grouped by family. Under this model, one gomphothere (KNM-MO 71279) was a C₃-C₄ mixed feeder with a diet

of 70% C₃ and 30% C₄ while one anthracothere (KNM-WK 16924) was still a C₃ dominated feeder, but with a diet of 76% C₃ and 24% C₄. A total of 61 out of 95 specimens show incorporation of some C₄ vegetation into their diet.

Table 7: Calculated percentage of individuals, using the standard dietary model, classified by dietary types, grouped by family.

Family	Diet Type (%)
Suidae/Sanitheriidae	47% C ₃ Pure C ₃ Feeders 53% C ₃ Dominated Feeders
Giraffidae/Pecora	8% C ₃ Pure C ₃ Feeders 92% C ₃ Dominated Feeders
Tragulidae	18% C ₃ Pure C ₃ Feeders 82% C ₃ Dominated Feeders
Rhinocerotidae	45% C ₃ Pure C ₃ Feeders 55% C ₃ Dominated Feeders
Gomphotheriidae	31% C ₃ Pure C ₃ Feeders 65% C ₃ Dominated Feeders 4% C ₃ -C ₄ Mixed Feeder
Deinotheriidae	80% Pure C ₃ Feeders 20% C ₃ Dominated Feeders
Anthracotheriidae	43% C ₃ Pure C ₃ Feeders 57% C ₃ Dominated Feeders
Titanohyracidae	56% C ₃ Pure C ₃ Feeders 44% C ₃ Dominated Feeders

4.1.3 Species Differences

The goal of this section is to determine if there are dietary differences between species. This section will focus on the anthracotheres, giraffids/pecorans, suids/sanitheres, and tragulids because these families each include multiple species (Figure 7). These species were plotted on box and whisker plots and compared using Mann-Whitney U tests (Figure 8; Table 8). These values show that the species in each family show no statistical differences indicating that there was no dietary separation among species.

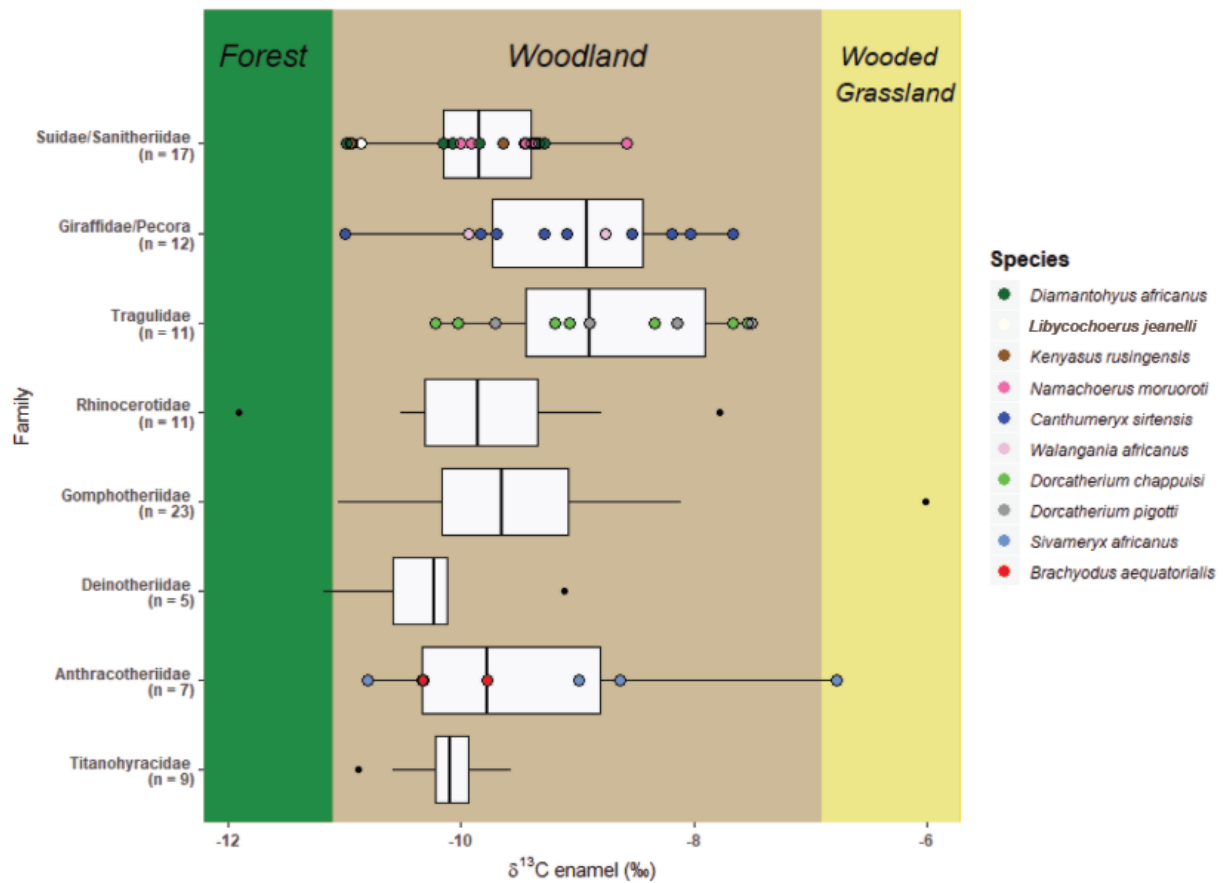


Figure 6: Summary of species distribution along with box and whisker plots of $\delta^{13}\text{C}$ enamel values of families at both Kalodirr and Moruorot.

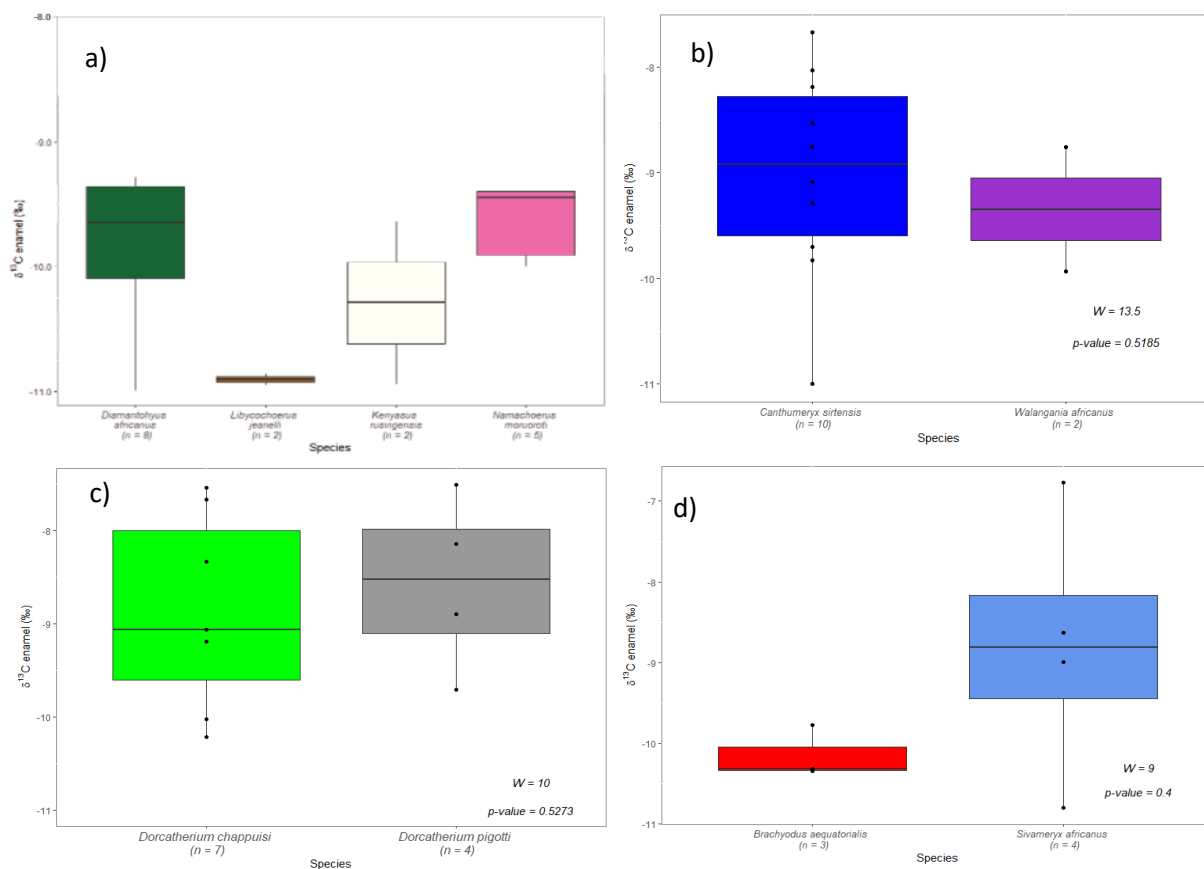


Figure 7: Box and whisker plots comparing $\delta^{13}\text{C}$ enamel range of individual species; a) suid/sanither species *Diamantohyus africanus*, *Kenyasus rusingensis*, *Libycochoerus jeanelli* and *Namachoerus moruoroti*, b) giraffid/pecoran species *Canthumeryx sirtensis* and *Walangania africanus*, c) tragulids species *Dorcatherium chappuisi* and *Dorcatherium pigotti*, d) anthracothere species *Brachyodus aequatorialis* and *Sivameryx africanus*.

Table 8: Results of comparative Mann-Whitney U tests of $\delta^{13}\text{C}$ enamel values between Suidae/Sanitheriidae species from Kalodirr and Moruorot.

	<i>Diamantohyus africanus</i>	<i>Kenyasus rusingensis</i>	<i>Libycochoerus jeanelli</i>	<i>Namachoerus moruoroti</i>
<i>Diamantohyus africanus</i>				
<i>Kenyasus rusingensis</i>	W = 11 p-value = 0.5333			
<i>Libycochoerus jeanelli</i>	W = 14 p-value = 0.1778	W = 1 p-value = 0.6667		
<i>Namachoerus moruoroti</i>	W = 16 p-value = 0.6216	W = 2 p-value = 0.381	W = 0 p-value = 0.09524	

Although there are no clear statistical differences, the suids show interesting dietary values that warrant some discussion. The values of the suids indicate a dietary divide between the smaller *Diamantohyus africanus* and *Namachoerus moruoroti* which are more lophodont, and the larger *Kenyasus rusingensis* and *Libycochoerus jeanelli* which are more bunodont. In general, this appears to be an isotopic separation between the smaller suids with more lophodont molars, *Diamantohyus africanus* and *Namachoerus moruoroti*, and the larger suids with more bunodont molars, *Kenyasus rusingensis* and *Libycochoerus jeanelli*. The smaller, lophodont suids appear to incorporate more enriched plant sources in comparison to the larger, bunodont suids indicating a diet sourced from more open environments and/or more C₄ sources.

4.1.4 Habitat Reconstruction

The calculated $\delta^{13}\text{C}_{\text{enamel}}$ for a closed forest system, using values collected from Kakamega and Ituri, is $\leq -12\text{‰}$ (Cerling et al. 2003; Cerling et al. 2004). Our values indicate an environment with $\delta^{13}\text{C}_{\text{enamel}}$ values too enriched to represent a closed forest system and instead likely represent a woodland environment. When the data are compared to calculated environmental analogues, they fall into the range of a woodland environment (Figure 9). Two specimens, a rhino (KNM-MO 64764) and a deinotheres (KNM-WK-16920) indicate the presence of a forest, while a gomphotheres (KNM-MO 71279) and an anthracotheres (KNM-WK 16924) indicate a wooded grassland environment. All other $\delta^{13}\text{C}_{\text{enamel}}$ values indicate the presence of a woodland environment.

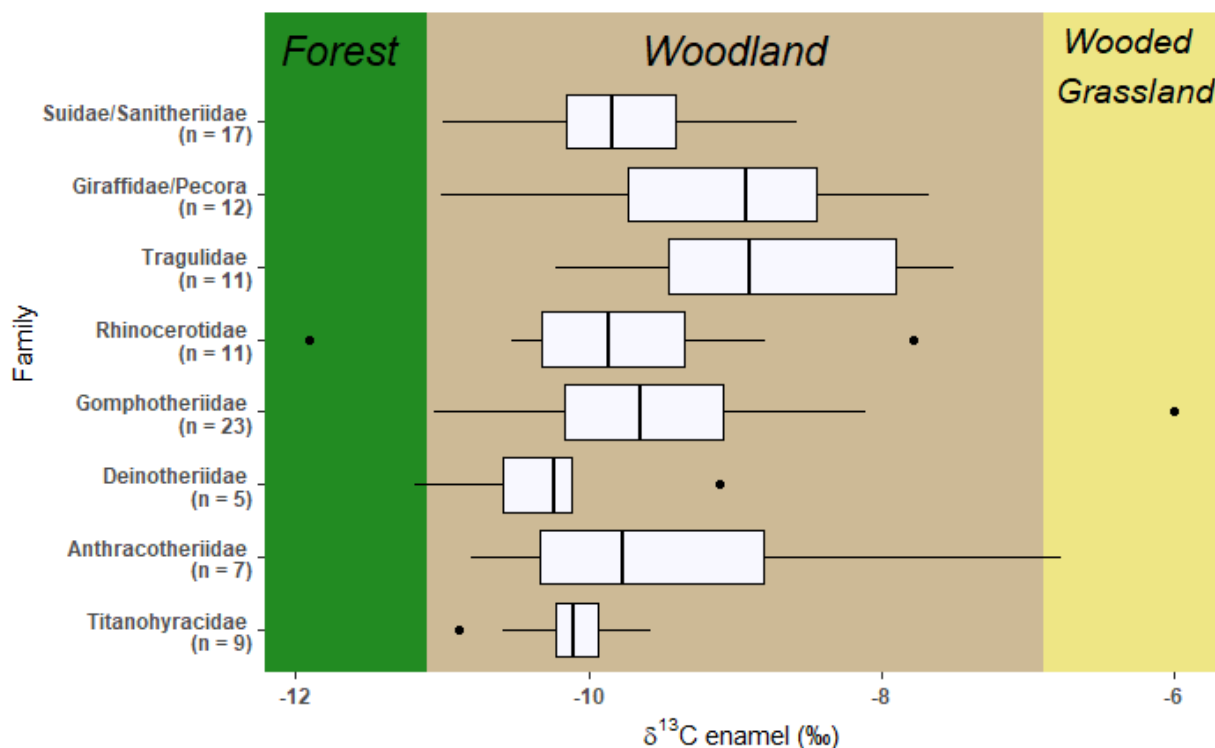


Figure 8: Box and whisker plot of $\delta^{13}\text{C}$ enamel values of families at both Kalodirr and Moruorot

According to White (1984), a woodland is classified as an open stand of trees with a canopy cover of 40% or more with crowns that are often in contact but are not densely interlocking. Groundcover typically consists primarily of grasses along with shrubs and other herbs (White 1984). Due to the values observed in this dataset, there are two potential groundcover hypotheses: C_3 grasses, shrubs and herbs and/or C_4 grasses and dicots. These will be explored in the discussion, “4.2.1 C_3 vs C_4 Diets.”

In comparison to the $\delta^{13}\text{C}_{\text{enamel}}$ values collected from the other early Miocene sites, Kalodirr and Moruorot have a more enriched $\delta^{13}\text{C}$ range. The most depleted $\delta^{13}\text{C}_{\text{enamel}}$ values are from Bukwa, Kenya (~19 Ma) with a range of -16.1‰ to -8.2‰ (Kingston et al. 2018). Napak and Moroto (21 to 20 Ma) had a $\delta^{13}\text{C}_{\text{enamel}}$ range of -15‰ to -7‰ (Kingston et al. 2009, 2011) and Tinderet (20 Ma) had a $\delta^{13}\text{C}_{\text{enamel}}$ range of -12.74‰ to -7.34‰ (Arney et al. 2017). Rusinga Island also had $\delta^{13}\text{C}_{\text{enamel}}$ data collected but the ranges have not been published, though the authors predict a woodland environment (Garrett et al. 2015). The $\delta^{13}\text{C}_{\text{enamel}}$ range for Kalodirr and Moruorot is -11.91‰ to -6.01‰, which indicates a more open

environment than these other sites. In general, this collective data indicates the early Miocene of Kenya had a patchy environmental distribution ranging from broken forests to open woodlands at the scale of individual fossil localities.

4.2 Discussion

The primary goal of this study was to determine the environments of Kalodirr and Moruorot in order to test the hypothesis that forest canopies began opening before the middle Miocene. The $\delta^{13}\text{C}_{\text{enamel}}$ values collected in this study are too enriched to represent a closed forest environment, supporting this hypothesis. The following sections will discuss these results, beginning with diets and then exploring possible vegetation sources and environments.

4.2.1 Isotopic Signals

Regardless of the dietary model used, these results indicate pure C_3 and C_3 dominated diets, indicating C_3 vegetation as the primary dietary source. The pure C_3 feeders (100% C_3) were likely fed on leaves and shrubs. The C_3 dominated feeders, indicating potential C_4 sources, are likely incorporating highly enriched C_3 foliage and grasses and potentially C_4 grasses and/or dicots. These sources are discussed in the following section (4.2.2 C_3 vs C_4). The two families that warrant individual discussion are the pecorans and the tragulids.

The $\delta^{13}\text{C}_{\text{enamel}}$ values of the pecorans indicate a wide dietary range with more enriched sources than hypothesized. The $\delta^{13}\text{C}_{\text{enamel}}$ range of -11 ‰ to -7.67 ‰ indicates diets of both denser C_3 foliage as well as the incorporation of highly enriched vegetation. This is consistent with the findings at Tinderet, as *Walangania africanus* specimens had a $\delta^{13}\text{C}_{\text{enamel}}$ range of -12.17 ‰ to -7.34 ‰ (Arney, Personal Communication). Due to the selenodont cheek teeth of *Walangania* and *Canthumeryx* (Archer & Sanson 2002; Janis 2008) and angle of the tooth rows of *Canthumeryx* (Solounias 2007) they were hypothesized to have a browsing diet.

Tragulids are often hypothesized to have a diet of dense browse due to their modern analogues, which have a heavily specialized diet of closed forest forage (ie. fruits, seeds, leaves, stems etc.; Rossner 2007). Although this study hypothesized a flexible diet of multiple C_3 sources, the values from Rusinga Island (Garrett et al. 2015) and Tinderet (Arney et al. 2017) indicate feeding from closed canopy sources. The $\delta^{13}C_{\text{enamel}}$ values of -10.22 ‰ to -7.51 ‰ indicates diets of C_3 foliage as well as highly enriched vegetation. These values support the hypothesis of a flexible diet from multiple sources, although the incorporation of such enriched values was unexpected.

4.2.2 C_3 vs C_4

This study considers two dietary models, a standard dietary model and a conservative dietary model, resulting in a wide range of interpretations. The conservative model indicates that the majority of individuals are pure C_3 feeders, with only 2% of individuals incorporating C_4 into their diet. Under the standard dietary model we have a wider spectrum of diets including pure C_3 feeders, C_3 dominated feeders and mixed feeders, with 64% of individuals incorporating C_4 into their diet.

The conservative dietary model hypothesizes the presence of highly enriched C_3 vegetation. This may be due to C_3 grasses, C_3 dicots, or a C_3 plant with no modern analogue. The most positive $\delta^{13}C_{\text{plant}}$ values for C_3 vegetation in East Africa are from C_3 dicots from Mpala, Kenya (Cerling et al. 2003). These plants likely made up some groundcover of this woodland but are not enriched enough by modern standards to account for all the values observed, which may be explained by C_3 grasses. Although majority of modern C_3 grasses are restricted to elevations of 1500m and higher, due to lower irradiance, lower temperatures and lack of water stress, there are a few specialized C_3 grasses found in the understories of closed canopy forests (Tieszen et al. 1979). Additionally, C_3 dominant grasslands are considered to be the first stage to a two-stage progression in the evolution of grassland habitats, which are then followed by the spread of C_4 grasslands (Pagani et al. 1999; Edwards et al. 2010; McInerney et al. 2011; Stromberg 2011). C_3 grasses collected from Mongolia, Utah and Argentina by Cerling & Harris

(1999) have a $\delta^{13}\text{C}_{\text{enamel}}$ range, calculated for to account for atmospheric change, of -10.3 ‰ to -6.3 ‰ with an average of -8 ‰. This range encompasses many of our specimens and may explain the more enriched values.

However, the conservative model may also be indicating C_3 values that are more enriched than those observed in modern ecosystems. Modern C_3 plants demonstrate that their carbon signatures are highly influenced by environmental factors (Deines 1980; van der Merwe & Medina 1989). The lower atmospheric pCO_2 , high temperatures, and lack of competition with C_4 vegetation may have allowed C_3 vegetation to expand their $\delta^{13}\text{C}$ values, becoming more enriched in ^{13}C (Pagani et al. 1999). As climate began to change and topography shifted these C_3 species may have been outcompeted by C_4 vegetation, which increased in abundance during the middle and late Miocene.

Alternatively, the standard model indicates that C_4 vegetation was incorporated into the diets of the majority of these herbivores. These C_4 plants could be either monocot grasses, monocot sedges, and/or herbaceous dicots. Due to the complex nature of the dicot physiology it has been proposed that the C_4 monocot grasses (Poaceae) and sedges (Cyperaceae) developed before C_4 dicots (Sage 2001). Additionally, the record from North America indicates that early Poaceae species were adapted to warm and closed canopies (Osborne & Freckleton 2009; Edwards & Smith 2010; Stromberg 2011) and may have developed in the closed forests of East Africa and further expanded when the forest canopies began opening. New phytolith data from Bukwa (~19 Ma) and Rusinga Island (site R3; 18 Ma) indicate the presence of the C_4 grasses (GPWG 2001; Stromberg 2011; Novello et al. 2017; Kingston et al. 2018; Peppe et al. 2018). These new data indicate that C_4 grass was represented in these early Miocene landscapes in an unknown abundance and is a possible contributor to the enriched values observed. These C_4 plants may not have been common in the landscape but may have been selectively eaten by the herbivores of this study. However, the dental morphologies of these mammals indicate diets of folivory so they may instead be incorporating leafy dicots.

Today, C_4 leafy dicots are represented by 10 genera in eastern and southern Africa and are found in the openings of woodlands and at the edge of forests (Jeffrey 1961; Elffers et al. 1964; Nabil El Hadidi

1985; Townsend 1985; Whitehouse 1996; Peters & Vogel 2005). The $\delta^{13}\text{C}_{\text{plant}}$ ranges of these dicots are similar to NADP-ME (NADP-malic enzyme) species, which are the more negative of the C_4 grasses (-11 ‰ to -8 ‰; Fraquhar 1983). Examples of C_4 dicots present in modern Africa include *Gisekia* (ice plant), *Amaranthus* (pigweed), and *Tribulus* (devil's-weed; Peter & Vogel 2005). Molecular evidence suggests that C_4 dicots first developed in the Miocene of Africa (21 to 15 Ma; Sage 2004). Dicots are believed to have an advantage over C_4 monocots during times of environmental disturbance (Ehleringer et al. 1997) and may have thrived in the dynamic environments of the Miocene. This advantage is typically in times of low CO_2 , very high temperatures (i.e. desert), and in saline ecosystems (Ehleringer et al. 1997). While the aquatic environments of Kalodirr and Moruorot were likely freshwater environments, the early Miocene was a period of low CO_2 , higher temperatures (Pagani et al. 1999), and localized environmental disturbances, supporting this hypothesis.

4.2.3 Habitat Interpretation

Cerling et al. (2011, 2013, 2015) collected data from modern environments in order to create a wood cover density continuum. For further description and environmental classifications please refer to section '3.4.4 Habitat reconstructions using dietary isotopes.' The values collected from this study were too enriched in ^{13}C to indicate a closed forest environment and are more like modern woodland environments. A woodland is an open stand of trees with wood cover of 40% or more, with crowns that are in contact with one another (White 1984).

Following Cerling et al. (2011, 2013, 2015) our values indicate that majority of the landscape fell between 80% to 60% wood cover with some evidence of open areas with 40% to 20% wood cover. Using these analogues, Kalodirr and Moruorot indicate a patchy network of woodlands with heterogeneous densities of wood cover. This is consistent with the geology, which indicates an abundance of ephemeral and perennial braided stream beds. Braided channels are characterized by divisions and rejoinings of flows around unstable alluvial islands (Puhakka et al. 1992). The banks of these islands are unstable and

subject to erosion, therefore are characterized by young successional vegetation (eg. grasses, herbs, small bushes; Puhakka et al. 1992). The flow of these rivers was likely fast moving, as evidenced by the large clast and grain sizes of the conglomerates found, which would further contribute to this instability. This would support more rapidly maturing vegetation, such as grasses, sedges and herbs. These banks would likely be the primary source of the more enriched $\delta^{13}\text{C}$ vegetation. The larger and more stable islands likely had central areas where older, secondary vegetation could grow (eg. trees; Puhakka et al. 1992; Morley 2000). This would cause the tree canopies to connect at different densities throughout the landscape, dependent on the size and stability of the islands. Although this model appears to agree with the geological interpretations of these sites, it assumes that the herbivores are incorporating all of the natural vegetation from the surrounding environment. Rather, these values could represent dietary specializations and/or different rates of incorporating vegetation types.

Chapter 5: Pretreatment Analysis

Isotopic studies use pretreatments in order to remove organic material and secondary carbonates from tooth enamel. Traditionally, enamel samples are reduced to a powder form and exposed to diluted NaOCl or H₂O₂ followed by acetic acid (Lee-Thorp 1989; Koch et al. 1997). However, this process has begun to vary among labs, including concentrations and exposure times. These treatment processes are becoming less common in deep time studies (> 1 Ma; Kingston, personal communication). This is due to a lack of understanding on how these acids effect the $\delta^{13}\text{C}_{\text{enamel}}$ values of fossilized teeth. Additionally, there is increased pressure from museums to collect smaller samples. Acid treatments cause an average of 50% material loss and therefore cannot be applied to small samples. I have excluded the pretreatment process for the majority of my samples due to the small samples collected. Additionally, other researchers working on the early Miocene have stopped pretreating fossil samples. This allows us to better compare our isotopic signals with these other early Miocene sites, although it complicates comparisons with studies that do pretreat their samples.

5.1 Enamel Formation and Diagenesis

It is important to understand the structure, formation and chemistry of tooth enamel and how post-depositional environments affect the enamel. Any alteration after deposition may alter the $\delta^{13}\text{C}$ values recovered; therefore, various acid treatments are used in isotopic studies with the goal of erasing these exogenous influences.

5.1.1 Formation and Chemistry

Enamel is secreted by ameloblasts at an angle to the enamel dentine junction (EDJ) marked by growth lines, including brown striae of Retzius (Hillson 1996). After the initial secretion of organic matrix, the ameloblasts replace the organic compounds with calcium and phosphate ions (Simmer &

Finchan 1995; Hillson 1996). At the end of this process, enamel is composed of mostly inorganic (mineral) composites, with <1% organic material, and very low porosity (Williams & Elliott 1979; LeGeros 1981; Wang & Cerling 1993). The timing of formation is variable for mammals depending on their circadian rhythm, ranging from a few weeks to a month for smaller mammals, and up to a year for larger herbivores such as elks or horses (Kohn & Cerling 2002; Passey & Cerling 2002).

The principle constituent of enamel is calcium hydroxyapatite, $\text{Ca}_{10}(\text{PO}_4)_6(\text{OH})_2$ (LeGeros 1981; Wang & Cerling 1993). The properties of biological apatites are different from the pure state of calcium hydroxyapatite, causing LeGeros (1981) to refer to these as “impure hydroxyapatites.” Biological apatites are microcrystalline in structure and variable in composition, including small amounts of “structural” carbonate substituting as carbonate ions (CO_3) for hydroxyl ions (OH) or phosphate (PO_4) in the lattice structure (LeGeros et al. 1969; LeGeros 1981; LeGeros & LeGeros 1984; Wang & Cerling 1993). These structural carbonates are analyzed for carbon and oxygen isotopes. In addition to these resistant, lattice-bound carbonates, hydroxylapatite may also contain carbonate in the hydration layers or in the amorphous zones near the crystal surface, known as “labile” components (Beshah et al. 1990; Kohn & Cerling 2002).

5.1.2 Diagenesis and Pretreatments

Diagenesis is the process of alteration or change to the original mineral matrix. This may include any recrystallization or secondary deposition of exogenous materials into the enamel. The CO_3 that substitutes for the lattice bound PO_4 or OH is believed to be diagenetically resistant (therefore preserving the original isotopic signatures), while the labile CO_3 may be subject to alteration (Lee-Thorp & van der Merwe 1987; Quade et al. 1992; Wang & Cerling 1994; Koch et al. 1997; Kohn & Cerling 2002). It is the goal of acid pretreatments to remove these labile constituents as well as any added material (Kruegar 1991; Koch et al. 1997; Kohn & Cerling 2002). Added material is in the form of simple carbonate, typically calcite (CaCO_3) or dolomite ($\text{CaMg}(\text{CO}_3)_2$), which can theoretically be removed through the use

of dilute acetic acid (Lee-Thorp & van der Merwe 1987; Lee-Thorp 1989; Kreugar 1991; Quade et al. 1992; Wang & Cerling 1994; Koch et al. 1997; Kohn & Cerling 2002).

Traditionally, samples are exposed to diluted NaOCl or H₂O₂ solutions in order to remove any traces of bacterial proteins and other organic matter followed by the introduction of 0.1 M or 1 M acetic acid or 1 M acetate buffer to remove secondary and absorbed carbonates without substantial dissolution of hydroxylapatite (Lee-Thorp 1989; Koch et al. 1997). Continued isotopic studies on mammalian enamel have complicated these traditional acid treatment methods, indicating that the diagenetic processes are more complicated than previously believed and affect the enamel structure in less uniform ways. For example, Rink & Schwarcz (1995) determined that fossil tooth enamel fragments are potentially more subject to chemical alteration than intact teeth, while Schoeninger et al. (2003) demonstrated that the surrounding depositional environment influences the outer 0.5mm of fossilized enamel.

Today, researchers use different treatment processes. A few researchers do not treat their samples at all (eg. Rink & Schwarcz 1995; Kingston, personal communication). Some labs have begun to treat enamel using only H₂O₂ (eg. Uno et al. 2011), while others react their samples with both H₂O₂ and 0.1 M buffered acetic acid (eg. Cerling et al. 2015). The dilution of acetic acid varies, with some labs using 1 M acetic acid and others using 0.1 M (eg. Quade et al. 1995; Cerling et al. 1997; Cerling et al. 2013). Additionally, the exposure of fossilized and modern teeth and bone in 1 M acetic acid promotes the recrystallization of biological hydroxylapatite, creating offsets in oxygen isotope analysis (Lee-Thorp & van der Merwe 1991; Sillen & Sealy 1995). The introduction of bone samples to 1 M acetic acid typically results in unacceptable loss (Lee-Thorp et al. 1997; Garvie-Lok et al. 2004). This is also the case in tooth enamel as the lowered pH levels cause a higher degree of erosion to enamel (Lee-Thorp et al. 1997; Hannig et al. 2005; Kingston, Personal Communication). With the increased pressure for smaller sample sizes 0.1 M acetic acid is preferable (Lee-Thorp et al. 1997). However, 0.1 M acetic acid creates smaller offsets than 1 M acetic acid making comparison to literature difficult. The timing of these reactions is also varied, ranging from 30 minutes to a few hours to 24 hours (eg. Quade et al. 1995; Bocherens et al. 1996;

Cerling & Harris 1999; Kingston et al. 2007). If the partial dissolution of acidic solutions changes the proportions of carbonate at lattice sites it could create isotopic effects (Kohn et al. 1999). The longer these sites are exposed to the acid treatments the further the change to isotopic values of the apatite and lattice until an eventual isotopic plateau (Kohn et al. 1999). These changes would be dependent on the amount of alteration as well as the pH and exposure times of the fossil to the acids.

Due to small sample sizes of fossil samples, some researchers have begun to treat their larger samples collected from each site to determine the isotopic offset and calculate the untreated values accordingly (eg. Uno et al. 2011; Cerling et al. 2015). Using this method, Cerling et al. (2015) found that for > 200 samples the average alteration between treated and untreated samples was by -0.4 ‰ after reactions with 3% H₂O₂ and 0.1 M acetic acid. The untreated samples were then corrected for the calculated change between untreated and treated samples in order to replicate acid treatment on all samples (Cerling et al. 2015). I do not agree with this method, as enamel alteration varies due to the extent of exposed cracks or micro-cracks in the enamel as well as the exposure time during weathering and fossilization, as this is when secondary deposition occurs (Boaz & Behrensmeyer 1976; Kohn et al. 1999; Schoeninger et al. 2003). This creates variation among enamel samples based on exposure time and depositional environment. Schoeninger et al. (2003) demonstrate this variability, indicating while most samples were changed by a value of < 1 ‰, others showed a difference of > 2 ‰ when treated. Fossil fragments are also altered in the direction of the sediments that surround the enamel during fossilization, therefore differential deposition could also cause different extents of $\delta^{13}\text{C}$ alteration (Lee-Thorp 2000, Schoeninger et al. 2003). This would make a standardized adjustment inaccurate. However, this may be viewed as a better approach than an all or nothing acid treatment approach as it addresses both the small sample sizes and potential alteration. In general, this lack of agreement on pretreatment protocols may cause variation in isotopic offsets that are independent of depositional environments.

5.2 Study Design

This study aims to test the effects of four treatment types on fossilized mammalian tooth enamel. These treatments include: treatment A (no treatment), treatment B (~2% NaOHCl), treatment C (0.1 M CH₃COOH), and treatment D (~2% NaOHCl and 0.1 M CH₃COOH). Large samples, collected from rhinos, gomphotheres, and deinotheres, were divided into four equal parts and treated with one of the four treatment types. The weights of these samples were taken before and after treatment in order to calculate the percent of sample lost for each treatment to determine if the percent loss is consistent for treatment type. The isotopic values of these four treatments were compared to one another to determine the offsets between the treatments. I hypothesize that these different treatments will cause significant isotopic offsets. I predict that:

1. Treatment B (bleach only) will not be significantly different from the untreated samples but will be significantly different from treatments C (acetic acid only) and D (bleach and acetic acid).
 - a. Bleach is introduced to enamel samples in order to remove any organic matter. These fossils are ~17 Ma and therefore any organic material on my samples would be modern. As all the teeth were cleaned before sampling and the outer layer of enamel discarded, all modern organics should have been cleaned off. Therefore, the untreated and bleach treated samples should have similar carbon isotope values.
 - b. The introduction of acetic acid is meant to eliminate any secondary or diagenic altered labile carbonates. Therefore, the $\delta^{13}\text{C}$ signatures recovered for treatments C and D should be significantly different from treatment B.

5.2.1 Methods

This section will outline the samples that were chosen and how the pretreatments are performed. All other details, including sampling and sample analysis, are described in section '3.4 Methods.'

5.2.1.1 Sample Subset

Of the 95 specimens sampled for this study, only 11 samples were subject to pretreatment due to small samples sizes ($< 0.03\text{g}$). Additionally, six samples from Karungu, Kenya ($\sim 18\text{ Ma}$) were sampled and treated for this analysis. Two rhino, deinotheres and gomphotheres samples were treated from each site, with the exception of deinotheres as only one sample was available from Kalodirr. These 17 samples were split into four parts and subjected to pretreatment processes described in the subsequent section. After splitting the samples, the smallest sample size being subjected to acid treatments weighed $\sim 0.002\text{ g}$ while the largest was 0.005 g . Weights of each sample before and after treatment are available on Table S2.

5.2.1.2 Pretreatment Process

A subset of 17 samples were divided to perform four different pretreatment types; (A) no treatment, (B) $\sim 2\%$ NaOHCl, (C) $0.1\text{ M CH}_3\text{COOH}$, and (D) $\sim 2\%$ NaOHCl and $0.1\text{ M CH}_3\text{COOH}$. These treatments are described below.

TREATMENT A:

Samples were untreated.

TREATMENT B:

1. $\sim 2\%$ NaOHCl was added to centrifuge tubes to the 1 mL line. $\sim 2\%$ NaOHCl was obtained by diluting unscented, pure bleach (5.25% NaOHCl) with double distilled water (DDW). Once NaOHCl was introduced to the sample, the samples were agitated using a VWR Fixed Speed Vortex Mixer for 1-3 seconds and placed back in the specimen box. The specimen box was then placed on top of a lab rotator on speed level 2 in order to keep them agitated. Samples were then left for 30 minutes.
2. After 30 minutes, samples were placed in a micro-centrifuge for 3 minutes. This allowed samples to form a pellet at the bottom of the centrifuge tube. Liquid was removed using transfer pipettes. Tubes were then filled with DDW, agitated using the vortex mixer, re-spun and the liquid was

pipetted out. This was repeated 3 times. After the third time pH balance was checked for neutrality.

3. Samples were then placed in a freezer (~-18° Celsius) for 24 hours.

TREATMENT C:

1. 0.1 M CH₃COOH (acetic acid) was added to centrifuge tubes to the 1 mL line. 0.1M acetic acid was obtained by diluting 1.0 M acetic acid with DDW (18 mL DDW added to 2mL 1 M acetic acid). Once acetic acid was introduced to the samples, the samples were agitated using a VWR Fixed Speed Vortex Mixer for 1-3 seconds and placed back in the specimen box. The specimen box was then placed on top of the lab rotator on speed level 2 in order to keep them agitated. Samples were left for 30 minutes.
2. After 30 minutes, samples were placed in a micro-centrifuge for 3 minutes. This allowed samples to form a pellet at the bottom of the centrifuge tube. Liquid was removed using transfer pipettes. Tubes were then filled with DDW, agitated using the vortex mixer, re-spun and the liquid was pipetted out. This was repeated 3 times. After the third time pH balance was checked for neutrality.
3. Samples were then placed in a freezer (~-18° Celsius) for 24 hours.

TREATMENT D:

1. ~2% NaOCl was added to centrifuge tubes to the 1 mL line. ~2% NaOCl was obtained by diluting unscented, pure bleach (5.25% NaOCl) with double distilled water (DDW). Once NaOCl was introduced to the sample, the samples were agitated using a VWR Fixed Speed Vortex Mixer for 1-3 seconds and placed back in the specimen box. The specimen box was then placed on top of a lab rotator on speed level 2 in order to keep them agitated. Samples were then left for 30 minutes.

2. After 30 minutes, samples were placed in a micro-centrifuge for 3 minutes. This allowed samples to form a pellet at the bottom of the centrifuge tube. Liquid was removed using transfer pipettes. Tubes were then filled with DDW, agitated using the vortex mixer, re-spun and the liquid was pipetted out. This was repeated 3 times. After the third time pH balance was checked for neutrality.
3. Following NaOHCl treatment, 0.1 M CH_3COOH (acetic acid) was added to centrifuge tubes to the 1 mL line. 0.1M acetic acid was obtained by diluting 1.0 M acetic acid with DDW (18 mL of DDW added to 2mL 1 M acetic acid). Once acetic acid was introduced to the samples, the samples were agitated using a VWR Fixed Speed Vortex Mixer for 1-3 seconds and placed back in the specimen box. The specimen box was then placed on top of the lab rotator on speed level 2 in order to keep them agitated. Samples were left for 30 minutes.
4. After 30 minutes, samples were placed in a micro-centrifuge for 3 minutes. This allowed samples to form a pellet at the bottom of the centrifuge tube. Liquid was removed using transfer pipettes. Tubes were then filled with DDW, agitated using the vortex mixer, re-spun and the liquid was pipetted out. This was repeated 3 times. After the third time pH balance was checked for neutrality.
5. Samples were then placed in a freezer ($\sim 18^\circ$ Celsius) for 24 hours.

Freeze drying process:

1. After 24 hours, samples were removed and parafilm was placed over the mouth of the centrifuge tube. A hole was poked in the parafilm and centrifuge tubes were placed into a small glass jar and taped in place, so they did not shift while drying.
2. The freeze-drying process took place over 24 hours using the VirTis Sentry Benchtop 3L.
 - a. Samples were loosely packed into the freeze drier glass containers.
 - b. Containers were placed on top of pads to reduce vibration and were attached to the freeze drier spouts.

- c. The vacuum was then turned on slowly for each jar, checking to ensure that the vacuum and condenser lights indicated the system was running smoothly.
 - d. Containers were checked to be sure the vacuum was running and left for 24 hours.
3. After samples were dried, they were removed from the vacuum and the system was shut down. Samples were then weighed, packaged and sent to the University of Florida for isotopic measurement, described in section '3.4.1 Sampling Protocol'.

5.3 Results

The results of the various acid treatments were analyzed using both the resulting $\delta^{13}\text{C}$ signals as well as the percentage of sample weight lost. Treatment A was ignored while analyzing the percentage weight lost, as all samples kept their total weight. A Shapiro-Wilk normality test was run on these data and returned a normal distribution for the $\delta^{13}\text{C}$ values (Table 9) and a non-normal distribution for the percent weight lost (Table 10).

Table 9: Results of Shapiro-Wilk normality tests for the $\delta^{13}\text{C}$ enamel values of the treatment types.

	Results	Normal?
Treatment A	W = 0.9525 p-value = 0.4973	Yes
Treatment B	W = 0.94066 p-value = 0.3261	Yes
Treatment C	W = 0.94318 p-value = 0.3578	Yes
Treatment D	W = 0.93725 p-value = 0.2871	Yes

Table 10: Results of Shapiro-Wilk normality tests for the percentage of weight loss of treatment types B, C, and D.

	Results	Normal?
Treatment B	W = 0.75702 p-value = 0.0005534	No
Treatment C	W = 0.90603 p-value = 0.08576	Yes
Treatment D	W = 0.93835 p-value = 0.2992	Yes

The mean $\delta^{13}\text{C}_{\text{enamel}}$ values for each treatment type were: treatment A = -9.53 ‰, treatment B = -9.77 ‰, treatment C = -10.32 ‰, and treatment D = -10.4 ‰ (Table 11). Treatments B, C, and D were compared to treatment A using paired t-tests (Figure 9) due to the normal distribution of the data (Table 9). All three of these pretreatment values are significantly different from the untreated samples (treatment A; Table 12). It was surprising that treatment B was significantly different, as the function of bleach was to remove any organic materials. As these specimens are 17.5 to 16.8 Ma all organics should have been removed during the cleaning process. A Welch two-sample t-test determined that Treatment B was significantly different from Treatments C and D (Table 12). This indicates that while the bleach pretreatment significantly altered $\delta^{13}\text{C}_{\text{enamel}}$ values, the introduction of acetic acid further altered these $\delta^{13}\text{C}_{\text{enamel}}$ values.

These results indicate that each treated sample became more negative than the untreated samples, apart from sample SC-2010-10 treatment B which remained the same and SC-2017-62 treatment be which became more positive by 0.02 ‰. The average change in $\delta^{13}\text{C}_{\text{enamel}}$ values from treatment A for each sample were: treatment B = -0.24 ‰, treatment C = -0.55 ‰, and treatment D = -0.87 ‰. Table 11 demonstrates the largest change from A for each sample, which ranges from -0.62 ‰ to -1.5 ‰, which may significantly alter the ecological interpretations of these mammals.

Table 11: List of the alteration of enamel weight and $\delta^{13}\text{C}$ by pretreatment type for all specimens in this experiment. KAL = Kalodirr, KAR = Karungu, MOR = Moruorot.

Sample Number	Family	Locality	$\delta^{13}\text{C}_{\text{enamel}}$ by Treatment Type (‰)				Times New Roman Largest change in $\delta^{13}\text{C}_{\text{enamel}}$ from Treatment A (‰)	Weight loss by Treatment Type (%)			Largest change in Weight from Treatment A (%)
			A	B	C	D		B	C	D	
SC-2017-29	Deinothere	KAL	-10.23	-10.31	-10.9	-11.53	-1.3	33	33	67	67
SC-2017-61	Deinothere	KAR	-11.3	-11.45	-12.37	-12.8	-1.5	33	0	75	75
SC-2017-62	Deinothere	KAR	-9.82	-9.8	-11.04	-10.96	-1.22	0	33	33	33
SC-2017-33	Deinothere	MOR	-10.12	-10.35	-10.74	-10.63	-0.62	0	67	25	67
SC-2017-34	Deinothere	MOR	-9.11	-9.39	-9.89	-9.96	-0.85	0	40	40	40
SC-2017-28	Gomphothere	KAL	-9.42	-9.81	-10.04	-9.93	-0.62	0	33	0	33
SC-2017-31	Gomphothere	KAL	-9.7	-9.99	-10.5	-10.37	-0.8	50	33	33	50
SC-2017-70	Gomphothere	KAR	-8.52	-8.87	-9.23	-9.17	-0.71	33	0	25	33
SC-2017-71	Gomphothere	KAR	-8.13	-8.44	-8.75	-8.8	-0.67	0	25	25	25
SC-2017-27	Gomphothere	MOR	-9.65	-9.88	-10.62	-10.69	-1.04	20	25	40	40
SC-2017-30	Gomphothere	MOR	-9.82	-10.21	-10.56	-10.52	-0.74	0	33	25	33
SC-2017-10	Rhino	KAL	-9.86	-9.86	-11.02	-10.99	-1.16	0	50	0	50
SC-2017-14	Rhino	KAL	-9.38	-9.6	-10.42	-10.69	-1.31	0	0	50	50
SC-2017-52	Rhino	KAR	-9.45	-9.69	-10.09	-10.21	-0.76	50	50	50	50
SC-2017-54	Rhino	KAR	-9.42	-9.77	-10.31	-10.31	-0.89	50	50	0	50
SC-2017-11	Rhino	MOR	-9.3	-9.56	-10.21	-10.27	-0.97	0	33	50	50
SC-2017-13	Rhino	MOR	-8.79	-9.03	-8.9	-8.97	-0.24	33	66	25	66
		Mean =	-9.53	-9.77	-10.32	-10.4	-0.91	18	34	33	48

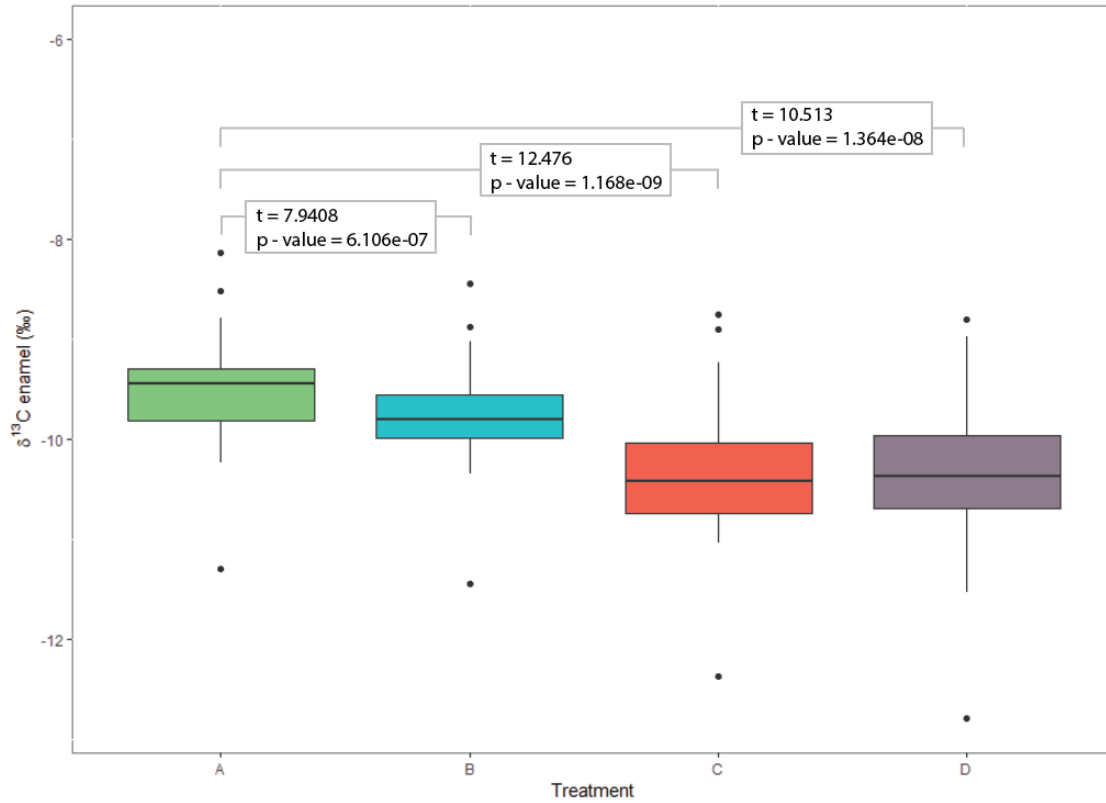


Figure 9: Box and whisker plot displaying the $\delta^{13}\text{C}_{\text{enamel}}$ values of the various treatment types.

Table 12: Results of a Welch Two Sample t-test comparing the acid treatments B, C and D $\delta^{13}\text{C}_{\text{enamel}}$ values. Significant values are highlighted in light grey.

	Treatment B	Treatment C	Treatment D
Treatment B			
Treatment C	t = 2.1336 df = 30.041 p-value = 0.04116		
Treatment D	t = 2.2527 df = 28.585 p-value = 0.03213	t = 0.2283 df = 31.689 p-value = 0.8209	

The percentage of weight loss of treatment B was non-normally distributed, while treatments C and D were normal (Table 10). The percentage of weight loss comparing treatment B to treatments C and D were compared using a Mann-Whitney U test, due to the non-normal distribution of Treatment B

(Table 10). This indicated that there was a significant difference between treatment B and C and a non-significant difference between treatment B and D, although it was close to significance (Table 13). A Welch Two Sample t-test determined that treatment C and D were not significantly different (Table 13). Although these statistical tests indicate that the change in weight significantly alters with the introduction of acetic acid, the range of weight loss for each treatment type indicates that this is not consistent (Table 11; Figure 10).

The average percentage of weight loss for each treatment type was as follows: treatment B = 18%, treatment C = 34% and treatment D = 33% (Table 11). It is interesting to note that treatment C and not treatment D had the most loss of sample. It was expected that treatment D would have the largest loss due to its treatment with both bleach and acetic acid, which should both react with separate components and contribute to further weight loss. It is important to note that substantial sample was also lost, with the highest loss of 75% (Table 11).

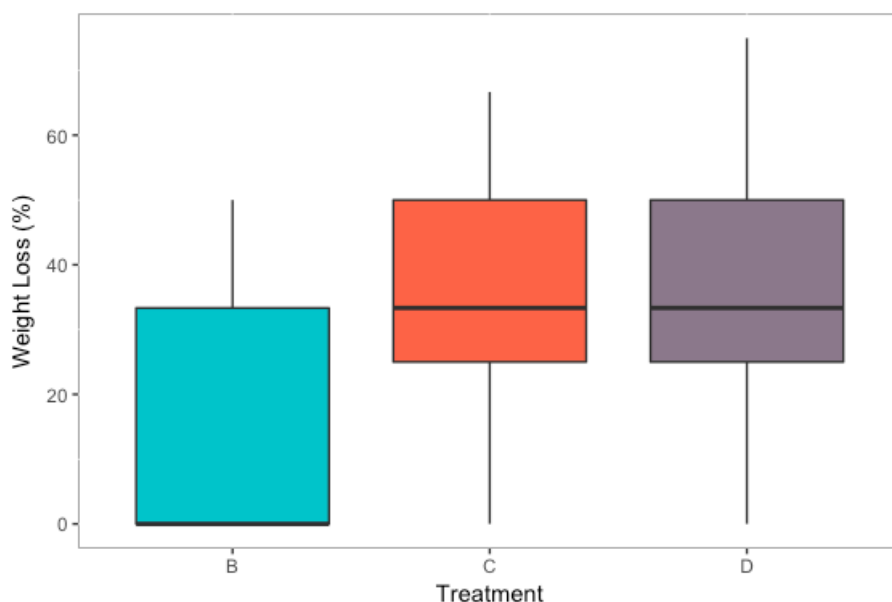


Figure 10: Box and whisker plot displaying the percentage of weight lost in treatments B, C and D.

Table 13: Weight percent loss comparisons between treatment types. The type of statistical tests used are listed where Mann-Whitney U tests are used when at least one of the treatments are non-normal and Welch Two Sample t-test are used when both treatments have a normal distribution. Significant results are highlighted in grey.

	Treatment B	Treatment C	Treatment D
Treatment B			
Treatment C	Mann-Whitney U Test W = 89 p-value = 0.04893		
Treatment D	Mann-Whitney U Test W = 93 p-value = 0.07037	Welch Two Sample t-test t = 0.081937 df = 31.874 p-value = 0.9352	

A Pearson's Correlation was used to test the strength of the linear association between the percentage of weight loss and the change in $\delta^{13}\text{C}_{\text{enamel}}$ for acid treatments B, C, and D (Laerd Statistics 2018). This test indicated that the $\delta^{13}\text{C}_{\text{enamel}}$ does correlate with the percentage of weight loss ($t = 2.3749$, $df = 49$, $p\text{-value} = 0.02027$). This could indicate that secondary carbonates are being removed, and the true $\delta^{13}\text{C}_{\text{enamel}}$ values are being expressed.

5.4 Discussion

This study shows that the introduction of any pretreatment significantly alters the samples from the untreated samples, with every treated sample becoming depleted relative to untreated samples, as well as between the treatment types. These changes are not surprising due to the different functions of these treatments. The role of bleach is to remove any organic matter and therefore was predicted to be non-significant from the untreated samples, due to the prehistoric nature of our samples. However, treatment B was significant from the untreated samples ($p\text{-value} = 6.106 \times 10^{-7}$). The introduction of acetic acid further alters these samples, indicated by a significant difference between treatments B and C and D ($p\text{-value}_{B \text{ vs } C} = 0.04116$; $p\text{-value}_{B \text{ vs } D} = 0.03213$), while treatments C and D were not significantly different ($p\text{-value} = 0.8209$). This difference between bleach and acetic acid treatments are unsurprising, as the function of

acetic acid would influence the labile or secondary carbonates. Treatments B, C and D expressed average $\delta^{13}\text{C}_{\text{enamel}}$ alterations of -0.24 ‰, -0.79 ‰ and -0.87 ‰, respectively. These alterations were completed after only 30-minute cycles, indicating that isotopic alteration occurs quickly. Further study on these acid treatments is required, including exposure times and acids used.

These treatments indicate that there is a significant change in $\delta^{13}\text{C}_{\text{enamel}}$ when treated, typically < 1 ‰. The greatest alteration was -1.5 ‰ after treatment D. As my samples are untreated, they may be artificially enriched in ^{13}C due to exogenous materials. If this study was to follow the calculations demonstrated by Cerling et al. (2015), our samples would be adjusted by the isotopic offsets of treatment D (~ -0.87 ‰). Although this is a minimal alteration it would alter the interpretations of diet for some of our samples. For example, under the current standard dietary model 37 % of specimens are pure C_3 feeders, 62 % are C_3 dominant feeders, and 1 % are mixed feeders. However, after adjusting the values for the treatment offset the data reflects 72 % pure C_3 feeders, 27 % C_3 dominated feeders, and 1 % mixed feeders. While the dietary interpretations change the environmental interpretation does not greatly alter, shifting to a slightly more ^{13}C depleted woodland environment. The majority of samples would still have values too enriched in ^{13}C to indicate a closed forest environment. While this is a caveat of this study, other labs are beginning to remove the pretreatment process. This is largely due to the pressure from museums for smaller sampling and the loss of sample that can occur during any of the sampling protocols, as demonstrated on Table 11 / Figure 10. With the average change in $\delta^{13}\text{C}_{\text{enamel}}$ values being < 1 ‰ it does not significantly skew environmental interpretations and may not be worth the potential loss of sample.

Chapter 6: Conclusions

6.1 Summary

The environmental history of East Africa is long and complex, influenced by a variety of factors such as volcanic activity, climate and tectonics. Slowed movement of the underlying mantle, due to the collision between Arabia and Eurasia, resulted in an increase of rifting and volcanic activity (McConnell 1972; Schilling 1973; Karson & Curtis 1989; Nyblade & Robinson 1994; Burke 1996; Chorowicz 2005; Partridge 2010). Rifting resulted in the uplift of the East African Plateau by 10 Ma leading to changes in climatic patterning (Pickford et al. 1993; Sepulchre et al. 2006; Maslin & Christensen 2007; Kasper et al. 2010; Prommel et al. 2012). This uplift was believed to be the major cause of environmental change in East Africa, causing closed canopy forests to remain stable until this uplift led to an aridification event and the opening of forest canopies during the middle Miocene (Kennett 1995; Zachos et al. 2001; Sepulchre et al. 2006; Maslin & Christensen 2007; Kasper et al. 2010; Uno et al. 2011; Prommel et al. 2012).

However, smaller localized rifting and volcanic occurrences likely influenced these environments on a smaller scale. Continued rifting creating the two branches of the EARS and a heavy concentration of volcanic activity along the eastern branch indicate that while the continent may have appeared relatively stable the local environments were exposed to unstable conditions. This is supported by the vegetation history of East Africa. The first indication of more open environments was at the Lokichar Basin, Kenya, dated to the Oligo-Miocene boundary, which indicated a mosaic of forests and woodlands with some Poaceae grasses (Vincens et al. 2006). Opened environments continued to be described in other Early Miocene sites such as Rusinga Island (20-18 Ma), Bukwa (~19 Ma), and Karungu (17.8 Ma) in the form of individual mosaics of forests, woodlands, and/or wooded grasslands at each site (Brock & MacDonald 1969; Evans et al. 1981; Bonnefille 1985; Pickford 2002; Collinson et al. 2009; Ungar et al. 2012; Driese et al. 2015; Lukens et al. 2017; Novello et al. 2017; Kingston et al. 2018). Continued isotopic analysis of

mammalian tooth enamel from Napak, Moroto, and Bukwa, Uganda and Rusinga Island and Tinderet, Kenya indicate either open forest or woodland conditions with C₃ and C₄ vegetation (Kingston et al. 2009, 2011, 2018; Garrett et al. 2015; Arney et al. 2017). Additionally, C₄ grass phytoliths were found at both Rusinga Island and Bukwa, Kenya (Stromberg 2011; Novello et al. 2017; Hillis et al. 2018). This is the earliest indication of C₄ grasses, typically associated with open environments, since its previous discovery from paleosol collected at the Tugen Hills at 15.5 Ma, and incorporation into mammalian enamel at 15.3 Ma (Kingston et al. 1994; Morgan et al. 1994). This new data supports the hypothesis of environmental instability and the opening of forest canopies during the early Miocene.

This study serves to augment this large body of literature by introducing new data from Kalodirr and Moruorot, which represent the latest early Miocene (17.5 to 16.8 Ma). Both standard and conservative dietary models are presented in this study in order to show the potential diets of these mammals. If C₄ grasses were not present, or present in small proportions, the conservative dietary model would be more representative of this environment and indicate diets reliant on the incorporation of enriched C₃ sources such as open canopy leaves, shrubs, herbs and grasses. However, the standard dietary model is more accurate when comparing to modern environments and is used in a number of paleontological studies (i.e. Lee-Thorp et al. 1989; Quade et al. 1992; Bocherens et al. 1996; Macfadden & Cerling 1996; Harris & Cerling 2002; Sponheimer et al. 2003; Kingston & Harrison 2007; Cerling et al. 2011). This model would indicate either a large proportion of C₄ in the environments of Kalodirr and Moruorot or preferential feeding on a few C₄ plants. The $\delta^{13}\text{C}_{\text{enamel}}$ values indicate environments too enriched in ¹³C to indicate a closed forest environment. Additionally, the $\delta^{13}\text{C}_{\text{enamel}}$ values from Kalodirr and Moruorot are more enriched than the $\delta^{13}\text{C}_{\text{enamel}}$ values from the other early Miocene sites of Napak, Moroto, and Bukwa, Uganda and Rusinga Island and Tinderet, Kenya. This indicates more open dietary C₃ and C₄ dietary sources from a woodland system.

6.2 Significance

This study has three important findings:

1. The $\delta^{13}\text{C}_{\text{enamel}}$ values indicate the incorporation of C_4 vegetation into diets.

The $\delta^{13}\text{C}_{\text{enamel}}$ values from these mammals indicate feeding from enriched ^{13}C vegetation sources. These sources could have been in the form of highly enriched C_3 browse, C_3 dicots, C_3 grasses, C_4 dicots, and/or C_4 grasses. However, regardless of the dietary model used, standard or conservative, there are indications of C_4 vegetation. This is consistent with the current understanding that the C_4 pathway first arose in species that were well adapted to warm, mesic and closed environments (Osborne & Freckleton 2009; Edwards & Smith 2010; Stromberg 2011), as well as phytolith data collected from Rusinga Island and Bukwa that indicates the presence of C_4 grasses in Kenya during the early Miocene (Stromberg 2011; Novello et al. 2017; Hillis et al. 2018). The abundance of this C_4 vegetation is still unknown, as the mammals of Kalodirr may have been selectively feeding. Further work is required to determine the abundance and form of these C_4 sources.

2. The environments of Kalodirr and Moruorot were not closed forests.

The $\delta^{13}\text{C}_{\text{enamel}}$ range of -11.91 ‰ to -6.01 ‰ collected falls outside of the range of closed canopy forests ($\delta^{13}\text{C}_{\text{enamel}}$ range is ≤ -12 ‰; Cerling et al. 2003, 2004), indicating that Kalodirr and Moruorot were more open. Instead, the $\delta^{13}\text{C}_{\text{enamel}}$ range indicates a woodland environment. This is consistent with the findings at the other East African early Miocene sites of Napak, Moroto, and Bukwa, Uganda and Rusinga Island, Karungu and Tinderet, Kenya which indicate a series of mosaic environments with individual incorporations of forests, woodlands and/or wooded grasslands (Brock & MacDonald 1969; Evans et al. 1981; Bonnefille 1985; Pickford 2002; Collinson et al. 2009; Ungar et al. 2012; Driese et al. 2015; Lukens et al. 2017; Novello et al. 2017; Kingston et al. 2018). The $\delta^{13}\text{C}_{\text{enamel}}$ range of Kalodirr and Moruorot is also more enriched than those of Napak, Moroto, Bukwa and Tinderet (Kingston et al. 2009, 2011, 2018; Garrett et al. 2015; Arney et al. 2017), indicating that the environments of the younger sites of Kalodirr and Moruorot were more open than the older early Miocene sites.

3. The fossil apes at Kalodirr and Moruorot were not living in a closed canopy forest.

Three apes are known to have lived in Kalodirr and Moruorot: *Simiolus enjiessi*, *Afropithecus turkanensis*, and *Turkanapithecus kalakolensis* (Leakey & Leakey 1986a, 1986b, 1987). The morphology of these apes suggests an arboreal lifestyle and aided in the interpretation of these sites as a forest. However, these data suggest a more open environment likely in the form of a woodland. This has implications for the larger bodied apes *Afropithecus* and *Turkanapithecus*. Due to their large body sizes they would require branches that could support their weights of 10kg to 55 kg (Rose et al. 1992; Rose 1994, 1997; Ward 1997, 1998; Harrison 2002, 2010). These branches would be rare in a woodland habitat, potentially influencing their locomotor and feeding behaviours. This does explain the tooth morphology of *Afropithecus*, which indicates sclerocarp foraging (Rossie & MacLachy 2013). This suggests feeding on hard fruits surrounded by a tough pericarp and seeds or more abrasive materials, which are typically found in drier habitats (Rossie & MacLachy 2013), such as the woodland environments demonstrated here.

Ultimately, this study has augmented the understanding of East African early Miocene environments. This study can confidently conclude that the $\delta^{13}\text{C}_{\text{enamel}}$ values recovered do not represent feeding from a closed canopy environment. Instead these values suggest the presence of a woodland habitat with some C_4 incorporations.

6.3 Future Directions

This study used an indirect method of assessing the environments of Kalodirr and Moruorot, using $\delta^{13}\text{C}_{\text{enamel}}$ values to indicate diet and extrapolate these results to reconstruct environment. Therefore, these data can only be used to interpret the vegetation and habitats that these mammals were actively feeding on. If these mammals had specialized diets, they would not be incorporating the entire range of vegetation present during this time. This would create a false vegetative and environmental signal. C_4 plants may have been widespread during this time but were not being regularly consumed due to a dietary lag in relation to environmental shifts. This was the case in North America, where environmental change

was recorded by phytoliths and carbonate data before and during the C₃ to C₄ shift of mammalian diets (Fox & Koch 2003; Stromberg 2011; Stromberg & McInerney 2011). Additionally, the $\delta^{13}\text{C}$ of modern vegetation used as an end member in the mixing model (3.4.3 Dietary Calculations) can also influence dietary interpretations. This is demonstrated between the standard and conservative models in this study, which show changes between pure C₃ and C₃ dominated diets.

These dietary factors would ultimately influence the environmental interpretations of Kalodirr and Moruorot. As this study uses a secondary inference, extrapolating diet into environment, it is subject to the errors above. Future work conducted at Kalodirr and Moruorot should consist of direct environmental methods, such as paleosol and phytolith analysis. However, as the preservation of direct proxies can be rarely represented in the fossil record, indirect methods are often necessary in order to gain an understanding of the environment.

Citations

- Allen, M., Jackson, J., Walker, R. (2004). Late Cenozoic reorganization of the Arabia-Eurasia collision and the comparison of short-term and long-term deformation rates. *Tectonics*, 23(2).
- Andrews, P., Lord, J. M., Evans, E. M. N. (1979). Patterns of ecological diversity in fossil and modern mammalian faunas. *Biological Journal of the Linnean Society*, 11(2), 177-205.
- Arambourg, C. (1947). *Contribution à l'étude géologique et paléontologique du bassin du lac Rodolphe et de la basse vallée de l'Omo. 2. ptie. Paléontologie*. Éditions du Muséum.
- Archer, D., Sanson, G. (2002). Form and function of the selenodont molar in southern African ruminants in relation to their feeding habits. *Journal of Zoology*, 257(1), 13-26.
- Arney, I., Cote, S., Fox, D.L., Kingston, J., MacLatchy, L., Mbua, E., McNulty, K., Nengo, I. (2017) Stable isotopic evidence of paleoenvironments at early Miocene localities from Tinderet, Kenya. (Abstract, Society of Vertebrate Paleontology).
- Azzaroli, A. (1968). On the evolution of the Gulf of Aden. In *International Geological Congress Report of Sessions 23rd* (1), 125-134.
- Bärmann, E. V., Rössner, G. E. (2011). Dental nomenclature in Ruminantia: Towards a standard terminological framework. *Mammalian Biology-Zeitschrift für Säugetierkunde*, 76(6), 762-768.
- Barry, J. C., Johnson, N. M., Raza, S. M., Jacobs, L. L. (1985). Neogene mammalian faunal change in southern Asia: correlations with climatic, tectonic, and eustatic events. *Geology*, 13(9), 637-640.
- Bernor, R. L., Brunet, M., Ginsburg, L., Mein, P., Pickford, M., Rögl, F., Thomas, H. (1987). A consideration of some major topics concerning Old World Miocene Mammalian chronology, migrations and paleogeography. *Geobios*, 20(4), 431-439.
- Beshah, K., Rey, C., Glimcher, M. J., Schimizu, M., Griffin, R. G. (1990). Solid state carbon-13 and proton NMR studies of carbonate-containing calcium phosphates and enamel. *Journal of Solid State Chemistry*, 84(1), 71-81.
- Bishop, L. C. (2010). Suoidea. Chapter XLII. In *Cenozoic Mammals of Africa* (pp. 829-850). University of California Press.
- Boaz, N. T., Behrensmeyer, A. K. (1976). Hominid taphonomy: transport of human skeletal parts in an artificial fluvial environment. *American Journal of Physical Anthropology*, 45(1), 53-60.
- Bocherens, H., Koch, P. L., Mariotti, A., Geraads, D., Jaeger, J. J. (1996). Isotopic biogeochemistry (13 C, 18 O) of mammalian enamel from African Pleistocene hominid sites. *Palaaios*, 306-318.
- Bonnefille, R. (1985). Evolution of the continental vegetation: the palaeobotanical record from East Africa. *South African journal of science*, 81(5), 267-270.
- Boschetto, H.B. (1988). Geology of the Lothidok Range, northern Kenya (Master's thesis). Accessed from The University of Utah Database:
<http://content.lib.utah.edu/utis/getfile/collection/etd3/id/2476/filename/2478.pdf>

- Boschetto, H.B., Brown, F.H., McDougall, I. (1992) Stratigraphy of the Lothidok Range, northern Kenya, and K/Ar ages of its Miocene primates. *Journal of Human Evolution* 22; 47-71.
- Bosworth, W., Huchon, P., McClay, K. (2005). The Red Sea and Gulf of Aden basins. *Journal of African Earth Sciences*, 43(1-3), 334-378.
- Bouchenak-Khelladi, Y., Verboom, G. A., Savolainen, V., Hodkinson, T. R. (2010). Biogeography of the grasses (Poaceae): a phylogenetic approach to reveal evolutionary history in geographical space and geological time. *Botanical Journal of the Linnean Society*, 162(4), 543-557.
- Brock, P. W. G., Macdonald, R. (1969). Fossil Mammal Locality on Mount Elgon, Eastern Uganda: Geological Environment of the Bukwa Mammalian Fossil Locality, Eastern Uganda. *Nature*, 223(5206), 593.
- Bullard, E. C. (1936). Gravity measurements in east Africa. *Phil. Trans. R. Soc. Lond. A*, 235(757), 445-531.
- Burke, K. (1996). The African plate. *South African Journal of Geology*, 99(4), 341-409.
- Cerling, T. E. (1992). Development of grasslands and savannas in East Africa during the Neogene. *Palaeogeography, Palaeoclimatology, Palaeoecology*, 97(3), 241-247.
- Cerling, T. E., Andanje, S. A., Blumenthal, S. A., Brown, F. H., Chritz, K. L., Harris, J. M., Leakey, M. G. (2015). Dietary changes of large herbivores in the Turkana Basin, Kenya from 4 to 1 Ma. *Proceedings of the National Academy of Sciences*, 112(37), 11467-11472.
- Cerling, T. E., Ehleringer, J. R., Harris, J. M. (1998). Carbon dioxide starvation, the development of C4 ecosystems, and mammalian evolution. *Philosophical Transactions of the Royal Society of London B: Biological Sciences*, 353(1365), 159-171.
- Cerling, T.E., Harris, J.M. (1999). Carbon isotope fractionation between diet and bioapatite in Ungulate mammals and implications for ecological and paleoecological studies. *Oecologia* 120(3); 347-363.
- Cerling, T. E., Harris, J. M., Ambrose, S. H., Leakey, M. G., Solounias, N. (1997a). Dietary and environmental reconstruction with stable isotope analyses of herbivore tooth enamel from the Miocene locality of Fort Ternan, Kenya. *Journal of Human Evolution*, 33(6), 635-650.
- Cerling, T. E., Harris, J. M., MacFadden, B. J., Leakey, M. G., Quade, J., Eisenmann, V., & Ehleringer, J. R. (1997b). Global vegetation change through the Miocene/Pliocene boundary. *Nature*, 389(6647), 153.
- Cerling, T.E., Harris, J.M., Passey, B.H. (2003). Diets of East African Bovidae based on stable isotope analysis. *Journal of Mammalogy* 84(2); 456-470.
- Cerling, T.E., Hart, J.A., Hart, T.B. (2004) Stable isotope ecology in the Ituri forest. *Oecologia* 138 (1); 5-12.
- Cerling, T. E., Wynn, J. G., Andanje, S. A., Bird, M. I., Korir, D. K., Levin, N. E., Remien, C. H. (2011). Woody cover and hominin environments in the past 6 million years. *Nature*, 476(7358), 51.
- Cerling, T. E., Manthi, F. K., Mbua, E. N., Leakey, L. N., Leakey, M. G., Leakey, R. E., Roche, H. (2013). Stable isotope-based diet reconstructions of Turkana Basin hominins. *Proceedings of the National Academy of Sciences*, 110(26), 10501-10506.

- Cerling, T. E., Quade, J., Ambrose, S. H., Sikes, N. E. (1991). Fossil soils, grasses, and carbon isotopes from Fort Ternan, Kenya: grassland or woodland?. *Journal of Human Evolution*, 21(4), 295-306.
- Chesters, K. I. (1957). The Miocene flora of Rusinga Island, Lake Victoria, Kenya. *Palaeontographica Abteilung B*, 30-71.
- Christin, P. A., Besnard, G., Samaritani, E., Duvall, M. R., Hodkinson, T. R., Savolainen, V., Salamin, N. (2008). Oligocene CO₂ decline promoted C₄ photosynthesis in grasses. *Current Biology*, 18(1), 37-43.
- Chorowicz, J. (2005). The east African rift system. *Journal of African Earth Sciences*, 43(1-3), 379-410.
- Collinson, M. E., Andrews, P., Bamford, M. K. (2009). Taphonomy of the early Miocene flora, Hiwegi Formation, Rusinga Island, Kenya. *Journal of Human Evolution*, 57(2), 149-162.
- Cote, S. M. (2010). Pecora *Incertae Sedis*. Chapter XXXVII. In *Cenozoic Mammals of Africa* (pp.731-739). University of California Press.
- Crepet, W. L., Feldman, G. D. (1991). The earliest remains of grasses in the fossil record. *American Journal of Botany*, 78(7), 1010-1014.
- Deines, P. (1980). The isotopic composition of reduced organic carbon. *Handbook of environmental isotope geochemistry*, 329-406.
- DeNiro, M. J., Epstein, S. (1978). Influence of diet on the distribution of carbon isotopes in animals. *Geochimica et cosmochimica acta*, 42(5), 495-506.
- Driese, S. G., Peppe, D. J., Beverly, E. J., DiPietro, L. M., Arellano, L. N., Lehmann, T. (2016). Paleosols and paleoenvironments of the early Miocene deposits near Karungu, Lake Victoria, Kenya. *Palaeogeography, palaeoclimatology, palaeoecology*, 443, 167-182.
- Ebinger, C. J., Yemane, T., Harding, D. J., Tesfaye, S., Kelley, S., Rex, D. C. (2000). Rift deflection, migration, and propagation: Linkage of the Ethiopian and Eastern rifts, Africa. *Geological Society of America Bulletin*, 112(2), 163-176.
- Edwards, A. R. (1968). The calcareous nannoplankton evidence for New Zealand Tertiary marine climate. *Tuatara*, 16(1), 26-31.
- Edwards, E. J., Smith, S. A. (2010). Phylogenetic analyses reveal the shady history of C₄ grasses. *Proceedings of the National Academy of Sciences*, 107(6), 2532-2537.
- Ehleringer, J. R., Cerling, T. E., Helliker, B. R. (1997). C₄ photosynthesis, atmospheric CO₂, and climate. *Oecologia*, 112(3), 285-299.
- Ehleringer, J. R., Sage, R. F., Flanagan, L. B., Pearcy, R. W. (1991). Climate change and the evolution of C₄ photosynthesis. *Trends in Ecology & Evolution*, 6(3), 95-99.
- Elffers, L., Graham, R.A., DeWolfe, G.P. (1964). Capparidaeeae. *Flora of Tropical East Africa*. Crown Agents for Oversea Governments and Administrations, London.
- Evans, E. N., Van Couvering, J. A., Andrews, P. (1980). Palaeoecology of Miocene sites in western Kenya. *Journal of Human Evolution*, 10(1), 99-116.
- Evans, E. N., Van Couvering, J. A., & Andrews, P. (1981). Palaeoecology of Miocene sites in western Kenya. *Journal of Human Evolution*, 10(1), 99-116.

- Farquhar, G. D., Ehleringer, J. R., & Hubick, K. T. (1989). Carbon isotope discrimination and photosynthesis. *Annual review of plant biology*, 40(1), 503-537.
- Flower, B. P., & Kennett, J. P. (1993). Middle Miocene ocean-climate transition: High-resolution oxygen and carbon isotopic records from Deep Sea Drilling Project Site 588A, southwest Pacific. *Paleoceanography and Paleoclimatology*, 8(6), 811-843.
- Fortelius, M., Heissig, K., Saraç, G., Sen, S. (2003). Rhinocerotidae (Perissodactyla). *Geology and Paleontology of the Miocene Sinap Formation, Turkey. Columbia University Press, New York*, 282-307.
- Fox, D. L., Koch, P. L. (2003). Tertiary history of C4 biomass in the Great Plains, USA. *Geology*, 31(9), 809-812.
- Frakes, L. A., Kemp, E. M. (1972). Influence of continental positions on early Tertiary climates. *Nature*, 240(5376), 97.
- Fredlund, G. G., Tieszen, L. T. (1994). Modern phytolith assemblages from the North American great plains. *Journal of Biogeography*, 321-335.
- Freeman, K. H., Hayes, J. M. (1992). Fractionation of carbon isotopes by phytoplankton and estimates of ancient CO2 levels. *Global Biogeochemical Cycles*, 6(2), 185-198.
- Fuchs, V. E. (1939). The geological history of the Lake Rudolf basin, Kenya Colony. *Phil. Trans. R. Soc. Lond. B*, 229(560), 219-274.
- Garrett, N.D., Fox, D.L., McNulty, K.P., Mitchel, L., Peppe, D.J. (2015) Early Miocene paleoenvironments of Rusinga Island, Kenya: new data from fossil mammalian tooth enamel stable isotope compositions. (Abstract, Society of Vertebrate Paleontology).
- Garvie-Lok, S. J., Varney, T. L., Katzenberg, M. A. (2004). Preparation of bone carbonate for stable isotope analysis: the effects of treatment time and acid concentration. *Journal of Archaeological Science*, 31(6), 763-776.
- Geraads, D. (2010a). Rhinocerotidae. Chapter XXXIV. In *Cenozoic Mammals of Africa* (pp. 669-729). University of California Press.
- Geraads, D. (2010b). Tragulidae. Chapter XXXVI. In *Cenozoic Mammals of Africa* (pp. 723-729). University of California Press.
- Geraads, D., Miller, E. (2013). *Brachypotherium minor* n. sp., and other Rhinocerotidae from the Early Miocene of Buluk, Northern Kenya. *Geodiversitas*, 35(2), 359-375.
- Grass Phylogeny Working Group, Barker, N. P., Clark, L. G., Davis, J. I., Duvall, M. R., Guala, G. F., Mathews, S. Y. (2001). Phylogeny and subfamilial classification of the grasses (Poaceae). *Annals of the Missouri Botanical Garden*, 373-457.
- Graham, A. (1999). *Late Cretaceous and Cenozoic history of North American vegetation: north of Mexico*. Oxford University Press on Demand.
- Guiraud, R., Bosworth, W., Thierry, J., Delplanque, A. (2005). Phanerozoic geological evolution of Northern and Central Africa: an overview. *Journal of African Earth Sciences*, 43(1-3), 83-143.

- Hamilton, W. R. (1978). Fossil giraffes from the Miocene of Africa and a revision of the phylogeny of the Giraffoidea. *Phil. Trans. R. Soc. Lond. B*, 283(996), 165-229.
- Hannig, C., Hamkens, A., Becker, K., Attin, R., & Attin, T. (2005). Erosive effects of different acids on bovine enamel: release of calcium and phosphate in vitro. *Archives of Oral Biology*, 50(6), 541-552.
- Harris, J. M. (1975). Evolution of feeding mechanisms in the family Deinotheriidae (Mammalia: Proboscidea). *Zoological Journal of the Linnean Society*, 56(4), 331-362.
- Harris, J. M., Cerling, T. E. (2002). Dietary adaptations of extant and Neogene African suids. *Journal of Zoology*, 256(1), 45-54.
- Harris, J.M., Solounias, N., Geraads, D. (2010). Giraffoidea. Chapter XXXIX. In *Cenozoic Mammals of Africa* (pp.797-811). University of California Press.
- Harrison, T. (2002). Late Oligocene to middle Miocene catarrhines from Afro-Arabia. *The primate fossil record*, 311-338.
- Harrison, T. (2010). Dendropithecoidea, proconsuloidea, and hominoidea. *Cenozoic mammals of Africa*, 429-469.
- Haq, B. U. (1980). Biogeographic history of Miocene calcareous nannoplankton and paleoceanography of the Atlantic Ocean. *Micropaleontology*, 414-443.
- Hedges, R. E., Van Klinken, G. J. (2002). "Consider a Spherical Cow..."—on Modeling and Diet. In *Biogeochemical approaches to paleodietary analysis* (pp. 211-241). Springer, Boston, MA.
- Hembree, D. I., Hasiotis, S. T. (2007). Paleosols and ichnofossils of the White River Formation of Colorado: Insight into soil ecosystems of the North American Midcontinent during the Eocene-Oligocene transition. *Palaaios*, 22(2), 123-142.
- Hillis, K.R., Michel, L.A., Fox, D.L., Driese, S.G., Peppe, D.L., Lehmann, T., McNulty, K.P. (2018). Paleoclimate reconstruction from pedogenic carbonates from the early Miocene Wayando Formation, Mfangano Island, Lake Victoria, Kenya and the impact on early ape evolution. (Abstract, American Association of Physical Anthropology).
- Holroyd, P. A., Lihoreau, F., Gunnell, G. F., Miller, E. R., Werdelin, L., Sanders, W. J. (2010). Anthracotheriidae. In *Cenozoic mammals of Africa*, 843-851.
- Hooijer, D. A. (1968). A note on the mandible of *Aceratherium acutirostratum* (Deraniyagala) from Moruaret Hill, Turkana District, Kenya. *Zoologische Mededelingen, Leiden*, 42(21), 231-235.
- Jacobs, B. F. (1999). Estimation of rainfall variables from leaf characters in tropical Africa. *Palaeogeography, Palaeoclimatology, Palaeoecology*, 145(1-3), 231-250.
- Janis, C. (2008). An evolutionary history of browsing and grazing ungulates. In *The ecology of browsing and grazing* (pp. 21-45). Springer, Berlin, Heidelberg.
- Janis, C. M., Damuth, J., Theodor, J. M. (2000). Miocene ungulates and terrestrial primary productivity: where have all the browsers gone?. *Proceedings of the National Academy of Sciences*, 97(14), 7899-7904.

- Janis, C. M., Damuth, J., Theodor, J. M. (2002). The origins and evolution of the North American grassland biome: the story from the hoofed mammals. *Palaeogeography, Palaeoclimatology, Palaeoecology*, 177(1-2), 183-198.
- Jeffrey, C. (1961). Aizoaceae. *Flora of Tropical East Africa*. Crown Agents for Oversea Governments and Administrations, London.
- Karson, J. A., Curtis, P. C. (1989). Tectonic and magmatic processes in the eastern branch of the East African rift and implications for magmatically active continental rifts. *Journal of African Earth Sciences (and the Middle East)*, 8(2-4), 431-453.
- Kaspar, F., Prömmel, K., Cubasch, U. (2010). Impacts of tectonic and orbital forcing on East African climate: a comparison based on global climate model simulations. *International Journal of Earth Sciences*, 99(7), 1677-1686.
- Kay, R. F., Ungar, P. S. (1997). Dental evidence for diet in some Miocene catarrhines with comments on the effects of phylogeny on the interpretation of adaptation. In *Function, Phylogeny, and Fossils* (pp. 131-151). Springer, Boston, MA.
- Kellogg, E. A. (2001). Evolutionary history of the grasses. *Plant physiology*, 125(3), 1198-1205.
- Kennett, J. P. (1995). A review of polar climate evolution during the Neogene, Based on the marine sediment record. In *Paleoclimate and Evolution, with Emphasis on Human Origins* (pp. 49-64). Yale University Press, New Haven.
- Khan, M. A., Akhtar, M. (2011). *Dorcatherium* cf. *nagrii* from the Chinji type locality (Chakwal, northern Pakistan) of the Chinji Formation, Lower Siwaliks, Pakistan. *Pakistan Journal of Zoology*, 43(6).
- Kingston, J. D. (1999). Environmental determinants in early hominid evolution: issues and evidence from the Tugen Hills, Kenya. *Late Cenozoic Environments and Hominid Evolution: a tribute to Bill Bishop*. London: Geological Society, 69-84.
- Kingston, J. D., Harrison, T. (2007). Isotopic dietary reconstructions of Pliocene herbivores at Laetoli: Implications for early hominin paleoecology. *Palaeogeography, Palaeoclimatology, Palaeoecology*, 243(3-4), 272-306.
- Kingston, J. D., Hill, A., Marino, B. D. (1994). Isotopic evidence for Neogene hominid paleoenvironments in the Kenya Rift Valley. *Science*, 264(5161), 955-959.
- Kingston, J. D., Jacobs, B. F., Hill, A., & Deino, A. (2002). Stratigraphy, age and environments of the late Miocene Mpesida Beds, Tugen Hills, Kenya. *Journal of Human Evolution*, 42(1-2), 95-116.
- Kingston, J., MacLatchy, L., Cote, S., Kinyanjui, R. (2018) Isotopic evidence of habitat heterogeneity at Bukwa, an early Miocene catarrhine site in Uganda. (Abstract, American Association of Physical Anthropology).
- Kingston, J., MacLatchy, L., Cote, S., Kityo, R., Sanders, W. (2009). Paleoenvironments of early Miocene vertebrate localities at Napak and Moroto, Uganda: lithofacies and isotopic analysis. *Journal of Vertebrate Paleontology* S29: 127A.
- Kingston, J., MacLatchy, L., Cote, S., Kityo, R., Sanders, W. (2011) Isotopic evidence of paleoenvironments and niche partitioning of early Miocene fossil fauna from Napak and Moroto, Uganda. *Journal of Vertebrate Paleontology* S31: 136A.

- Koch, P. L., Tuross, N., Fogel, M. L. (1997). The effects of sample treatment and diagenesis on the isotopic integrity of carbonate in biogenic hydroxylapatite. *Journal of Archaeological Science*, 24(5), 417-429.
- Kohn, M. J. (2010). Carbon isotope compositions of terrestrial C3 plants as indicators of (paleo) ecology and (paleo) climate. *Proceedings of the National Academy of Sciences*, 107(46), 19691-19695.
- Kohn, M. J., Cerling, T. E. (2002). Stable isotope compositions of biological apatite. *Reviews in mineralogy and geochemistry*, 48(1), 455-488.
- Kohn, M. J., Schoeninger, M. J., Barker, W. W. (1999). Altered states: effects of diagenesis on fossil tooth chemistry. *Geochimica et cosmochimica acta*, 63(18), 2737-2747.
- Koufos, G. D., Kostopoulos, D. S., & Vlachou, T. D. (2005). Neogene/Quaternary mammalian migrations in eastern Mediterranean. *Belgian Journal of Zoology*, 135(2), 181.
- Kreuser, T. (1995). Rift to drift evolution in Permian-Jurassic basins of East Africa. *Geological Society, London, Special Publications*, 80(1), 297-315.
- Krueger, H. W. (1991). Exchange of carbon with biological apatite. *Journal of Archaeological Science*, 18(3), 355-361.
- Laerd Statistics. (2018). Pearson Product-Moment Correlation. Lund Research Ltd. Accessed from: <https://statistics.laerd.com/statistical-guides/pearson-correlation-coefficient-statistical-guide.php>
- Leakey, M., Grossman, A., Gutierrez, M., Fleagle, J.G. (2011) Faunal change in the Turkana Basin during the Late Oligocene and Miocene. *Evolutionary Anthropology* 20; 238-253.
- Leakey, R. E. F., Leakey, M. G. (1986a). A new Miocene hominoid from Kenya. *Nature* 324:143–146.
- Leakey, R. E. F., Leakey, M. G. (1986b). A second new Miocene hominoid from Kenya. *Nature* 324:146–149.
- Leakey, R. E., Leakey, M. G. (1987). A new Miocene small-bodied ape from Kenya. *Journal of Human Evolution*, 16(4), 369-387.
- Leakey, M., Walker, A. (1997). *Afropithecus*. In *Function, phylogeny, and fossils* (pp. 225-239). Springer, Boston, MA.
- LeGeros, R. Z., Trautz, O. R., Klein, E., LeGeros, J. P. (1969). Two types of carbonate substitution in the apatite structure. *Experientia*, 25(1), 5-7.
- LeGeros, R. Z. (1981). Apatites in biological systems. *Progress in crystal growth and characterization*, 4(1-2), 1-45.
- LeGeros, R. Z., Legeros, J. P. (1984). Phosphate minerals in human tissues. In *Phosphate minerals* (pp. 351-385). Springer, Berlin, Heidelberg.
- Lee-Thorp, J. A. (1989). Stable carbon isotopes in deep time: the diets of fossil fauna and hominids (Doctoral dissertation, University of Cape Town).
- Lee-Thorp, J. A. (2002). Preservation of biogenic carbon isotopic signals in Plio-Pleistocene bone and tooth mineral. In *Biogeochemical approaches to paleodietary analysis* (pp. 89-115). Springer, Boston, MA.

- Lee-Thorp, J. A., Manning, L., Sponheimer, M. (1997). Problems and prospects for carbon isotope analysis of very small samples of fossil tooth enamel. *Bulletin de la Société géologique de France*, 168(6), 767-773.
- Lee-Thorp J. A., van der Merwe N. J. (1987) Carbon isotope analysis of fossil bone apatite. *South African Journal of Science* 83:712-715
- Lee-Thorp, J. A., van der Merwe, N. J. (1991). Aspects of the chemistry of modern and fossil biological apatites. *Journal of Archaeological Science*, 18(3), 343-354.
- Lee-Thorp, J. A., van der Merwe, N. J., Brain, C. K. (1989). Isotopic evidence for dietary differences between two extinct baboon species from Swartkrans. *Journal of Human Evolution*, 18(3), 183-189.
- Lihoreau, F., & Ducrocq, S. (2007). Family Anthracotheriidae. In *The evolution of artiodactyls*, 89-105.
- Liem, K. F. (1980). Adaptive significance of intra-and interspecific differences in the feeding repertoires of cichlid fishes. *American zoologist*, 20(1), 295-314.
- Lukens, W. E., Lehmann, T., Peppe, D. J., Fox, D. L., Driese, S. G., McNulty, K. P. (2017). The Early Miocene Critical Zone at Karungu, Western Kenya: An Equatorial, Open Habitat with Few Primate Remains. *Frontiers in Earth Science*, 5, 87.
- MacGregor, D. (2015). History of the development of the East African Rift System: A series of interpreted maps through time. *Journal of African Earth Sciences*, 101, 232-252.
- Macfadden, B. J., Cerling, T. E. (1996). Mammalian herbivore communities, ancient feeding ecology, and carbon isotopes: a 10 million-year sequence from the Neogene of Florida. *Journal of Vertebrate Paleontology*, 16(1), 103-115.
- Madden, G. T. (1972). *A Miocene Mammalian Fauna from Lothidok Hill, Kenya*. University of California.
- Maslin, M. A., Christensen, B. (2007). Tectonics, orbital forcing, global climate change, and human evolution in Africa: introduction to the African paleoclimate special volume. *Journal of Human Evolution*, 53(5), 443-464.
- McConnell, R. B. (1972). Geological development of the rift system of eastern Africa. *Geological Society of America Bulletin*, 83(9), 2549-2572.
- McCrossin, M. L., Benefit, B. R. (1997). On the relationships and adaptations of Kenyapithecus, a large-bodied hominoid from the middle Miocene of eastern Africa. In *Function, Phylogeny, and Fossils* (pp. 241-267). Springer, Boston, MA.
- McInerney, F. A., Strömberg, C. A., White, J. W. (2011). The Neogene transition from C 3 to C 4 grasslands in North America: stable carbon isotope ratios of fossil phytoliths. *Paleobiology*, 37(1), 23-49.
- Michener, R., Lajtha, K. (Eds.). (2008). *Stable isotopes in ecology and environmental science*. John Wiley & Sons.
- Mihlbachler, M. C., Rivals, F., Solounias, N., Semprebon, G. M. (2011). Dietary change and evolution of horses in North America. *Science*, 331(6021), 1178-1181.

- Mihlbachler, M. C., Solounias, N. (2006). Coevolution of tooth crown height and diet in oreodonts (Merycoidodontidae, Artiodactyla) examined with phylogenetically independent contrasts. *Journal of Mammalian Evolution*, 13(1), 11-36.
- Morgan, M. E., Kingston, J. D., Marino, B. D. (1994). Carbon isotopic evidence for the emergence of C4 plants in the Neogene from Pakistan and Kenya. *Nature*, 367(6459), 162.
- Morley, R. J. (2000). Chapter 2: Present-day tropical rain forests. Origin and evolution of tropical rain forests. John Wiley & Sons. 8-42.
- Morley, C. K., Wescott, W. A., Stone, D. M., Harper, R. M., Wigger, S. T., Karanja, F. M. (1992). Tectonic evolution of the northern Kenyan Rift. *Journal of the Geological Society*, 149(3), 333-348.
- Mucciarone, D. (2003). Standard Operating Procedures Manual. *Stanford University Stable Isotope Laboratory*.
- Nabil El Hadidi, M. (1985). Zygophyllaceae. *Flora of Tropical East Africa*. A.A. Balkema, Rotterdam.
- Nambudiri, E. M. V., Tidwell, W. D., Smith, B. N., Hebbert, N. P. (1978). A C4 plant from the Pliocene. *Nature*, 276(5690), 816.
- Novello, A., Stromberg, C.A., Jacobs, B.F., McNulty, K.P., Michel, L.A., Uno, K.T. (2017). The role of grasses in East Africa vegetation during the past 30 million years: New results and perspectives from plant silica (phytolith) analysis. (Abstract, Society of Vertebrate Paleontology).
- Nyblade, A. A., Robinson, S. W. (1994). The african superswell. *Geophysical research letters*, 21(9), 765-768.
- Osborne, C. P., Freckleton, R. P. (2009). Ecological selection pressures for C4 photosynthesis in the grasses. *Proceedings of the Royal Society of London B: Biological Sciences*, 276(1663), 1753-1760.
- Pagani, M., Freeman, K. H., Arthur, M. A. (1999). Late Miocene atmospheric CO2 concentrations and the expansion of C4 grasses. *Science*, 285(5429), 876-879.
- Park, R., Epstein, S. (1960). Carbon isotope fractionation during photosynthesis. *Geochimica et Cosmochimica Acta*, 21(1-2), 110-126.
- Park, R., Epstein, S. (1961). Metabolic fractionation of C13 & C12 in plants. *Plant Physiology*, 36(2), 133.
- Partridge, T. C. (2010) Tectonics and geomorphology of Africa during the Phanerozoic. Chapter I. In *Cenozoic Mammals of Africa* (pp. 3-26). University of California Press.
- Passey, B. H., Cerling, T. E. (2002). Tooth enamel mineralization in ungulates: implications for recovering a primary isotopic time-series. *Geochimica et Cosmochimica Acta*, 66(18), 3225-3234.
- Passey, B. H., Robinson, T. F., Ayliffe, L. K., Cerling, T. E., Sponheimer, M., Dearing, M. D., Ehleringer, J. R. (2005). Carbon isotope fractionation between diet, breath CO2, and bioapatite in different mammals. *Journal of Archaeological Science*, 32(10), 1459-1470.
- Peppe, D. J., Cote, S., Deino, A., Driese, S. G., Fox, D. L., Kingston, J., Jenkins, K. (2018, April). Adaptable apes: reconstructing habitats through space and time in the early Miocene of East Africa. In *American Journal of Physical Anthropology* (Vol. 165, pp. 203-203).

- Peters, C. R., Vogel, J. C. (2005). Africa's wild C4 plant foods and possible early hominid diets. *Journal of human evolution*, 48(3), 219-236.
- Pickford, M. (2002). Early Miocene grassland ecosystem at Bukwa, Mount Elgon, Uganda. *Comptes Rendus Palevol*, 1(4), 213-219.
- Pickford, M., Senut, B., Hadoto, D. P. M. (1993). *Geology and Palaeobiology of the Albertine Rift Valley, Uganda-Zaire: Geology* (Vol. 1). Cifeg.
- Prodehl, C. (1981). Structure of the crust and upper mantle beneath the central European rift system. *Tectonophysics*, 80(1-4), 255-269.
- Prömmel, K., Cubasch, U., Kaspar, F. (2013). A regional climate model study of the impact of tectonic and orbital forcing on African precipitation and vegetation. *Palaeogeography, Palaeoclimatology, Palaeoecology*, 369, 154-162.
- Puhakka, M., Kalliola, R., Rajasilta, M., Salo, J. (1992). River types, site evolution and successional vegetation patterns in Peruvian Amazonia. *Journal of Biogeography*, 651-665.
- Quade, J., Cerling, T. E., Bowman, J. R. (1989). Development of Asian monsoon revealed by marked ecological shift during the latest Miocene in northern Pakistan. *Nature*, 342(6246), 163-166.
- Quade, J., Cerling, T. E., Barry, J. C., Morgan, M. E., Pilbeam, D. R., Chivas, A. R., van der Merwe, N. J. (1992). A 16-Ma record of paleodiet using carbon and oxygen isotopes in fossil teeth from Pakistan. *Chemical Geology*, 94(3), 183-192.
- Rasmussen, D.T., Gutierrez, M. (2010). Hyracoidea. Chapter XIII. In *In Cenozoic Mammals of Africa* (pp. 123-145). University of California Press.
- Retallack, G. J. (1997). Neogene expansion of the North American prairie. *Palaios*, 12(4), 380-390.
- Retallack, G. J. (2007). Cenozoic paleoclimate on land in North America. *The Journal of Geology*, 115(3), 271-294.
- Retallack, G. J., Wynn, J. G., Benefit, B. R., McCrossin, M. L. (2002). Paleosols and paleoenvironments of the middle Miocene, Maboko Formation, Kenya. *Journal of Human Evolution*, 42(6), 659-703.
- Rink, W. J., Schwarcz, H. P. (1995). Tests for diagenesis in tooth enamel: ESR dating signals and carbonate contents. *Journal of Archaeological Science*, 22(2), 251-255.
- Rose, M. D. (1994). Quadrupedalism in some Miocene catarrhines. *Journal of Human Evolution*, 26(5-6), 387-411.
- Rose, M. D. (1997). Functional and phylogenetic features of the forelimb in Miocene hominoids. In *Function, phylogeny, and fossils* (pp. 79-100). Springer, Boston, MA.
- Rose, M. D., Leakey, M. G., Leakey, R. E. F., Walker, A. C. (1992). Postcranial specimens of *Simiolus enjiessi* and other primitive catarrhines from the early Miocene of Lake Turkana, Kenya. *Journal of Human Evolution*, 22(3), 171-237.
- Rossie, J. B., MacLatchy, L. (2013). Dentognathic remains of an *Afropithecus* individual from Kalodirr, Kenya. *Journal of human evolution*, 65(2), 199-208.
- Rössner, G. E. (2007). Family Tragulidae. The evolution of artiodactyls, 213-220.

- Rowan, J., Adrian, B., Grossman, A. (2015). The first skull of *Sivameryx africanus* (Anthracotheriidae, Bothriodontinae) from the early Miocene of East Africa. *Journal of Vertebrate Paleontology*, 35(3), e928305.
- Sage, R. F. (2001). Environmental and evolutionary preconditions for the origin and diversification of the C4 photosynthetic syndrome. *Plant Biology*, 3(3), 202-213.
- Sage, R. F. (2004). The evolution of C4 photosynthesis. *New phytologist*, 161(2), 341-370.
- Sanders, W.J., Gheerbrant, E., Harris, J. M., Saegusa, H., Delmer, C. (2010) Proboscidea. Chapter XXVI. In *Cenozoic Mammals of Africa* (pp. 161-251). University of California Press.
- Schilling, J. G. (1973). Afar mantle plume: rare earth evidence. *Nature Physical Science*, 242(114), 2.
- Schilling, J. G., Kingsley, R. H., Hanan, B. B., McCully, B. L. (1992). Nd-Sr-Pb isotopic variations along the Gulf of Aden: Evidence for Afar mantle plume-continental lithosphere interaction. *Journal of Geophysical Research: Solid Earth*, 97(B7), 10927-10966.
- Schoeninger, M. J., Hallin, K., Reeser, H., Valley, J. W., Fournelle, J. (2003). Isotopic alteration of mammalian tooth enamel. *International Journal of Osteoarchaeology*, 13(1-2), 11-19.
- Sepulchre, P., Ramstein, G., Fluteau, F., Schuster, M., Tiercelin, J. J., Brunet, M. (2006). Tectonic uplift and Eastern Africa aridification. *Science*, 313(5792), 1419-1423.
- Shapiro, S. S., Wilk, M. B. (1965). An analysis of variance test for normality (complete samples). *Biometrika*, 52(3/4), 591-611.
- Sillen, A., & Sealy, J. C. (1995). Diagenesis of strontium in fossil bone: A reconsideration of Nelson et al. (1986). *Journal of Archaeological Science*, 22(2), 313-320.
- Slingo, J., Spencer, H., Hoskins, B., Berrisford, P., Black, E. (2005). The meteorology of the Western Indian Ocean, and the influence of the East African Highlands. *Philosophical Transactions of the Royal Society of London A: Mathematical, Physical and Engineering Sciences*, 363(1826), 25-42.
- Smith, A. G., Hurley, A. M., Briden, J. C. (1982). *Paläokontinentale Weltkarten des Phanerozoikums*. Enke.
- Solounias, N. (2007). Family Giraffidae. The evolution of artiodactyls, 257.
- Sponheimer, M., Lee-Thorp, J. A., DeRuiter, D. J., Smith, J. M., Van Der Merwe, N. J., Reed, K., Marcus, W. (2003). Diets of southern African Bovidae: stable isotope evidence. *Journal of Mammalogy*, 84(2), 471-479.
- Steininger, F. F., Rögl, F. (1984). Paleogeography and palinspastic reconstruction of the Neogene of the Mediterranean and Paratethys. *Geological Society, London, Special Publications*, 17(1), 659-668.
- Stromberg, C. A. (2003). The origin and spread of grass-dominated ecosystems during the Tertiary of North America and how it relates to the evolution of hypsodonty in equids (Vol. 2). University of California, Berkeley.

- Strömberg, C. A. (2004). Using phytolith assemblages to reconstruct the origin and spread of grass-dominated habitats in the great plains of North America during the late Eocene to early Miocene. *Palaeogeography, Palaeoclimatology, Palaeoecology*, 207(3-4), 239-275.
- Strömberg, C. A. (2005). Decoupled taxonomic radiation and ecological expansion of open-habitat grasses in the Cenozoic of North America. *Proceedings of the National Academy of Sciences*, 102(34), 11980-11984.
- Strömberg, C. A. (2011). Evolution of grasses and grassland ecosystems. *Annual Review of Earth and Planetary Sciences*, 39, 517-544.
- Strömberg, C. A., McInerney, F. A. (2011). The Neogene transition from C 3 to C 4 grasslands in North America: assemblage analysis of fossil phytoliths. *Paleobiology*, 37(1), 50-71.
- Tassy, P. (1990). The “Proboscidean Datum Event:” How Many Proboscideans and How Many Events?. In *European Neogene Mammal Chronology*. 237-252. Springer, Boston, MA.
- Tieszen, L. L., Senyimba, M. M., Imbamba, S. K., Troughton, J. H. (1979). The distribution of C3 and C4 grasses and carbon isotope discrimination along an altitudinal and moisture gradient in Kenya. *Oecologia*, 37(3), 337-350.
- Tipple, B. J., & Pagani, M. 2010. A 35Myr North American leaf-wax compound-specific carbon and hydrogen isotope record: implications for C 4 grasslands and hydrologic cycle dynamics. *Earth and Planetary Science Letters*, 299(1), 250-262.
- Townsend, C.C. (1985). *Amaranthaceae. Flora of Tropical East Africa*. A.A. Balkema, Rotterdam.
- Ungar, P. S., Scott, J. R., Curran, S. C., Dunsworth, H. M., Harcourt-Smith, W. E. H., Lehmann, T., McNulty, K. P. (2012). Early Neogene environments in East Africa: Evidence from dental microwear of tragulids. *Palaeogeography, Palaeoclimatology, Palaeoecology*, 342, 84-96.
- Uno, K.T., Cerling, T.E., Harris, J.M., Kunimatsu, Y., Leakey, M.G., Nakatsukasa, M., Nakaya, H. (2011). Late Miocene to Pliocene carbon isotope record of differential diet change among east African herbivores. *PNAS* 108(16); 6509- 6514
- van der Merwe, N. J., Medina, E. (1989). Photosynthesis and $^{13}\text{C}/^{12}\text{C}$ ratios in Amazonian rain forests. *Geochimica et Cosmochimica Acta*, 53(5), 1091-1094.
- Verdcourt, B. (1963). The Miocene non-marine mollusca of Rusinga Island, Lake Victoria and other localities in Kenya. *Palaeontographica Abteilung A*, 1-37.
- Vincens, A., Tiercelin, J. J., Buchet, G. (2006). New Oligocene–early Miocene microflora from the southwestern Turkana Basin: Palaeoenvironmental implications in the northern Kenya Rift. *Palaeogeography, Palaeoclimatology, Palaeoecology*, 239(3-4), 470-486.
- Vogel, J. C. (1978). Isotopic assessment of the dietary habits of ungulates. *South African Journal of Science*, 74(8), 298-301.
- Walker, A. (1969). Fossil Mammal Locality on Mount Elgon, Eastern Uganda: Lower Miocene Fossils from Mount Elgon Uganda. *Nature*, 223(5206), 591.
- Walsh, J., Dodson, R. G. (1969). *Geology of northern Turkana, degree sheets 1, 2, 9, and 10* (No. 82). Geological Survey of Kenya.

Wang, Y., Cerling, T. E. (1994). A model of fossil tooth and bone diagenesis: implications for paleodiet reconstruction from stable isotopes. *Palaeogeography, Palaeoclimatology, Palaeoecology*, 107(3-4), 281-289.

Wang, Y., Cerling, T. E., & MacFadden, B. J. (1994). Fossil horses and carbon isotopes: new evidence for Cenozoic dietary, habitat, and ecosystem changes in North America. *Palaeogeography, Palaeoclimatology, Palaeoecology*, 107(3-4), 269-279.

Ward, C. V. (1997). Functional anatomy and phyletic implications of the hominoid trunk and hindlimb. In *Function, phylogeny, and fossils* (pp. 101-130). Springer, Boston, MA.

Ward, C. V. (1998). Afropithecus, Proconsul, and the primitive hominoid skeleton. In *Primate locomotion* (pp. 337-352). Springer, Boston, MA.

White F (1983) The Vegetation of Africa (United Nations Scientific and Cultural Organization, Paris), Vol 20.

Whitehouse, C. (1996). Nyctaginaceae. *Flora of Tropical East Africa*. A.A. Balkema, Rotterdam.

Wynn, J. G., Retallack, G. J. (2001). Paleoenvironmental reconstruction of middle Miocene paleosols bearing Kenyapithecus and Victoriapithecus, Nyakach Formation, southwestern Kenya. *Journal of human evolution*, 40(4), 263-288.

Zachos, J., Pagani, M., Sloan, L., Thomas, E., Billups, K. (2001). Trends, rhythms, and aberrations in global climate 65 Ma to present. *science*, 292(5517), 686-693.

Supplementary Information

List of Figures

Figure S 1 Stratigraphy of Kalodirr	pdf
Figure S 2 Stratigraphy of Moruorot	pdf

List of Tables

Table S 1 Calculations of $\delta^{13}\text{C}$ plant and enamel values adjusting for atmospheric values between 17.5 to 16.8 Ma. Atmospheric values are from Tipple & Pagani (2010) high resolution benthic data. The maximum C_3 plant values were collected from a savannah in Mpala, Kenya while the minimum C_4 range was collected from a bushland drought in Turkana, Kenya by Cerling et al. (2003).	88
Table S 2 Acid treated enamel samples.	89
Table S 3 Conservative dietary classification values.	92
Table S 4 Non-conservative dietary classifications.	97

Table S 1 Calculations of $\delta^{13}\text{C}$ plant and enamel values adjusting for atmospheric values between 17.5 to 16.8 Ma. Atmospheric values are from Tippie & Pagani (2010) high resolution benthic data. The maximum C_3 plant values were collected from a savannah in Mpala, Kenya while the minimum C_4 range was collected from a bushland drought in Turkana, Kenya by Cerling et al. (2003).

	ATMOSPHERIC VALUES		PLANT VALUES				ENAMEL VALUES			
Age (Ma)	$\delta^{13}\text{C}$ atm CO_2 high estimate	$\delta^{13}\text{C}$ atm CO_2 low estimate	$\delta^{13}\text{C}$ plant Average C_3 plant	$\delta^{13}\text{C}$ plant Max. C_3 plant	$\delta^{13}\text{C}$ plant Average C_4 plant	$\delta^{13}\text{C}$ plant Min. C_4 plant	$\delta^{13}\text{C}$ enamel Average C_3 enamel	$\delta^{13}\text{C}$ enamel Max. C_3 enamel	$\delta^{13}\text{C}$ enamel Average C_4 enamel	$\delta^{13}\text{C}$ enamel Min C_4 enamel
Present	-8.2	--	-27.3	-24.6	-12.8	-14.4	-13.2	-10.5	1.3	-0.3
16.82	-4.87	-6.08	-23.97	-21.27	-10.68	-12.28	-9.87	-7.17	3.42	1.82
16.823	-4.81	-6.02	-23.91	-21.21	-10.62	-12.22	-9.81	-7.11	3.48	1.88
16.89	-4.93	-6.14	-24.03	-21.33	-10.74	-12.34	-9.93	-7.23	3.36	1.76
16.95	-4.97	-6.18	-24.07	-21.37	-10.78	-12.38	-9.97	-7.27	3.32	1.72
17.12	-4.91	-6.12	-24.01	-21.31	-10.72	-12.32	-9.91	-7.21	3.38	1.78
17.12	-4.77	-5.98	-23.87	-21.17	-10.58	-12.18	-9.77	-7.07	3.52	1.92
17.25	-5.06	-6.27	-24.16	-21.46	-10.87	-12.47	-10.06	-7.36	3.23	1.63
17.27	-5.19	-6.4	-24.29	-21.59	-11	-12.6	-10.19	-7.49	3.1	1.5
17.45	-5.19	-6.4	-24.29	-21.59	-11	-12.6	-10.19	-7.49	3.1	1.5
17.45	-5.27	-6.48	-24.37	-21.67	-11.08	-12.68	-10.27	-7.57	3.02	1.42
Average	-5.603	-6.207	-24.097	-21.397	-10.807	-12.407	-9.997	-7.297	3.293	1.693

Table S 2 Acid treated enamel samples.

Specimen Number	Family	Treatment	Weight Before (g)	Weight After (g)	Weight change (g)	Percent Lost (%)	$\delta^{13}\text{C}$ (‰, vs VPDB)
KNM-KA 68745	Deinotheriidae	A	0.004	0.004	0	0	-11.3
KNM-MO 64770	Deinotheriidae	A	0.003	0.003	0	0	-10.12
KNM-MO 64771	Deinotheriidae	A	0.003	0.003	0	0	-9.11
KNM-WK 64768	Deinotheriidae	A	0.003	0.003	0	0	-10.23
KNM-MO 64778	Gomphotheriidae	A	0.001	0.001	0	0	-9.82
KNM-MO 64780	Gomphotheriidae	A	0.003	0.003	0	0	-9.65
KNM-WK 64777	Gomphotheriidae	A	0.002	0.002	0	0	-9.42
KNM-WK 64785C	Gomphotheriidae	A	0.003	0.003	0	0	-9.7
KNM-KA 71085	Rhinocerotidae	A	0.001	0.001	0	0	-9.45
KNM-KA 71096	Rhinocerotidae	A	0.001	0.001	0	0	-9.42
KNM-MO 64765	Rhinocerotidae	A	0.003	0.003	0	0	-8.79
KNM-MO 64766	Rhinocerotidae	A	0.003	0.003	0	0	-9.3
KNM-WK 64763A	Rhinocerotidae	A	0.003	0.003	0	0	-9.86
KNM-WK 64767	Rhinocerotidae	A	0.001	0.001	0	0	-9.38
KNM-KA 71100	Deinotheriidae	A	0.002	0.002	0	0	-9.82
KNM-KA 71079	Gomphotheriidae	A	0.001	0.001	0	0	-8.52
KNM-KA 71080	Gomphotheriidae	A	0.002	0.002	0	0	-8.13
KNM-KA 68746	Deinotheriidae	B	0.003	0.002	0.001	33	-11.45
KNM-KA 71101	Deinotheriidae	B	0.003	0.003	0	0	-9.8
KNM-MO 64770	Deinotheriidae	B	0.003	0.003	0	0	-10.35
KNM-MO 64771	Deinotheriidae	B	0.004	0.004	0	0	-9.39
KNM-WK 64768	Deinotheriidae	B	0.003	0.002	0.001	33	-10.31
KNM-KA 71080	Gomphotheriidae	B	0.003	0.002	0.001	33	-8.87
KNM-MO 64778	Gomphotheriidae	B	0.003	0.003	0	0	-10.21
KNM-MO 64780	Gomphotheriidae	B	0.005	0.004	0.001	20	-9.88
KNM-WK 64777	Gomphotheriidae	B	0.003	0.003	0	0	-9.81
KNM-WK 64785C	Gomphotheriidae	B	0.004	0.002	0.002	50	-9.99

KNM-KA 71081	Gomphotheriidae	B	0.004	0.004	0	0	-8.44
KNM-KA 71086	Rhinocerotidae	B	0.002	0.001	0.001	50	-9.69
KNM-KA 71097	Rhinocerotidae	B	0.002	0.001	0.001	50	-9.77
KNM-MO 64765	Rhinocerotidae	B	0.003	0.002	0.001	33	-9.03
KNM-MO 64766	Rhinocerotidae	B	0.003	0.003	0	0	-9.56
KNM-WK 64763A	Rhinocerotidae	B	0.002	0.002	0	0	-9.86
KNM-WK 64767	Rhinocerotidae	B	0.002	0.002	0	0	-9.6
KNM-KA 68747	Deinotheriidae	C	0.003	0.003	0	0	-12.37
KNM-KA 71102	Deinotheriidae	C	0.003	0.002	0.001	33	-11.04
KNM-MO 64770	Deinotheriidae	C	0.003	0.001	0.002	67	-10.74
KNM-MO 64771	Deinotheriidae	C	0.005	0.003	0.002	40	-9.89
KNM-WK 64768	Deinotheriidae	C	0.003	0.002	0.001	33	-10.9
KNM-KA 71081	Gomphotheriidae	C	0.003	0.003	0	0	-9.23
KNM-KA 71082	Gomphotheriidae	C	0.004	0.003	0.001	25	-8.75
KNM-MO 64778	Gomphotheriidae	C	0.003	0.002	0.001	33	-10.56
KNM-MO 64780	Gomphotheriidae	C	0.004	0.003	0.001	25	-10.62
KNM-WK 64777	Gomphotheriidae	C	0.003	0.002	0.001	33	-10.04
KNM-WK 64785C	Gomphotheriidae	C	0.003	0.002	0.001	33	-10.5
KNM-KA 71087	Rhinocerotidae	C	0.002	0.001	0.001	50	-10.09
KNM-KA 71098	Rhinocerotidae	C	0.002	0.001	0.001	50	-10.31
KNM-MO 64765	Rhinocerotidae	C	0.003	0.001	0.002	67	-8.9
KNM-MO 64766	Rhinocerotidae	C	0.003	0.002	0.001	33	-10.21
KNM-WK 64763A	Rhinocerotidae	C	0.002	0.001	0.001	50	-11.02
KNM-WK 64767	Rhinocerotidae	C	0.002	0.002	0	0	-10.42
KNM-KA 68748	Deinotheriidae	D	0.004	0.001	0.003	75	-12.8
KNM-KA 71103	Deinotheriidae	D	0.003	0.002	0.001	33	-10.96
KNM-MO 64770	Deinotheriidae	D	0.004	0.003	0.001	25	-10.63
KNM-MO 64771	Deinotheriidae	D	0.005	0.003	0.002	40	-9.96
KNM-WK 64768	Deinotheriidae	D	0.003	0.001	0.002	67	-11.53

KNM-KA 71082	Gomphotheriidae	D	0.004	0.003	0.001	25	-9.17
KNM-KA 71083	Gomphotheriidae	D	0.004	0.003	0.001	25	-8.8
KNM-MO 64778	Gomphotheriidae	D	0.004	0.003	0.001	25	-10.52
KNM-MO 64780	Gomphotheriidae	D	0.005	0.003	0.002	40	-10.69
KNM-WK 64777	Gomphotheriidae	D	0.003	0.003	0	0	-9.93
KNM-WK 64785C	Gomphotheriidae	D	0.003	0.002	0.001	33	-10.37
KNM-KA 71088	Rhinocerotidae	D	0.002	0.001	0.001	50	-10.21
KNM-KA 71099	Rhinocerotidae	D	0.003	0.003	0	0	-10.31
KNM-MO 64765	Rhinocerotidae	D	0.004	0.003	0.001	25	-8.97
KNM-MO 64766	Rhinocerotidae	D	0.004	0.002	0.002	50	-10.27
KNM-WK 64763A	Rhinocerotidae	D	0.003	0.003	0	0	-10.99
KNM-WK 64767	Rhinocerotidae	D	0.002	0.001	0.001	50	-10.69

Table S 3 Conservative dietary classification values.

Locality	Sample Number	Specimen Number	Family	Species	$\delta^{13}\text{C}$	% C3	% C4	Classification
KAL	SC-2017-20	KNM-WK 64761	Anthracotheriidae	<i>Brachyodus aequatorialis</i>	-9.77	100	0	C ₃ Pure Feeder
KAL	JK-2016-07	KNM-WK-16919	Anthracotheriidae	<i>Brachyodus aequatorialis</i>	-10.32	100	0	C ₃ Pure Feeder
KAL	JK-2016-12	KNM-WK-16924	Anthracotheriidae	<i>Sivameryx africanus</i>	-6.77	94	6	C ₃ Dominated Feeder
KAL	JK-2016-09	KNM-WK-16943D	Anthracotheriidae	<i>Brachyodus aequatorialis</i>	-10.34	100	0	C ₃ Pure Feeder
KAL	JK-2016-22	KNM-WK-16963C	Anthracotheriidae	<i>Sivameryx africanus</i>	-8.99	100	0	C ₃ Pure Feeder
KAL	JK-2016-23	KNM-WK-18129A	Anthracotheriidae	<i>Sivameryx africanus</i>	-10.8	100	0	C ₃ Pure Feeder
KAL	JK-2016-10	KNM-WK-18202	Anthracotheriidae	<i>Sivameryx africanus</i>	-8.63	100	0	C ₃ Pure Feeder
KAL	SC-2017-29	KNM-WK 64768	Deinotheriidae	<i>Prodeinotherium hobleyi</i>	-10.23	100	0	C ₃ Pure Feeder
KAL	SC-2016-06	KNM-WK-16920	Deinotheriidae	<i>Prodeinotherium hobleyi</i>	-11.18	100	0	C ₃ Pure Feeder
KAL	SC-2017-15	KNM-WK 64756	Giraffidae/Pecora	<i>Canthumeryx sirtensis</i>	-9.83	100	0	C ₃ Pure Feeder
KAL	SC-2016-17	KNM-WK-16967	Giraffidae/Pecora	<i>Canthumeryx sirtensis</i>	-11	100	0	C ₃ Pure Feeder
KAL	SC-2016-28	KNM-WK-17083	Giraffidae/Pecora	<i>Walangania africanus</i>	-8.76	100	0	C ₃ Pure Feeder
KAL	SC-2016-13	KNM-WK-17126	Giraffidae/Pecora	<i>Canthumeryx sirtensis</i>	-9.09	100	0	C ₃ Pure Feeder
KAL	SC-2016-16	KNM-WK-18135	Giraffidae/Pecora	<i>Canthumeryx sirtensis</i>	-8.53	100	0	C ₃ Pure Feeder
KAL	SC-2016-14	KNM-WK-18199C	Giraffidae/Pecora	<i>Canthumeryx sirtensis</i>	-8.19	100	0	C ₃ Pure Feeder
KAL	SC-2017-07	KNM-WK 64776	Gomphotheriidae		-8.65	100	0	C ₃ Pure Feeder
KAL	SC-2017-28	KNM-WK 64777	Gomphotheriidae		-9.42	100	0	C ₃ Pure Feeder
KAL	SC-2017-08	KNM-WK 64779	Gomphotheriidae		-9.67	100	0	C ₃ Pure Feeder
KAL	SC-2017-32	KNM-WK 64783	Gomphotheriidae		-10.56	100	0	C ₃ Pure Feeder

KAL	SC-2017-09	KNM-WK 64784	Gomphotheriidae		-9.52	100	0	C ₃ Pure Feeder
KAL	SC-2017-31	KNM-WK 64785C	Gomphotheriidae		-9.7	100	0	C ₃ Pure Feeder
KAL	SC-2016-05	KNM-WK 71075	Gomphotheriidae		-9.22	100	0	C ₃ Pure Feeder
KAL	SC-2016-04	KNM-WK 71078	Gomphotheriidae		-9.76	100	0	C ₃ Pure Feeder
KAL	SC-2016-01	KNM-WK 71280	Gomphotheriidae		-9.39	100	0	C ₃ Pure Feeder
KAL	SC-2016-02	KNM-WK 71281	Gomphotheriidae		-8.35	100	0	C ₃ Pure Feeder
KAL	SC-2016-07	KNM-WK-16926B	Gomphotheriidae	<i>Protanacus macinnesi</i>	-8.52	100	0	C ₃ Pure Feeder
KAL	SC-2016-08	KNM-WK-17005	Gomphotheriidae	<i>Protanacus macinnesi</i>	-8.11	100	0	C ₃ Pure Feeder
KAL	SC-2016-12	KNM-WK-17138	Gomphotheriidae		-8.99	100	0	C ₃ Pure Feeder
KAL	JK-2016-03	KNM-MO 71074	Rhinocerotidae		-7.78	100	0	C ₃ Pure Feeder
KAL	JK-2016-04	KNM-MO 71077	Rhinocerotidae		-10.12	100	0	C ₃ Pure Feeder
KAL	SC-2017-10	KNM-WK 64763A	Rhinocerotidae		-9.86	100	0	C ₃ Pure Feeder
KAL	SC-2017-14	KNM-WK 64767	Rhinocerotidae		-9.38	100	0	C ₃ Pure Feeder
KAL	JK-2016-02	KNM-WK-17007C	Rhinocerotidae		-10.12	100	0	C ₃ Pure Feeder
KAL	JK-2016-01	KNM-WK-18391A	Rhinocerotidae		-10.52	100	0	C ₃ Pure Feeder
KAL	JK-2016-05	KNM-WK-46450	Rhinocerotidae		-9.62	100	0	C ₃ Pure Feeder
KAL	SC-2017-45	KNM-WK 18108E	Suidae/Sanitheriidae	<i>Diamantohyus africanus</i>	-9.33	100	0	C ₃ Pure Feeder
KAL	SC-2017-24	KNM-WK 64758	Suidae/Sanitheriidae	<i>Namachoerus moruoroti</i>	-10	100	0	C ₃ Pure Feeder
KAL	JK-2016-14	KNM-WK 71076	Suidae/Sanitheriidae	<i>Diamantohyus africanus</i>	-9.37	100	0	C ₃ Pure Feeder
KAL	SC-2017-46	KNM-WK-16977	Suidae/Sanitheriidae	<i>Namachoerus moruoroti</i>	-9.4	100	0	C ₃ Pure Feeder
KAL	JK-2016-16	KNM-WK-17049	Suidae/Sanitheriidae	<i>Diamantohyus africanus</i>	-9.46	100	0	C ₃ Pure Feeder

KAL	SC-2017-44	KNM-WK-17075B	Suidae/Sanitheriidae	<i>Namachoerus moruoroti</i>	-8.58	100	0	C ₃ Pure Feeder
KAL	JK-2016-24	KNM-WK-17088A	Suidae/Sanitheriidae	<i>Kenyasus rusingensis</i>	-10.94	100	0	C ₃ Pure Feeder
KAL	SC-2017-47	KNM-WK-17094	Suidae/Sanitheriidae	<i>Namachoerus moruoroti</i>	-9.91	100	0	C ₃ Pure Feeder
KAL	JK-2016-15	KNM-WK-17097B	Suidae/Sanitheriidae	<i>Diamantohyus africanus</i>	-10.15	100	0	C ₃ Pure Feeder
KAL	JK-2016-20	KNM-WK-17127	Suidae/Sanitheriidae	<i>Libycochoerus jeanelli</i>	-10.86	100	0	C ₃ Pure Feeder
KAL	JK-2016-17	KNM-WK-17128	Suidae/Sanitheriidae	<i>Diamantohyus africanus</i>	-10.07	100	0	C ₃ Pure Feeder
KAL	JK-2016-19	KNM-WK-17131	Suidae/Sanitheriidae	<i>Kenyasus rusingensis</i>	-9.64	100	0	C ₃ Pure Feeder
KAL	JK-2016-18	KNM-WK-18204	Suidae/Sanitheriidae	<i>Diamantohyus africanus</i>	-9.29	100	0	C ₃ Pure Feeder
KAL	SC-2017-38	KNM-WK-16925A	Titanohyracidae	<i>Afrohyrax championi</i>	-10.14	100	0	C ₃ Pure Feeder
KAL	SC-2017-37	KNM-WK-16990B	Titanohyracidae	<i>Afrohyrax championi</i>	-10.22	100	0	C ₃ Pure Feeder
KAL	SC-2017-42	KNM-WK-17125D	Titanohyracidae	<i>Afrohyrax championi</i>	-9.93	100	0	C ₃ Pure Feeder
KAL	SC-2017-40	KNM-WK-18066	Titanohyracidae	<i>Afrohyrax championi</i>	-9.93	100	0	C ₃ Pure Feeder
KAL	SC-2017-39	KNM-WK-18104A	Titanohyracidae	<i>Afrohyrax championi</i>	-9.57	100	0	C ₃ Pure Feeder
KAL	SC-2017-36	KNM-WK-18105A	Titanohyracidae	<i>Afrohyrax championi</i>	-9.74	100	0	C ₃ Pure Feeder
KAL	SC-2017-41	KNM-WK-18206B	Titanohyracidae	<i>Afrohyrax championi</i>	-10.1	100	0	C ₃ Pure Feeder
KAL	SC-2017-19	KNM-WK 64750	Tragulidae	<i>Dorcatherium chappuisi</i>	-10.22	100	0	C ₃ Pure Feeder
KAL	SC-2017-17	KNM-WK 64752	Tragulidae	<i>Dorcatherium chappuisi</i>	-8.34	100	0	C ₃ Pure Feeder
KAL	SC-2017-48	KNM-WK 71283	Tragulidae	<i>Dorcatherium pigotti</i>	-8.9	100	0	C ₃ Pure Feeder
KAL	SC-2016-27	KNM-WK-16975B	Tragulidae	<i>Dorcatherium chappuisi</i>	-9.19	100	0	C ₃ Pure Feeder
KAL	SC-2016-23	KNM-WK-16987A	Tragulidae	<i>Dorcatherium pigotti</i>	-7.51	100	0	C ₃ Pure Feeder
KAL	SC-2016-25	KNM-WK-17101A	Tragulidae	<i>Dorcatherium chappuisi</i>	-7.67	100	0	C ₃ Pure Feeder

KAL	SC-2016-24	KNM-WK-17111	Tragulidae	<i>Dorcatherium pigotti</i>	-9.71	100	0	C ₃ Pure Feeder
KAL	SC-2016-21	KNM-WK-18079	Tragulidae	<i>Dorcatherium chappuisi</i>	-10.03	100	0	C ₃ Pure Feeder
KAL	SC-2016-22	KNM-WK-18095C	Tragulidae	<i>Dorcatherium pigotti</i>	-8.15	100	0	C ₃ Pure Feeder
KAL	SC-2016-20	KNM-WK-18096	Tragulidae	<i>Dorcatherium chappuisi</i>	-7.54	100	0	C ₃ Pure Feeder
KAL	SC-2017-43	KNM-WK-18200	Tragulidae	<i>Dorcatherium chappuisi</i>	-9.07	100	0	C ₃ Pure Feeder
MOR	SC-2017-26	KNM-MO 64769	Deinotheriidae	<i>Prodeinotherium hobleyi</i>	-10.58	100	0	C ₃ Pure Feeder
MOR	SC-2017-33	KNM-MO 64770	Deinotheriidae	<i>Prodeinotherium hobleyi</i>	-10.12	100	0	C ₃ Pure Feeder
MOR	SC-2017-34	KNM-MO 64771	Deinotheriidae	<i>Prodeinotherium hobleyi</i>	-9.11	100	0	C ₃ Pure Feeder
MOR	SC-2017-18	KNM-MO 64751	Giraffidae/Pecora	<i>Canthumeryx sirtensis</i>	-9.7	100	0	C ₃ Pure Feeder
MOR	SC-2017-16	KNM-MO 64753A	Giraffidae/Pecora	<i>Canthumeryx sirtensis</i>	-9.29	100	0	C ₃ Pure Feeder
MOR	SC-2016-15	KNM-MO-17115	Giraffidae/Pecora	<i>Canthumeryx sirtensis</i>	-7.67	100	0	C ₃ Pure Feeder
MOR	SC-2016-26	KNM-MO-18114	Giraffidae/Pecora	<i>Walangania africanus</i>	-9.93	100	0	C ₃ Pure Feeder
MOR	SC-2016-18	KNM-MO-65	Giraffidae/Pecora	<i>Canthumeryx sirtensis</i>	-8.03	100	0	C ₃ Pure Feeder
MOR	SC-2016-19	KNM-MO-73	Giraffidae/Pecora	<i>Canthumeryx sirtensis</i>	-8.76	100	0	C ₃ Pure Feeder
MOR	SC-2017-03	KNM-MO 64772	Gomphotheriidae		-10.42	100	0	C ₃ Pure Feeder
MOR	SC-2017-04	KNM-MO 64773	Gomphotheriidae		-11.05	100	0	C ₃ Pure Feeder
MOR	SC-2017-05	KNM-MO 64774	Gomphotheriidae		-10.62	100	0	C ₃ Pure Feeder
MOR	SC-2017-06	KNM-MO 64775	Gomphotheriidae		-10.25	100	0	C ₃ Pure Feeder
MOR	SC-2017-30	KNM-MO 64778	Gomphotheriidae		-9.82	100	0	C ₃ Pure Feeder
MOR	SC-2017-27	KNM-MO 64780	Gomphotheriidae		-9.65	100	0	C ₃ Pure Feeder
MOR	SC-2017-01	KNM-MO 64781	Gomphotheriidae		-10.18	100	0	C ₃ Pure Feeder

MOR	SC-2017-02	KNM-MO 64782	Gomphotheriidae		-9.17	100	0	C ₃ Pure Feeder
MOR	SC-2016-09/10/11	KNM-MO 71279	Gomphotheriidae		-6.01	86	14	C ₃ Dominated Feeder
MOR	SC-2016-03	KNM-MO 71282	Gomphotheriidae		-10.14	100	0	C ₃ Pure Feeder
MOR	SC-2017-12	KNM-MO 64764	Rhinocerotidae		-11.91	100	0	C ₃ Pure Feeder
MOR	SC-2017-13	KNM-MO 64765	Rhinocerotidae		-8.79	100	0	C ₃ Pure Feeder
MOR	SC-2017-11	KNM-MO 64766	Rhinocerotidae		-9.3	100	0	C ₃ Pure Feeder
MOR	JK-2016-06	KNM-MO-43	Rhinocerotidae		-10.51	100	0	C ₃ Pure Feeder
MOR	SC-2017-25	KNM-MO 64757	Suidae/Sanitheriidae	<i>Namachoerus moruoroti</i>	-9.45	100	0	C ₃ Pure Feeder
MOR	SC-2017-22	KNM-MO 64759	Suidae/Sanitheriidae	<i>Diamantohyus africanus</i>	-10.99	100	0	C ₃ Pure Feeder
MOR	SC-2017-23	KNM-MO 64760	Suidae/Sanitheriidae	<i>Diamantohyus africanus</i>	-9.84	100	0	C ₃ Pure Feeder
MOR	JK-2016-21	KNM-MO-18127A	Suidae/Sanitheriidae	<i>Libycochoerus jeanelli</i>	-10.95	100	0	C ₃ Pure Feeder
MOR	SC-2017-21	KNM-MO 64762	Titanohyracidae	<i>Afrohyrax championi</i>	-10.58	100	0	C ₃ Pure Feeder
MOR	SC-2017-35	KNM-MO-1	Titanohyracidae	<i>Afrohyrax championi</i>	-10.88	100	0	C ₃ Pure Feeder

Table S 4 Non-conservative dietary classifications.

Locality	Sample Number	Specimen Number	Family	Species	$\delta^{13}C$	% C3	% C4	Classification
KAL	SC-2017-20	KNM-WK 64761	Anthracotheriidae	<i>Brachyodus aequatorialis</i>	-9.77	98	2	C ₃ Dominated Feeder
KAL	JK-2016-12	KNM-WK-16924	Anthracotheriidae	<i>Sivameryx africanus</i>	-6.77	76	24	C ₃ Dominated Feeder
KAL	JK-2016-22	KNM-WK-16963C	Anthracotheriidae	<i>Sivameryx africanus</i>	-8.99	92	8	C ₃ Dominated Feeder
KAL	JK-2016-10	KNM-WK-18202	Anthracotheriidae	<i>Sivameryx africanus</i>	-8.63	90	10	C ₃ Dominated Feeder
KAL	JK-2016-07	KNM-WK-16919	Anthracotheriidae	<i>Brachyodus aequatorialis</i>	-10.32	100	0	C ₃ Pure Feeder
KAL	JK-2016-09	KNM-WK-16943D	Anthracotheriidae	<i>Brachyodus aequatorialis</i>	-10.34	100	0	C ₃ Pure Feeder
KAL	JK-2016-23	KNM-WK-18129A	Anthracotheriidae	<i>Sivameryx africanus</i>	-10.8	100	0	C ₃ Pure Feeder
KAL	SC-2017-29	KNM-WK 64768	Deinotheriidae	<i>Prodeinotherium hobleyi</i>	-10.23	100	0	C ₃ Pure Feeder
KAL	SC-2016-06	KNM-WK-16920	Deinotheriidae	<i>Prodeinotherium hobleyi</i>	-11.18	100	0	C ₃ Pure Feeder
KAL	SC-2017-15	KNM-WK 64756	Giraffidae/Pecora	<i>Canthumeryx sirtensis</i>	-9.83	99	1	C ₃ Dominated Feeder
KAL	SC-2016-28	KNM-WK-17083	Giraffidae/Pecora	<i>Walangania africanus</i>	-8.76	90	10	C ₃ Dominated Feeder
KAL	SC-2016-13	KNM-WK-17126	Giraffidae/Pecora	<i>Canthumeryx sirtensis</i>	-9.09	93	7	C ₃ Dominated Feeder
KAL	SC-2016-16	KNM-WK-18135	Giraffidae/Pecora	<i>Canthumeryx sirtensis</i>	-8.53	89	11	C ₃ Dominated Feeder
KAL	SC-2016-14	KNM-WK-18199C	Giraffidae/Pecora	<i>Canthumeryx sirtensis</i>	-8.19	86	14	C ₃ Dominated Feeder
KAL	SC-2016-17	KNM-WK-16967	Giraffidae/Pecora	<i>Canthumeryx sirtensis</i>	-11	100	0	C ₃ Pure Feeder
KAL	SC-2017-07	KNM-WK 64776	Gomphotheriidae		-8.65	90	10	C ₃ Dominated Feeder
KAL	SC-2017-28	KNM-WK 64777	Gomphotheriidae		-9.42	96	4	C ₃ Dominated Feeder
KAL	SC-2017-08	KNM-WK 64779	Gomphotheriidae		-9.67	98	2	C ₃ Dominated Feeder

KAL	SC-2017-09	KNM-WK 64784	Gomphotheriidae		-9.52	96	4	C ₃ Dominated Feeder
KAL	SC-2017-31	KNM-WK 64785C	Gomphotheriidae		-9.7	98	2	C ₃ Dominated Feeder
KAL	SC-2016-05	KNM-WK 71075	Gomphotheriidae		-9.22	94	6	C ₃ Dominated Feeder
KAL	SC-2016-04	KNM-WK 71078	Gomphotheriidae		-9.76	98	2	C ₃ Dominated Feeder
KAL	SC-2016-01	KNM-WK 71280	Gomphotheriidae		-9.39	95	5	C ₃ Dominated Feeder
KAL	SC-2016-02	KNM-WK 71281	Gomphotheriidae		-8.35	88	12	C ₃ Dominated Feeder
KAL	SC-2016-07	KNM-WK-16926B	Gomphotheriidae	<i>Protanacus macinnesi</i>	-8.52	89	11	C ₃ Dominated Feeder
KAL	SC-2016-08	KNM-WK-17005	Gomphotheriidae	<i>Protanacus macinnesi</i>	-8.11	86	14	C ₃ Dominated Feeder
KAL	SC-2016-12	KNM-WK-17138	Gomphotheriidae		-8.99	92	8	C ₃ Dominated Feeder
KAL	SC-2017-32	KNM-WK 64783	Gomphotheriidae		-10.56	100	0	C ₃ Pure Feeder
KAL	JK-2016-03	KNM-MO 71074	Rhinocerotidae		-7.78	83	17	C ₃ Dominated Feeder
KAL	SC-2017-10	KNM-WK 64763A	Rhinocerotidae		-9.86	99	1	C ₃ Dominated Feeder
KAL	SC-2017-14	KNM-WK 64767	Rhinocerotidae		-9.38	95	5	C ₃ Dominated Feeder
KAL	JK-2016-05	KNM-WK-46450	Rhinocerotidae		-9.62	97	3	C ₃ Dominated Feeder
KAL	JK-2016-04	KNM-MO 71077	Rhinocerotidae		-10.12	100	0	C ₃ Pure Feeder
KAL	JK-2016-02	KNM-WK-17007C	Rhinocerotidae		-10.12	100	0	C ₃ Pure Feeder
KAL	JK-2016-01	KNM-WK-18391A	Rhinocerotidae		-10.52	100	0	C ₃ Pure Feeder
KAL	JK-2016-14	KNM-WK 71076	Suidae/Sanitheriidae	<i>Diamantohyus africanus</i>	-9.37	95	5	C ₃ Dominated Feeder
KAL	SC-2017-46	KNM-WK-16977	Suidae/Sanitheriidae	<i>Namachoerus moruoroti</i>	-9.4	96	4	C ₃ Dominated Feeder
KAL	JK-2016-16	KNM-WK-17049	Suidae/Sanitheriidae	<i>Diamantohyus africanus</i>	-9.46	96	4	C ₃ Dominated Feeder
KAL	SC-2017-44	KNM-WK-17075B	Suidae/Sanitheriidae	<i>Namachoerus moruoroti</i>	-8.58	89	11	C ₃ Dominated Feeder

KAL	SC-2017-47	KNM-WK-17094	Suidae/Sanitheriidae	<i>Namachoerus moruoroti</i>	-9.91	99	1	C ₃ Dominated Feeder
KAL	JK-2016-19	KNM-WK-17131	Suidae/Sanitheriidae	<i>Kenyasus rusingensis</i>	-9.64	97	3	C ₃ Dominated Feeder
KAL	JK-2016-18	KNM-WK-18204	Suidae/Sanitheriidae	<i>Diamantohyus africanus</i>	-9.29	95	5	C ₃ Dominated Feeder
KAL	SC-2017-45	KNM-WK 18108E	Suidae/Sanitheriidae	<i>Diamantohyus africanus</i>	-9.33	95	5	C ₃ Pure Feeder
KAL	SC-2017-24	KNM-WK 64758	Suidae/Sanitheriidae	<i>Namachoerus moruoroti</i>	-10	100	0	C ₃ Pure Feeder
KAL	JK-2016-24	KNM-WK-17088A	Suidae/Sanitheriidae	<i>Kenyasus rusingensis</i>	-10.94	100	0	C ₃ Pure Feeder
KAL	JK-2016-15	KNM-WK-17097B	Suidae/Sanitheriidae	<i>Diamantohyus africanus</i>	-10.15	100	0	C ₃ Pure Feeder
KAL	JK-2016-20	KNM-WK-17127	Suidae/Sanitheriidae	<i>Libycochoerus jeanelli</i>	-10.86	100	0	C ₃ Pure Feeder
KAL	JK-2016-17	KNM-WK-17128	Suidae/Sanitheriidae	<i>Diamantohyus africanus</i>	-10.07	100	0	C ₃ Pure Feeder
KAL	SC-2017-42	KNM-WK-17125D	Titanohyracidae	<i>Afrohyrax championi</i>	-9.93	99	1	C ₃ Dominated Feeder
KAL	SC-2017-40	KNM-WK-18066	Titanohyracidae	<i>Afrohyrax championi</i>	-9.93	99	1	C ₃ Dominated Feeder
KAL	SC-2017-39	KNM-WK-18104A	Titanohyracidae	<i>Afrohyrax championi</i>	-9.57	97	3	C ₃ Dominated Feeder
KAL	SC-2017-36	KNM-WK-18105A	Titanohyracidae	<i>Afrohyrax championi</i>	-9.74	98	2	C ₃ Dominated Feeder
KAL	SC-2017-38	KNM-WK-16925A	Titanohyracidae	<i>Afrohyrax championi</i>	-10.14	100	0	C ₃ Pure Feeder
KAL	SC-2017-37	KNM-WK-16990B	Titanohyracidae	<i>Afrohyrax championi</i>	-10.22	100	0	C ₃ Pure Feeder
KAL	SC-2017-41	KNM-WK-18206B	Titanohyracidae	<i>Afrohyrax championi</i>	-10.1	100	0	C ₃ Pure Feeder
KAL	SC-2017-17	KNM-WK 64752	Tragulidae	<i>Dorcatherium chappuisi</i>	-8.34	87	13	C ₃ Dominated Feeder
KAL	SC-2017-48	KNM-WK 71283	Tragulidae	<i>Dorcatherium pigotti</i>	-8.9	92	8	C ₃ Dominated Feeder
KAL	SC-2016-27	KNM-WK-16975B	Tragulidae	<i>Dorcatherium chappuisi</i>	-9.19	94	6	C ₃ Dominated Feeder
KAL	SC-2016-23	KNM-WK-16987A	Tragulidae	<i>Dorcatherium pigotti</i>	-7.51	81	19	C ₃ Dominated Feeder
KAL	SC-2016-25	KNM-WK-17101A	Tragulidae	<i>Dorcatherium chappuisi</i>	-7.67	82	18	C ₃ Dominated Feeder

KAL	SC-2016-24	KNM-WK-17111	Tragulidae	<i>Dorcatherium pigotti</i>	-9.71	98	2	C ₃ Dominated Feeder
KAL	SC-2016-22	KNM-WK-18095C	Tragulidae	<i>Dorcatherium pigotti</i>	-8.15	86	14	C ₃ Dominated Feeder
KAL	SC-2016-20	KNM-WK-18096	Tragulidae	<i>Dorcatherium chappuisi</i>	-7.54	82	18	C ₃ Dominated Feeder
KAL	SC-2017-43	KNM-WK-18200	Tragulidae	<i>Dorcatherium chappuisi</i>	-9.07	93	7	C ₃ Dominated Feeder
KAL	SC-2017-19	KNM-WK 64750	Tragulidae	<i>Dorcatherium chappuisi</i>	-10.22	100	0	C ₃ Pure Feeder
KAL	SC-2016-21	KNM-WK-18079	Tragulidae	<i>Dorcatherium chappuisi</i>	-10.03	100	0	C ₃ Pure Feeder
MOR	SC-2017-34	KNM-MO 64771	Deinotheriidae	<i>Prodeinotherium hobleiyi</i>	-9.11	93	7	C ₃ Dominated Feeder
MOR	SC-2017-26	KNM-MO 64769	Deinotheriidae	<i>Prodeinotherium hobleiyi</i>	-10.58	100	0	C ₃ Pure Feeder
MOR	SC-2017-33	KNM-MO 64770	Deinotheriidae	<i>Prodeinotherium hobleiyi</i>	-10.12	100	0	C ₃ Pure Feeder
MOR	SC-2017-18	KNM-MO 64751	Giraffidae/Pecora	<i>Canthumeryx sirtensis</i>	-9.7	98	2	C ₃ Dominated Feeder
MOR	SC-2017-16	KNM-MO 64753A	Giraffidae/Pecora	<i>Canthumeryx sirtensis</i>	-9.29	95	5	C ₃ Dominated Feeder
MOR	SC-2016-15	KNM-MO-17115	Giraffidae/Pecora	<i>Canthumeryx sirtensis</i>	-7.67	82	18	C ₃ Dominated Feeder
MOR	SC-2016-26	KNM-MO-18114	Giraffidae/Pecora	<i>Walangania africanus</i>	-9.93	99	1	C ₃ Dominated Feeder
MOR	SC-2016-18	KNM-MO-65	Giraffidae/Pecora	<i>Canthumeryx sirtensis</i>	-8.03	85	15	C ₃ Dominated Feeder
MOR	SC-2016-19	KNM-MO-73	Giraffidae/Pecora	<i>Canthumeryx sirtensis</i>	-8.76	91	9	C ₃ Dominated Feeder
MOR	SC-2016-09/10/11	KNM-MO 71279	Gomphotheriidae		-6.01	70	30	C ₃ – C ₄ Mixed Feeder
MOR	SC-2017-30	KNM-MO 64778	Gomphotheriidae		-9.82	99	1	C ₃ Dominated Feeder
MOR	SC-2017-27	KNM-MO 64780	Gomphotheriidae		-9.65	97	3	C ₃ Dominated Feeder
MOR	SC-2017-02	KNM-MO 64782	Gomphotheriidae		-9.17	94	6	C ₃ Dominated Feeder
MOR	SC-2017-03	KNM-MO 64772	Gomphotheriidae		-10.42	100	0	C ₃ Pure Feeder
MOR	SC-2017-04	KNM-MO 64773	Gomphotheriidae		-11.05	100	0	C ₃ Pure Feeder

MOR	SC-2017-05	KNM-MO 64774	Gomphotheriidae		-10.62	100	0	C ₃ Pure Feeder
MOR	SC-2017-06	KNM-MO 64775	Gomphotheriidae		-10.25	100	0	C ₃ Pure Feeder
MOR	SC-2017-01	KNM-MO 64781	Gomphotheriidae		-10.18	100	0	C ₃ Pure Feeder
MOR	SC-2016-03	KNM-MO 71282	Gomphotheriidae		-10.14	100	0	C ₃ Pure Feeder
MOR	SC-2017-13	KNM-MO 64765	Rhinocerotidae		-8.79	91	9	C ₃ Dominated Feeder
MOR	SC-2017-11	KNM-MO 64766	Rhinocerotidae		-9.3	95	5	C ₃ Dominated Feeder
MOR	SC-2017-12	KNM-MO 64764	Rhinocerotidae		-11.91	100	0	C ₃ Pure Feeder
MOR	JK-2016-06	KNM-MO-43	Rhinocerotidae		-10.51	100	0	C ₃ Pure Feeder
MOR	SC-2017-25	KNM-MO 64757	Suidae/Sanitheriidae	<i>Namachoerus moruoroti</i>	-9.45	96	4	C ₃ Dominated Feeder
MOR	SC-2017-23	KNM-MO 64760	Suidae/Sanitheriidae	<i>Diamantohyus africanus</i>	-9.84	99	1	C ₃ Dominated Feeder
MOR	SC-2017-22	KNM-MO 64759	Suidae/Sanitheriidae	<i>Diamantohyus africanus</i>	-10.99	100	0	C ₃ Pure Feeder
MOR	JK-2016-21	KNM-MO-18127A	Suidae/Sanitheriidae	<i>Libycochoerus jeanelli</i>	-10.95	100	0	C ₃ Pure Feeder
MOR	SC-2017-21	KNM-MO 64762	Titanohyracidae	<i>Afrohyrax championi</i>	-10.58	100	0	C ₃ Pure Feeder
MOR	SC-2017-35	KNM-MO-1	Titanohyracidae	<i>Afrohyrax championi</i>	-10.88	100	0	C ₃ Pure Feeder